SKB

TECHNICAL REPORT 90-38

Solute transport in fractured rock – Applications to radionuclide waste repositories

Ivars Neretnieks

Department of Chemical Engineering,
Royal Institute of Technology, Stockholm

December 1990

SVENSK KÄRNBRÄNSLEHANTERING AB
SWEDISH NUCLEAR FUEL AND WASTE MANAGEMENT CO

BOX 5864 S-102 48 STOCKHOLM

TEL 08-665 28 00 TELEX 13108 SKB S
TELEFAX 08-661 57 19

SOLUTE TRANSPORT IN FRACTURED ROCK - APPLICATIONS TO RADIONUCLIDE WASTE REPOSITORIES

Ivars Neretnieks

Department of Chemical Engineering,
Royal Institute of Technology, Stockholm

December 1990

SOLUTE TRANSPORT IN FRACTURED ROCK - APPLICATIONS TO RADIONUCLIDE WASTE REPOSITORIES

IVARS NERETNIEKS
DEPARTMENT OF CHEMICAL ENGINEERING
ROYAL INSTITUTE OF TECHNOLOGY
S-100 44 STOCKHOLM
SWEDEN

DEC 1989

ABSTRACT

Flow and solute transport in fractured rocks has been intensively studied in the last decade. The increased interest is mainly due to the plans in many countries to site repositories for high level nuclear waste in deep geologic formations. All investigated crystalline rocks have been found to be fractured and most of the water flows in the fractures and fracture zones. The water transports dissolved species and radionuclides. It is thus of interest to be able to understand and to do predictive modelling of the flowrate of water, the flowpaths and the residence times of the water and of the nuclides.

The dissolved species including the nuclides will interact with the surrounding rock in different ways and will in many cases be strongly retarded relative to the water velocity. Ionic species may be ion exchanged or sorbed on the mineral surfaces. Charged and neutral species may diffuse into the stagnant waters in the rock matrix and thus be withdrawn from the mobile water. These effects will be strongly dependent on how much rock surface is in contact with the flowing water. It has been found in a set of field experiments and by other observations that not all fractures conduct water. Furthermore it is found that conductive fractures only conduct the water in a small part of the fracture in what is called channels or preferential flowpaths. The channels form a conductive network in rock with strong variations in flowrates and velocities between different channels.

This report summarizes the present concepts of water flow and solute transport in fractured rocks. The data needs for predictive modelling are discussed and both field and laboratory measurements which have been used to obtain data are described. Several large scale field experiments which have been specially designed to study flow and tracer transport in crystalline rocks are described. In many of the field experients new techniques have been deveoped and used.

TABLE OF CONTENTS

1 BACKGROUND AND INTRODUCTION

2 SOME CONCEPTS OF FLOW OF WATER IN FRACTURED ROCK

2.1 Large scale flow
2.2 Flow in individual fractures

3 SOME CONCEPTS OF THE TRANSPORT AND INTERACTION OF DISSOLVED SPECIES IN FRACTURED ROCK

3.1 Dispersion and channeling
3.2 Matrix diffusion effects
3.3 Sorption and other interactions
3.4 A quantitative illustration of matrix diffusion effects
3.5 Impact of channeling on transport

4 EMERGING CONCEPTS OF CHANNELING

5 DATA NEEDS AND APPROACHES TO OBTAIN DATA

5.1 Availability of data

6 DIFFUSION IN THE ROCK MATRIX

6.1 Overview
6.1.1 Concept of transport in a porous rock matrix
6.1.2 Experimental approaches

6.2 Results from diffusion experiments with nonsorbing substances in crystalline rocks
6.3 Diffusion experiments with sorbing substances in crystalline rocks
6.4 Field investigations
6.4.1 A field diffusion experiment in Stripa
6.4.2 Salt water diffusion profiles in a granite block

7 FLOW AND TRANSPORT IN INDIVIDUAL FRACTURES

7.1 Laboratory experiments
7.2 Field experiments
7.2.1 Stripa 2D experiment
7.2.2 Chalk river experiments

8 LARGE SCALE FLOW AND TRACER EXPERIMENTS

8.1 Stripa 3D investigation
8.1.1 Overview
8.1.2 Experimental
8.1.3 Results

8.1.4 Evaluation and interpretation of experimental results
8.1.5 Summary of main results, discussion and conclusions

8.2 Fannay Augere investigation
8.2.1 Overview
8.2.2 Experimental
8.2.3 Conceptual model
8.2.4 Interpretation of hydraulic information
8.2.5 Interpretation of tracer information
8.2.6 Discussion and conclusions

9 REFERENCES

10 NOTATION

1 BACKGROUND AND INTRODUCTION

In recent years interest has increased considerably in the area of flow and transport in low permeability fractured rock. One important reason for this is that many countries are seriously considering to site final repositories for nuclear waste in such environments, at depths ranging from a few tens of meters for low and intermediate level waste, to 500 m up to more than a kilometer for high level waste.

There is considerably less information and experience on depths below a few hundred meters than at shallower depths. To assess if a repository is sufficiently isolated, information in several fields is needed. The flow rate and flow distribution at repository depth will strongly influence the rate of dissolution of many radionuclides. The flow paths and velocities will influence their travel time. This will in turn determine the decay of the radionuclides. Axial dispersion will dilute the species in time but also allow a fraction of the nuclides to travel faster. Channeling has the same effect. Transverse dispersion will cause dilution but also exchange species between fast and slow flow paths. For those nuclides which sorb on fissure surfaces and/or diffuse into the rock matrix, the frequency of water conducting channels and their exposed surface directly influences the contact area between flowing water and rock.

In Canada, Switzerland and Sweden large national research programs are underway to study radionuclide transport in crystalline rocks. Finland also intends to site their repository in similar rocks and has a research program directed towards this end. Other countries, France, Japan, Spain, the United Kingdom, and the USA, have or have had research programs oriented towards crystalline rocks. In addition an international field research program organized by the OECD/NEA in the Stripa mine in Sweden is in its third phase.

The investigations are aimed at assessing the long term safety of nuclear waste repositories where the time scales involved range from hundreds of years to many millions of years because of the very long half-lives of several of the radionuclides. The research is aimed at understanding the processes involved which determine the flowpaths and the flowrates of water in fractured rock masses. Also and at least as important is to assess the release rates, the transport capacity, and rate of transport of the radionuclides. The solute transport is very much affected by the chemistry of the waters and by reaction processes involving exchange of dissolved and suspended species with the rock in contact with the mobile water.

The water moving in the fractures in the rock may transport dissolved species such as radionuclides from a repository for radioactive waste. The assessment of how much and at what rate the nuclides are carried by the moving water is usually based on calculations of the flow rate of the water in the rock, its velocity, pathways and on the retardation of the radionuclides by physical and chemical interactions with the rock.

In three recent safety analyses for nuclear waste repositories KBS–3 (1983) in Sweden, NAGRA (1985) in Switzerland and SFR (Neretnieks 1988) in Sweden the water flow rate calculations were based on conventional hydrological models applying Darcy's law to a medium which was assumed to be well described by a porous medium equivalent. The results from such calculations were flow rates and pathways in all parts of rock included in the model.

The flow rates and flow paths were used in the transport models. These models describe the movement of the radionuclides with the water. The radionuclides do not, however, move with the velocity of the water in general. Their velocity will deviate from the average velocity because of variations in the water velocity and the mixing of different portions of the water. Some portion of the nuclides may move faster and some slower than the average velocity because of these processes which are summarized in the term "dispersion". In extreme cases when the pathways are few and far between some fast pathways may dominate the transport process. This is sometimes called "channeling".

Most of the nuclides are expected to be cat-ionic or neutral in the waters present in the crystalline rocks investigated. They will adsorb and/or ion-exchange on the negatively charged surfaces of the rock minerals. These processes may considerably retard the radionuclides which in some instances are expected to move many orders of magnitude slower than the water. For a given flow rate the retardation will be larger for a nuclide if there are more exposed surfaces with which the nuclides interact. One of the crucial questions thus is how much fracture surface the flowing water encounters. In addition to interaction with the fracture surface, the radionuclides may diffuse into the rock matrix and sorb onto the inner surfaces of the rock matrix. The inner surfaces are much larger (many orders of magnitude) than the fracture surfaces in contact with the flowing water. If the inner surfaces are accessed, the retardation may increase considerably.

It is usually implicitly assumed that the fractured rock even at depth is sufficiently fractured to allow an averaging to be performed of the properties in a volume of rock such that it is meaningful to assign an average value of the property to a "point" in the rock. The properties of interest for *flow* are the hydraulic conductivity and the porosity. The size of the volume over which the averaging is performed is called a "Representative Elementary Volume"- REV. This is the basis for the continuum models. It is implicitly assumed that the REV is considerably smaller than the rock volume studied. Darcy's law is used together with the appropriate boundary conditions to calculate the flow rate and flow directions in "all" points in the rock mass of interest. Known variations of properties in space, such as the presence of fracture zones and other large scale features are readily included. In principle only the amount of available information and the size of the computer limits the amount of detail which can be included in the model calculations. Having thus obtained a detailed map of the flow rates, flow paths and if needed the actual flow velocities, this information is then used directly in the transport models. This was done in KBS-3 (1983) and Nagra (1985).

When there is channeling the flowrates in the different pathways are assessed and the transport calculations can be done for the individual pathways. This approach was taken in the SFR (Neretnieks 1988) repository for low and intermediate level reactor waste where the site was shallower and the flow paths shorter.

This report starts by giving an overview of some concepts of flow and transport in fractured rock which have not yet become textbook material. It is based on general observations and large scale field investigations. Some general features of fractured rocks are discussed in relation to flow and transport of solutes. These concepts and ideas have formed a background when designing many of the experiments that will be discussed later. Thereafter some recent laboratory and field experiments are described and their interpretation is discussed in relation to the concepts discussed earlier. The experiments described have been selected because they have given new insights or data. Several other experiments are mentioned briefly only.

2 SOME CONCEPTS OF FLOW OF WATER IN FRACTURED ROCK

2.1 Large scale flow

The flow in large volumes of fractured rock is usually assumed to take place in a pseudo homogeneous porous medium. Darcy's law is often assumed to be valid also in sparsely fractured rock. The scale at which a fractured rock has enough fractures to become representative of the rock mass will depend on the frequency, orientation, length, other geometrical properties and permeability of the individual fractures and fracture clusters.

Recently five potential sites for a spent fuel repository were investigated in Sweden in great detail (KBS-3 1983). They cover gneissic and granitic rocks. Aerial photographs and geophysical measurements were used to locate fracture zones over areas on the scale of tens of kilometers. On the more local scale tens of bore holes intersecting the fracture zones were used for mapping them in depth and for obtaining fracture and hydrological data. The widths of the fracture zones range from a few meters to several 100 meters.

It was found that rock blocks between fracture zones of the order of several cubic kilometers could be found in which a repository could be sited. Rock blocks with a horizontal projected area smaller than a square km were not uncommon whereas considerably larger blocks seem to be scarce. Figure 2.1 shows the interpreted fracture zones around the Gideå site and Figure 2.2 shows a more localized view of the same site. The other sites are similar as regards fracture zones. Up to 15 deep (app. 700 m) diamond drilled holes were investigated in each site in addition to many shallower holes (app. 100 m). Fracture mapping of the cores show fracture frequencies varying between less than 1 and 4 fractures per meter at depths below a few hundred meters. This includes closed fractures. Double packer tests at distances of 5 and 10 m and in some holes at 2-3 m, show that only a fraction of the visual fractures are conducting water. At the Finnsjön and Sternö sites the distance between water conducting fractures below 200 m was between 5 and 10 m. This includes all fractures where even the lowest conductivity (above the measurement limit) was obtained. Fractures and fracture zones with high conductivities have been found at the largest depths. Similar observations have been made in deep boreholes in Switzerland which reach down to more than 1500 m (Nagra 1985). Because of thick sedimentary overburdens in the Swiss investigated sites surface mapping has not been possible.

Figure 2.3 shows a plot of hydraulic conductivity data from Kamlunge (KBS-3 IV). The hydraulic conductivities of the fracture zones were about an order of magnitude higher than that of the rock mass.

Within the STRIPA project (Abelin et al 1987), the 3D migration study has recently been finished. In this study tracer movements in a larger rock mass are observed. For this purpose a drift, 75 m long with two side arms 12.5 m each, has been excavated at the 360 m level in the granitic rock of the rock laboratory. The rock is saturated with water and there is a natural inflow of water to the drift. This experiment will be described in more detail later. At present just some observations which support the general concepts are outlined.

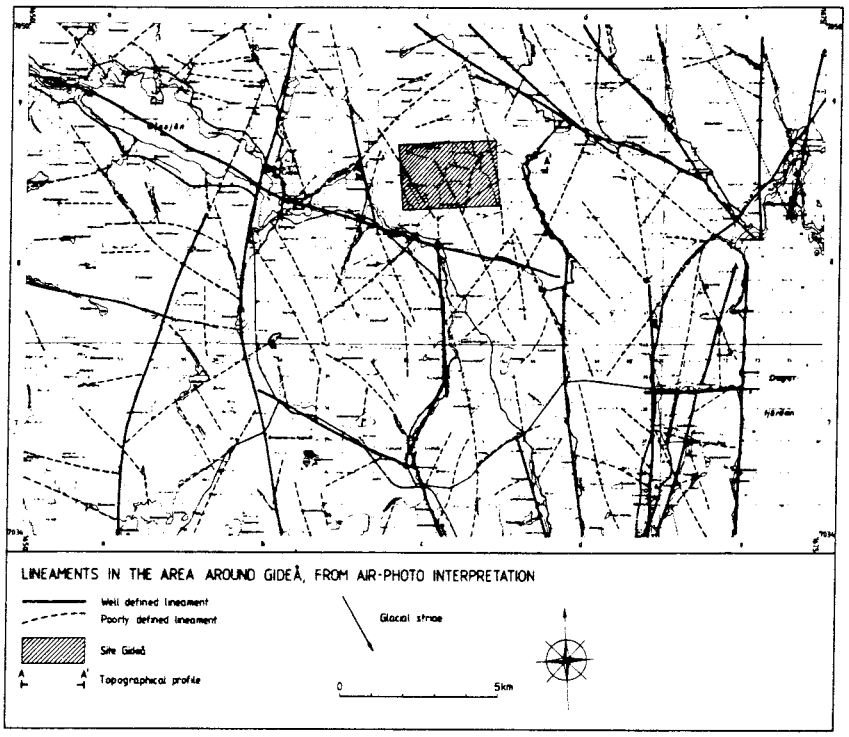

Figure 2.1 Interpreted lineaments in the area around Gideå.

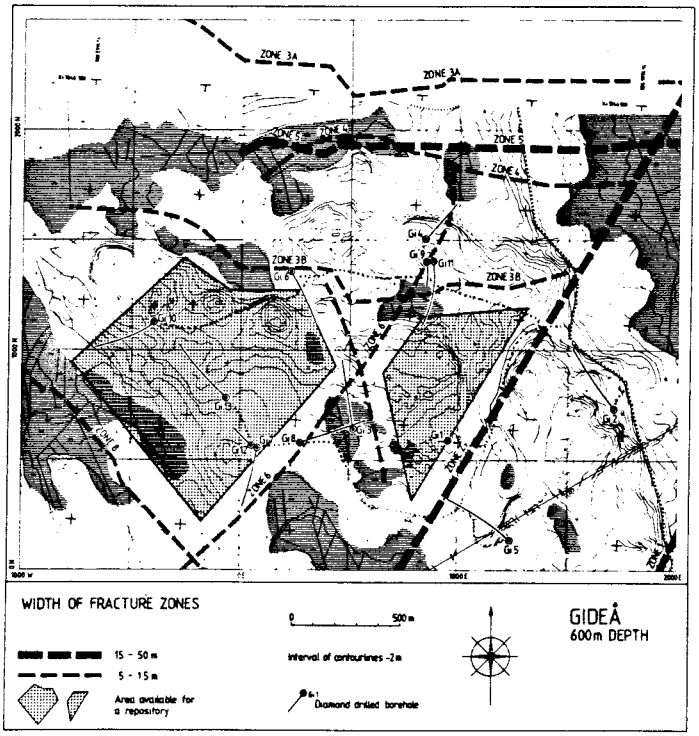

Figure 2.2 Location of fracture zones at 600 m depth in Gideå. Available area for possible repository at 500 and 600 m depth is indicated.

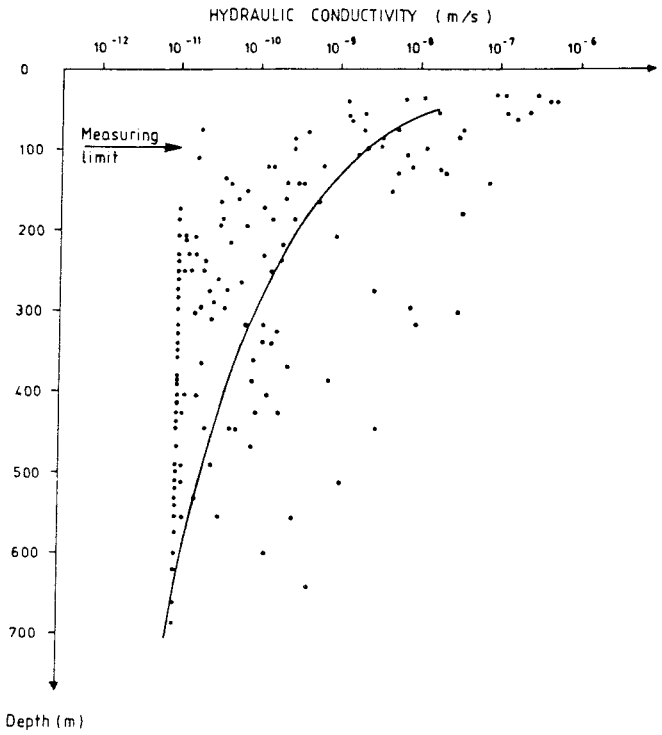

Figure 2.3 Correlation between hydraulic conductivity and depth for the rock mass.

The natural flow to the upper half of the drift has been monitored in considerable detail by gluing on approximately 375 plastic collector sheets about 2 m x 1 m in size. The water flow seeping into every sheet is monitored. The water flow was found to be very unevenly distributed over the 100 m long drift sections, covering a monitored area of more than 800 m. The total flow rate is less than 1 l/h. A third of the water flow takes place in about 2 % of the area covered. In about 70 % of the area no water flow has been found to take place.

A similar large scale flow and tracer experiment in central France at Fannay Augere was performed in a much more permeable rock than in Stripa (Cacas et al. 1990a,b). The length of the tunnel section used for the experiments was 100 m. The tracers arrived in three distinct locations in that section.

2.2 Flow in individual fractures

The flow in individual fractures is often assumed to be like flow between two parallel smooth plates. The relation between flow and pressure gradient will then be governed by the "cubic law". This has been experimentally shown for fresh fractures in granite (Witherspoon et al, 1980). Many natural fractures are old and weathered, filled with precipitated minerals or clays and cannot be expected to obey the cubic law. The pressure drop may more be determined by the physical size of the infilling material.

Analysis of tracer experiments between two boreholes in crystalline rock in three different experiments in Sweden indicate that the equivalent smooth plate fracture opening is different from that obtained from the residence time data of the conservative tracers. (Moreno et al 1983, 1989).

Similar results were obtained by analyzing flow and solute movement in three different natural fractures intersecting tunnels in the granite in the Stripa mine (Abelin et al, 1985). In this investigation it was also found that the same fracture when intersected by boreholes as close as 0.5 m distant had very different hydraulic properties. These observations indicated that the the fractures were closed or very tight (mostly) with less frequent open parts between the areas where the two fracture surfaces are in contact.

Observations in drifts and tunnels strengthen this impression. (Neretnieks 1987a,b).

The observed preferential pathways in a fracture plane may have several causes. In a fracture which has uneven surfaces, and where the aperture varies, the water will seek out the easiest paths for the prevailing gradient. The paths will change as the direction of the gradient changes. (Tsang et al. 1988, Moreno et al 1988) Such paths may be clogged or opened by chemical and erosion processes so that they are permanented in the fracture plane. Such chemical changes are frequently observed in old crystalline rocks where often several generations of fracture filling materials are found. Prominent dissolution channels have been found in fracture zones in Switzerland (Nagra 1985). In two investigations (Neretnieks 1987a, Abelin et al 1987 SFR) it was found that fracture intersections often make up high flowrate conduits.

Fracture zones have so far not been investigated in the same detail as the regular rock mass. There are indications that some fracture zones may have very variable properties (KBS-3 1983, Black et al 1987). On the other hand in an experiment in a very prominent and very highly conductive fracture zone at Finnsjön in Sweden the hydraulic properties were within an order of magnitude in several bore holes (Ahlbom and Smellie, 1989).

An ongoing investigation in Stripa aims to specifically measure the hydraulic conductivity variation in fracture planes on the scale of 2 m. First results (Abelin et al 1988) indicate that there are very strong variations in conductivity in the plane of the fractures.

The form of the channels and specifically the contact surface between the mobile water and the rock is of prime importance for the interaction of dissolved species with the rock. The interaction may be purely physical such as physical adsorption and diffusion into the rock matrix of solute molecules or it may be chemical such as ion exchange or precipitation.

3 SOME CONCEPTS OF THE TRANSPORT AND INTERACTION OF DISSOLVED SPECIES IN FRACTURED ROCK

Solutes which are dissolved in water will be carried by the moving water but will also move independently by various other mechanisms. The small molecules or ions diffuse in a concentration gradient and can move from one "stream tube" to another. Different water volumes move with different velocities and may mix at more or less regular intervals. A regular type of mixing may be described as a random process of the same type as molecular diffusion and is often described as such by the so called Fickian dispersion.

With only advection and dispersion active, the classical advection-dispersion equation results. It has been used extensively to describe tracer movement in porous media. It is easily modified to account for instantaneous chemical reaction with linear or nonlinear equilibria and can also easily accommodate reaction rates. The same equation can be used also to describe transport in parallel slits and in channels.

Ideally, hydrologic tracers are not supposed to react chemically with the solid material, but some naturally occurring tracers, e.g. C-14 does, and the effect cannot be neglected. Also in cases where it is of interest to describe the movement (and retardation) of reactive species e.g. chemical waste and many radionuclides, the chemical reactions are an integral part of the problem. In field experiments kinetic effects often influence the results and must be accounted for in the interpretations.

The dissolved species may also experience kinetic effects due to physical processes. One such process which may have a very large impact for solute transport in fractured rock is the diffusion in and out of zones with so slowly moving water that it for practical purposes can be assumed to be stagnant. Such stagnant zones can be expected in fractures with uneven surfaces and with fracture filling materials. In rocks with a connected matrix porosity the accessible pore volume of the matrix can be very much larger than the mobile water volume in the fracture. The species which has access to the pore water will then have a residence volume and residence time determined by the sum of the water volume in fractures with flow and the water volume accessed in stagnant areas. As the stagnant zones are reached by diffusion the volume of stagnant water accessed is dependent on the residence time of the flowing water. Rock fractures often seem to have preferential channels where the water flows. Channels in the same fracture may not meet and mix their water over considerable distances. The mixing required for the process to become one of hydrodynamic dispersion in the sense that it may be modelled as a Fickian process, may not be sufficient over the distances of interest. The situation may then be better described as stratified flow or channeling.

The properties of the medium can vary considerably in crystalline fractured rock. Fracture apertures and thus the transport capacity of the individual fractures are known to span several orders of magnitude. The porosity of and diffusivity in the rock matrix has similar variability. Fracture coating and filling materials also may vary considerably as to type and amount. In fracture zones the block sizes vary from very small particles up to blocks of considerable size. The size of the blocks will strongly influence the amount of stagnant volume accessible at a given contact time.

The details of the mathematical formulations or their solutions will not be discussed here. These have been discussed in some detail in the literature (Neretnieks, 1985). Instead some potential effects of channeling, matrix diffusion and sorption, will be discussed in more detail.

3.1 Dispersion and channeling

The advection-dispersion formulation implies that the dispersivity D_L is constant independent of the distance. This is expected to be true for large distances when the fluid in the different fractures has been repeatedly mixed. In fractured rock at depths larger than a few hundred meters the fissures are far apart and long distances are needed for mixing. As long as the channels do not intersect or only few of them intersect and incomplete mixing has taken place, the transport may not well be described by an advection-dispersion model with constant dispersivity D_L. Most tracer experiments in fissured rock have been performed over distances less than 50 m which may not be sufficient for frequent mixing.

The impact of the matrix diffusion for short residence time experiments should be small if laboratory diffusion data on crystalline rock are used for the estimation. In the Finnsjön field test (Moreno et al 1983) the condition of the fracture surface is not known. The regression analysis of the breakthrough curve indicated that the matrix diffusivity was much higher than that of intact granite. The matrix diffusion would account for most of the pulse spreading if the fissure surfaces are more porous than the granite further away from the surface. Experiments in granite at Studsvik in Sweden (Landström et al, 1978) over 22 and 51 m distance were reported to give dispersion lengths of 6.1 and 7.7 m respectively when matrix diffusion is not accounted for. Webster et al (1970) reported a dispersion length of 134 m for a migration distance of 538 m in fractured crystalline rock. The analysis does not account for matrix diffusion effects. Lallemand-Barres and Peaudecerf (1978) report on a confidential study in granite where a dispersion length of 0.8 m was obtained over a 11.8 m migration distance. Gelhar (1987) compiled a number of investigations which give dispersion data of varying quality. Some of these investigations were performed in fractured rocks. These data also indicate that the dispersion coefficients increase with travel distance.

Figure 3.1 shows some data on dispersion (Neretnieks 1985). The dispersion length increases with migration distance. This compilation of data is approximate because different methods have been used to determine the dispersivity.

An apparent increase in dispersion length can be caused by channeling and by various interaction mechanisms with the rock - e.g. matrix diffusion. Neretnieks (1983) has investigated a pure channeling model and shown that when pure channeling occurs, the apparent dispersion length is proportional to distance and never becomes constant. In the same work it is also shown that matrix diffusion may contribute considerably or even totally dominate the spreading of a tracer pulse when contact times are long. A large dispersion may dilute a contaminant plume and it has been argued that low dispersion cases therefore are of larger interest as the contaminant then would arrive in higher concentration. For radionuclide transport this is not necessarily the case because radionuclides decay. An early arrival of some portion of the plume may not have had time to decay and although diluted may have retained a considerably higher activity than that portion of the plume which travels with longer residence time.

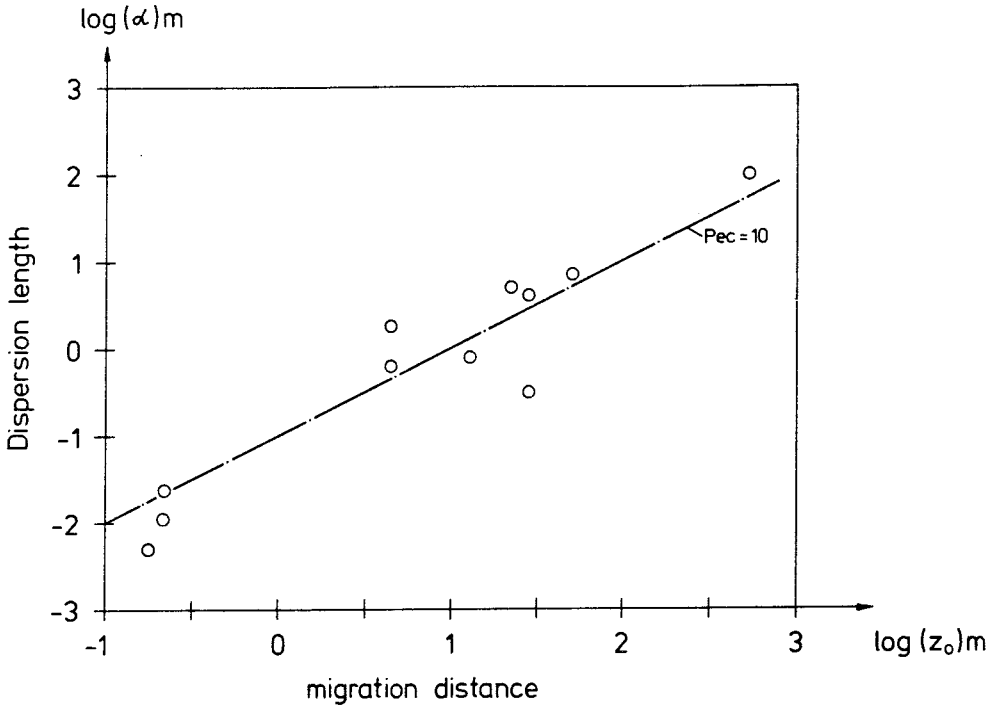

Figure 3.1 Dispersion in fractured rock as function of observation distance.

In view of the low frequency of fissures in the deeper regions of the rock, it is not clear that the mixing between channels is frequent enough to let the dispersivity become constant and independent of distance before the flow intersects fractures or fracture zones with other properties.

The non-connected channel models will not account for mixing between channels. In a recent model (Cacas et al. 1990a,b) the fractures are assumed to have channels connecting the centers of two intersecting fractures. The fracture network will, from the flow and transport point of view, form a network of connected tubes. This approach permits the channels to mix their water at intersections and can thus bridge the difference between an advection-dispersion concept and that of non-interacting channels. For the calculations of tracer transport the volume of the channels is needed in addition to the hydraulic properties. For interacting species also the contact surface must be known.

In other fracture network models the whole fracture plane is assumed to be available for the mobile water (Long et al 1985). Other approaches have also been used where the individual fracture is made up of regions with different apertures (Tsang et al 1988) Such fractures can then be combined in networks (Robinson 1984, 1986, Derschowitz et al 1985).

There has been a lack of data to test the various model concepts.

3.2 Matrix diffusion effects

Most rocks, even dense crystalline rocks, such as granites and gneisses, have microscopically small fissures between the crystals. These fissures comprise an at least partly interconnected pore system containing water. Small molecules are much smaller than the microfissures and can diffuse in and out of this pore system. The inner surfaces in the rock matrix are many times (thousands and more) larger than the surfaces in the fractures in which the water flows. The water volume in the microfissures is often much larger than the water volume in fractures. Over a long time scale molecular diffusion may play an important effect to exchange solutes between the mobile in the fractures and the stagnant or near stagnant water in the interior of the rock matrix. Cathles (1974) found in a field tracer experiment that the small molecule chloride did not arrive in the monitoring hole when colloidal silica particles did. This was interpreted as an effect of matrix diffusion where the small molecule was taken up by the porous matrix whereas the colloids with a much smaller diffusivity did not.

Gneisses and granites in Swedish Precambrian rock have been found to have a continuous pore system consisting of the microfissures between the crystals in the rock matrix. The porosity in this pore system varies between 0.06 % and 1 % (Skagius and Neretnieks 1986a) for the rock matrix. Similar results have been obtained by other investigators Brace (1965) and Bradbury (1982), Nagra (1985), Fracture minerals and rock in crushed zones have higher porosities. Values between 1 and 9 % have been measured. Substances dissolved in the water can diffuse into this pore system and sorb on the inner surfaces. Figure 3.2 shows the concept of penetration and sorption in the porous rock matrix.

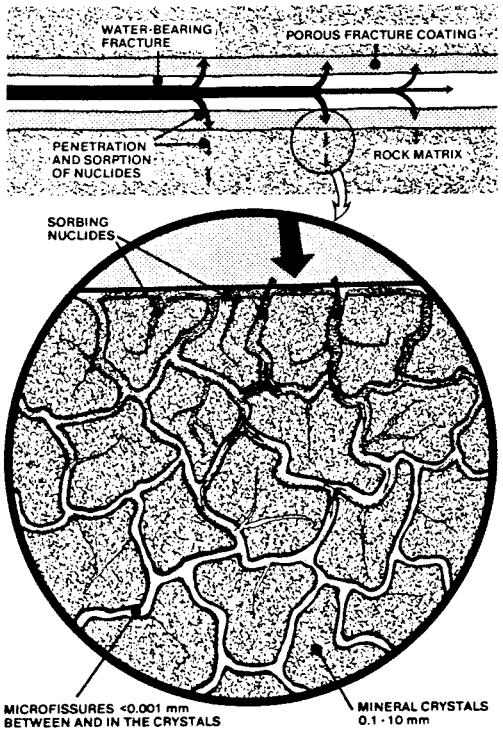

Figure 3.2 The figure shows the penetration and sorption of nuclides in the microfissures in the rock matrix.

The penetration depth increases with time. Non-sorbing species penetrate far into the matrix, while sorbing nuclides are retarded since they also have to fill up the sorption sites before they migrate further.

The penetration depth can be calculated with the aid of Fick's laws for diffusion, if the diffusivity is known, and by taking retardation due to sorption into account.

The size and form of the contact area will have a strong influence on the rate of interaction between the solutes and he rock matrix. Studies have been performed where the rock has been modelled as blocks or spheres of equal size, as blocks of unequal an irregular sizes and as circular or banded channels (Neretnieks and Rasmuson 1984, Rasmuson and Neretnieks 1986a,b). The rate of interaction was found to be primarily depending on the size of the wetted surface but also on the form of the blocks and channels in cases where the range of diffusion is larger than the channel dimensions.

3.3 Sorption and other Interactions

The minerals of crystalline rocks have a considerable cation exchange capacity. They also exhibit a capacity to form surface complexes with anions as well as cations. The capacity to bind different ions to the surface depends on the pH, the concentration of many of the other ions and on the form the species have in the solution. Many cations form complexes with the anions and other complexing agents in the water. The complexed metal ions which would have a positive charge if not complexed, may be positively charged, neutral species of even negatively charged species, depending on the composition of the water.

The component may be bound (adsorbed, ion exchanged) to the surface of the minerals of the rock, or it may form its own minerals by precipitation. It may also react irreversibly by mineralization into some very stable solids.

The different complexes will of course have different affinity to the mineral surfaces. Because of the complexity of the situation it is often convenient to summarize all the effects into a term "sorption coefficient" or K_d. This expresses how much of a component is bound to the surfaces of the rock and how much is in the water at equilibrium. One neglects which form (complexed or non-complexed) the various species containing the component have in the solution as well as in the bound state. K_d is the ratio of concentrations of the component in the two phases.

The component may simultaneously be a part of several species (complexes) which are sorbed in different ratios. K_d often varies very much with changes in the composition of the groundwater (pH, Eh, concentration of complexing agents etc.). It is therefore a very imprecise entity but because of its simplicity it has been found to be very useful in mathematical modelling and in transferring information from chemists to modellers.

Adsorption and ion exchange are often summarily called sorption and then denote fast reversible reactions of the dissolved components with the surface of the rocks. These processes are treated by the K_d-concept. Processes such as precipitation and irreversible mineralization are usually treated as such.

3.4 A quantitative illustration of matrix diffusion effects

The well known advection-diffusion equation is shown in equation (3.1). To it has been added a fourth term which accounts for the exchange of the solute with the matrix of rock by diffusion over the fracture surface. The fourth term consist of three parts. The concentration gradient in the matrix, the effective diffusivity in the matrix D_e and the surface to volume ratio, a, of the fracture surface in contact with the mobile water to the volume of the mobile water in the rock. The equation can be applied to a variety of cases with different geometries including flow in a porous medium with porous particles, flow in a fracture in a porous rock where the water in the rock matrix is stagnant, flow in channels etc.

$$\frac{\partial C}{\partial t} = -u_f \frac{\partial C}{\partial z} = D_L \frac{\partial^2 C}{\partial z^2} + a D_e \frac{\partial C_p}{\partial x}\Big|_{x=0} \qquad (3.1)$$

The movement by diffusion in the rock matrix is shown in equation (3.2). The right hand term contains the apparent diffusivity D_a which for diffusion in the pore water can be expressed as the ratio of the pore diffusivity D_p to the retardation coefficient R_d which accounts for sorption effects.

$$\frac{\partial C_p}{\partial t} = \frac{D_p}{R_d} \frac{\partial^2 C_p}{\partial x^2} = D_a \frac{\partial^2 C_p}{\partial x^2} \qquad (3.2)$$

R_d depends on the sorption coefficient K but also to a very large extent on the matrix porosity which for small values may make the retardation coefficient (equation 3.3) very large.

$$R_d = 1 + K (1-\varepsilon_p) / \varepsilon_p \qquad (3.3)$$

It has been shown (Neretnieks 1980) that for long contact times the matrix diffusion will have an important impact on the mobility of sorbing solutes and that also nonsorbing solutes such as tritiated water would potentially move considerably slower than the water velocity, making it difficult to utilize natural radionuclides to assess the water velocity (Neretnieks 1981). It was shown by Neretnieks (1980), Rasmuson and Neretnieks (1980) that for long contact times the velocity of the water may have an entirely negligible impact on the velocity of a solute, the velocity of the latter may be influenced only by the ratio of the flowrate of the water to the accessed sorption capacity of the rock.

These effects must be accounted for when designing and interpreting tracer tests.

To illustrate the effects quantitatively a simple example is given below based on a case where there is no hydrodynamic dispersion but only advection, matrix diffusion and sorption in the matrix. For a step injection of a solute in the stream of water flowing

in a medium with rock blocks where penetration depth is small compared to size of the blocks so that the geometry of the blocks can be approximated by flat surfaces, the solution to equations 3.1-3.3 is.

$$C/C_o = \text{erfc}\left(\frac{B\,a\,t_w}{2(t-t_w)^{1/2}}\right) \tag{3.4}$$

a is the wetted surface per volume of mobile water, B is defined in equation (3.6) and accounts for the uptake in the rock matrix by diffusion and sorption. Even if there is no sorption the uptake into the stagnant water in the matrix influences the movement of the solute as can be seen from equation (3.6) which gives B for no sorption.

$$B = (D_p \varepsilon_p (\varepsilon_p + (1-\varepsilon_p) K))^{1/2} \tag{3.5}$$

For K = 0, B becomes

$$B = (D_p)^{1/2} \varepsilon_p \tag{3.6}$$

For small porosities and high sorption B is given by equation (3.7).

$$B = (D_p \varepsilon_p K)^{1/2} \tag{3.7}$$

A simple criterion may be constructed from equation 3.4 to show when matrix diffusion becomes important as a retardation mechanism. It is formulated in the following way: "matrix diffusion is important when for a step input the resulting breakthrough curve has a C/C_0 equal to 0.5 at double the water residence time t_w". The argument in equation (3.4) is 0.477 for the left hand side to become 0.5 and so it is found that for $t_w = 0.91/(B \cdot a)^2$ matrix diffusion will become important.

Figure 3.3 shows the responses to a finite pulse, calculated by the advection-dispersion equation and by the advection-dispersion-matrix diffusion equations for a case with water residence time 1 year. Rock property data typical for Swedish granites have been used. The responses differ considerably. If in a field experiment the matrix diffusion curve was evaluated using the advection-dispersion model, erroneous water residence times and dispersivities would be obtained. The use of the obtained data and the advection-dispersion model for extrapolation to other cases might give very misleading results. Malozewski and Zuber (1985) have arrived at the same conclusion.

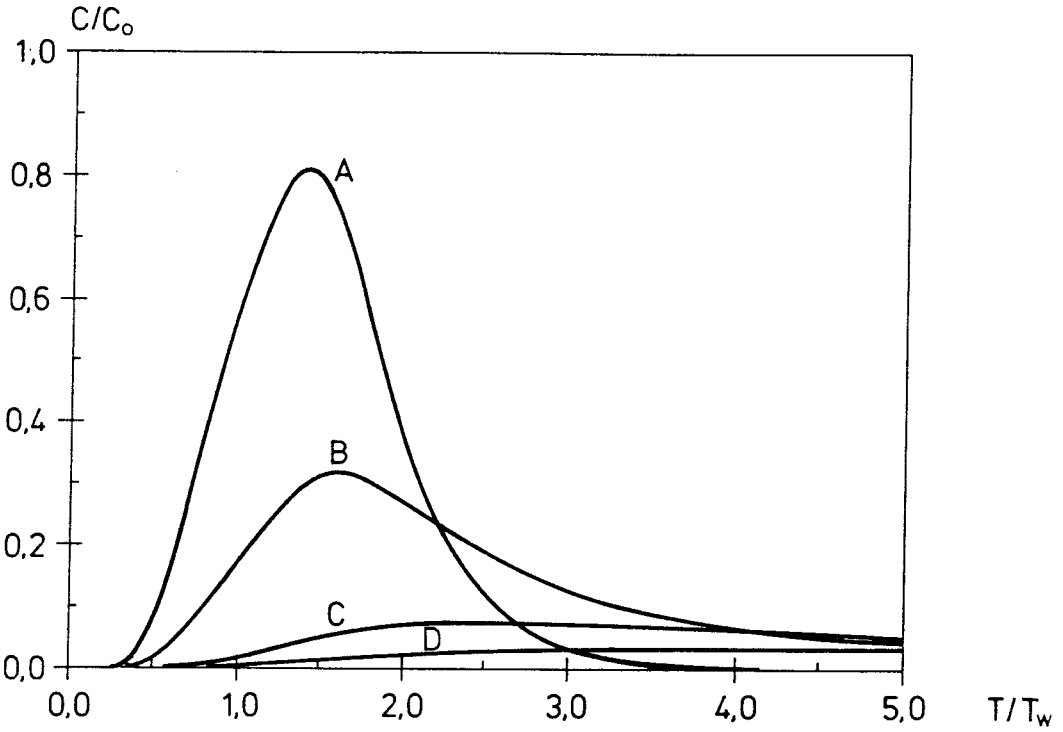

Figure 3.3 Response to a pulse in a 0.1 mm fracture. Influence of porosity and diffusivity. A: No matrix diffusion, B: $D_p=2.5\cdot10^{-11}$ m^2/s, $\varepsilon_p= 0.002$. C: $D_p=4\cdot10^{-11}$ m^2/s, $\varepsilon_p= 0.005$. D: $D_p=10\cdot10^{-11}$ m^2/s, $\varepsilon_p= 0.002$. Water residence time and injection pulse duration are 1 year.

3.5 Impact of channeling on transport

For media with largely unconnected channels the advection-dispersion equation may not be a good descriptor in the sense that the "dispersivity" of the overall system is governed by velocity differences between channels and not by the attenuating influence of mixing, although the transport in the individual channels may still be well described by the advection dispersion model. Radionuclides transported in fast channels which mix their water little or not at all with other channels will have shorter time in which to decay. In fast channels there will also be less time for the species to diffuse into the matrix. This may have quite strong effects as was found in a recent analysis of potential radionuclide migration from a repository for low and intermediate waste (Neretnieks 1988).

4 EMERGING CONCEPTS OF CHANNELING

The notion of channeling seems to be very old. It has, however, very seldom been described in the hydraulic literature. To water well drillers, miners and other underground workers it is well known that the water flow is unevenly distributed in the rock and that often unexpected "channels" are encountered when mining a new drift.

Below we describe some emerging concepts of channeling in an individual fracture.

A fracture is made up of two surfaces which are wavy and rough. The two surfaces are in contact with each other in some points but are at a distance from each other at other points. The openings in the fracture are potential channels. These are only potential conduits because they have to be connected to other open sections in order to form a continuous network.

When a hydraulic gradient is imposed over a fracture with variable aperture the water will seek out the easiest pathways. If there is a random but large variation in the transmissivities in different places, the water will seek out a tortuous path, always avoiding those sections where the transmissivity is low. In such a case most of the water may choose to flow along one path because this is the path with least resistance for that specific gradient.

Recently several model studies have been made on flow and transport in fractures with variable apertures (Smith et al 1987, Moreno et al 1988, Tsang et al 1988. Although based on very limited field data, the results indicate that considerable channeling is to be expected in such fractures.

It is possible that the flowing water will influence the transmissivity of the pathway in several ways. The pathways may be clogged due to filtering of particles or due to precipitation of minerals, or they may become larger due to erosion and dissolution. New pathways may open up due to small shearing movements in the fracture. All of these processes are known to occur. There are also several observations which indicate that fracture intersections form easy pathways (Abelin et al 1987, Neretnieks 1987b, Moreno and Neretnieks 1988).

The models indicate that here is a tendency for some pathways to carry much more water than others. In the limit one or a few pathways will dominate. Mixing between the pathways would be small and a tracer introduced in one channel may not reach the other channel even after considerable travel distances. There will then be distinct channeling from the transport point of view.

There are very few observations of channeling in a fracture plane (Bourke 1987, Abelin et al 1987,1988). Even less is known of what happens at fracture intersections. When fracture planes intersect, a channel may either connect to a closed or practically closed portion in the other fracture or to some open portion. In the latter case the channel will continue over more than one fracture. At fracture intersections several distinct possibilities exist. The fracture intersection may act as a conduit effectively connecting all channels from one fracture to the other. Another possibility is that the intersection has no properties of its own, so that if a channel from one

fracture does not meet a channel in the other fracture, there is no connection. A third possibility also exists. The fracture intersection has a low transmissivity effectively controlling (or hindering) the flow from one fracture plane to another.

In the first case there will be mixing "pools" at every fracture intersection. This will tend to average out concentration differences between channels. In the second case there will be considerably fewer channels which are connected from fracture to fracture. There will be a tendency that the more fractures that are involved the less channels will traverse them all. In the latter case there will in the limit be no water flow.

There is no information available today which would make it possible to distinguish between the cases. Probably all three cases exist in real rocks. It is more a question of how frequent the cases are.

When there is no mixing between channels they can be treated as a bundle of individual conduits. It would then be sufficient to characterize the properties and the variation of the properties of the channels. With such information it would be possible to statistically generate a (or many) bundle of channels and investigate their flow and transport properties. This is a very attractive notion because channels are essentially one dimensional features from the flow and transport point of view. It would in this case not be necessary to make 2-dimensional, much less 3-dimensional calculations of water flow and transport. A series of simple 1-dimensional calculations would suffice. This has been explored by theoretical calculations (Neretnieks 1983, Tsang et al 1987).

It is probably not possible to make such a radical simplification but it is non the less a very interesting approach because it is so simple and has so attractive properties. It is also probable that the fewer and the more widely spaced the channels there are the better such an approach is. It would also be possible, that if there are only few mixing points along the flowpath, to use the recently developed mixing rule methods (Rasmuson 1985) to determine the impact of mixing on the transport in a bundle of channels.

5 DATA NEEDS AND APPROACHES TO OBTAIN DATA

In the table below the most important data needed for assessing radionuclide escape rates to the biosphere are indicated and commented. Importance of the mechanism and data is based on experiences from the safety analyses: KBS-3 (1983), NAGRA (1985), SFR (1987) and WP-Cave (1988). The indicated importance may not be generally applicable for repositories of vastly different design.

Table 5.1 Data needed for radionuclide transport modelling.

Variable		Importance for near field	Importance for far field Nonsorbing	Sorbing
Q	Flowrate of water	**VL**	**VL**	**VL**
u	Water velocity	VL	VL	Negl
z	Travel path length	-	**VL**	**VL**
D_L	Hydrodynamic dispersion*	-	L	S
D_e	Diffusion in rock matrix	-	S	**VL**
K_d	Sorption in rock matrix	**VL**	-	**VL**
a	wetted surface	S	S	**VL**
Redox conditions, pH, complexing agents		**VL**	-	**VL**
Channel aperture, porosity		L	L	Negl
Channel frequency		L	S	**VL**
Channel flowrate distribution		L	L	**VL**

* in individual pathways. For overall dispersion see "Channel flowrate distribution".

VL	very large importance in the context
L	large importance in the context
S	small importance in the context
Negl	negligible in the context
-	not applicable in the context
VL	Very large importance for the over all safety assessment and final results.

5.1 Availability of data

The flowrate Q and its variability is assessed by hydraulic modelling using data on hydraulic conductivity K_p and its variations in the rock, topography and knowledge of the location and properties of fracture zones. These data are obtained by geologic and hydraulic investigations such as down hole conductivity measurements, surface mapping and by geophysical methods. Most of the investigation techniques give no detailed information on channel frequency, wetted surface, dispersivity or exchange with the matrix.

The water velocity u is obtained from Q and information on flow porosity. The latter entity is not well known for fractured crystalline rock. Good investigative techniques are lacking to determine flow porosity of large rock bodies. For sorbing nuclides in the far field this is uninteresting because it does not appreciable influence their velocity. For the nonsorbing nuclides it does not seem to be very critical in the safety assessments because the travel times are so short anyway that no appreciable nuclide decay (I-129, C-14) will take place.

The travel path length z is obtained from the hydraulic modelling and is a very important entity. It has the same impact on the radionuclide transport as the wetted surface a and flowrate Q.

The hydraulic dispersion D_L is not well understood for fractured rock. The dispersivities evaluated from available field tests seem to increase with distance which should rule out the use of the advection-dispersion model. The model is often used anyway to mimic the dispersion behavior. The dispersion in individual channels seems not to have a large impact. The velocity differences between channels dominate the overall "dispersion".

The flowrate, velocity and wetted surface may vary considerably between channels. The rather new concept of channeling in the context of radionuclide transport in fractured rock is far from fully understood but there are strong indications both experimentally in the field and theoretically that it may have a most profound influence on the RTD (Residence Time Distribution) of the nuclides, nonsorbing as well as sorbing. For the latter, channeling is very important because channels with high flowrates may have a very small wetted surface relative to the flowrate in the channel.

No well tested and accepted methods exist at present to investigate channeling.

Sorption on the minerals of crystalline rock has been much studied. There is a fair understanding of the processes involved and the confidence in the data is reasonably large. The uptake in the rock matrix by diffusion in the micropore waters is fairly well understood except the surface diffusion for some nuclides. Practically all investigations have been performed in the laboratory and there is a need to confirm the findings on the field scale and under natural stress and chemical conditions.

The matrix diffusion and sorption on the inner surfaces of the rock is the by far most important retardation mechanism for the sorbing nuclides. The sorption of the nuclides on fracture filling and coating materials is practically negligible compared to the sorption in the matrix. This is because there is so much more material to sorb on in depth in the matrix as compared to the thin layer on the surface.

Redox conditions, pH, and the presence of complexing agents very strongly influence the solubility and sorption properties of the nuclides and thus directly influence the nuclide mobility. The minerals in the rock such as ferrous iron minerals, silica and carbonates will play a dominating role in determining the water chemistry. The iron minerals for example which are abundant in the matrix of the rock may neutralize even quite large disturbances caused by the intrusion of surface waters or due to radiolysis.

Most of the data on these phenomena have been obtained in the laboratory and there is a clear need to make field experiments and observations. Transport modelling using coupled geochemical and transport models will play an important role to interpret the experiments.

The channel aperture and porosity influences the migration of the nonsorbing nuclides but this seldom influences the maximum rate of escaping nonsorbing nuclides because the important ones will not have time to decay anyway.

The channel geometry and the wetted surface have a very strong influence on the RTDs of the sorbing nuclides. The wetted surface has the same influence as the flowrate in a channel and as the travel distance.

Very little is know at present on channel geometry and wetted surface. Some first investigations have been made but there is a large need for both more field observations, investigations as well as theoretical deliberations.

The channel flowrate distribution has a very strong influence on the RTD of the sorbing nuclides. Not only does a channel with a high flowrate carry a nuclide in large amounts. It may also have a small surface to sorb on and from which the nuclide may diffuse into the matrix. A "fast" channel may then allow a certain portion of the sorbing nuclide to be little retarded by the sorption because the flowrate of water is large compared to the wetted surface in this channel.

Very little is know at present on channel flowrate distribution. Some first investigations have been made but there is large need for both more field observations, investigations as well as theoretical deliberations.

Available information suggests that the variability of flowrates and wetted areas may sometimes be more important than the level of the average flowrate along the flowpath.

The information on flowrate distribution is not normally obtained in the conventional hydraulic investigations. Special investigation methods must be developed, tested and present channeling models must be further developed.

In addition to what is said above the channel frequency has a large impact on the near field release. If there are only a few channels there may be many canisters which in practice will not have access to mobile water. On the other hand some canisters may be subjected to large flowrates if they are intersected by a channel with a high flowrate.

The views expressed above are based on the experiences of more than 10 years working with safety analyses and having had to devise and apply models for calculating radionuclide transport from repositories for radioactive waste. In the course of this work many concepts have changed as new observations and data have become available. It has been noted that a lot of effort has gone into hydraulic and geologic investigations in the field. Very little of that information has been possible to use directly when the migration of the radionuclides has had to be assessed. On the

other hand there has been a very noticeable lack of information in some areas. The wetted surface in still poorly known. The understanding of channeling is far from complete. The surface diffusion phenomena are not so well understood that it is possible to confidently predict how a solute will diffuse in the rock matrix.

To assess the transport of radionuclides those processes which are of importance for the migration of the nuclides should be put in the foreground. The hydraulic parameters make up only one part of the important parameters.

Below some recent experiments which have set out to investigate various aspects of the flow and transport in fractured crystalline rock are described.

6 DIFFUSION IN THE ROCK MATRIX

6.1 Overview

The rock matrix of even dense crystalline rocks has been observed to be porous. The porosity, if connected in depth, has a potential of acting as a sink for radionuclides and other dissolved substances in the mobile water in the fractures (Neretnieks 1980). Positively charged or neutral species will sorb on the mineral surfaces of the pores and micro-fractures of the matrix.

Matrix porosity, diffusivity in the pore waters and sorption properties of some sorbing species which do not sorb very strongly can be and are measured in the laboratory by simple experiments. If the data are to be used for predictions of transport over much larger time and space scales, however, the laboratory experiments must be supplemented by other experiments and observations. Some key issues which to varying extent have been addressed in various investigations are the following.

1 Connectivity of pore system over long distances.

2 Questions of constrictivity: Will larger molecules be less mobile than small, even accounting for the smaller diffusivity in water.

3 Effects of surface charge: Many mineral surfaces are negatively charged and may by electric repulsion "constrict" the pores for an-ions.

4 Sorption mechanisms and mobility: Are the sorbed cat-ions immobilized or are they mobile even in the "sorbed"state.

5 What influence does rock stress have on the porosity of the rock and diffusivity of the solutes.

6 Have the de-stressed samples taken to the laboratory been irreversibly changed.

7 Will fracture coating and filling material allow diffusing species to access the underlying matrix.

8 Do the transport and sorption properties change over long times.

This section will describe some of the theoretical background, techniques used and experiments performed.

6.1.1 Concept of transport in a porous rock matrix

Crystalline rocks are made up of small crystals ranging in size typically from 0.1 mm to many mm:s. There are micro fractures in and between the crystals which make up a connected pore system. Some pores are dead ended. Granites and gneisses have been found to have low hydraulic conductivity and transport by flow can usually be neglected compared to that by diffusion. Transport by flow in the rock matrix will not be discussed in this section.

When the pores of the matrix are water filled, the solutes will migrate by molecular diffusion. The movement will be restricted at narrow passages and the path length will be longer than the physical distance in the rock because the pores form tortuous pathways.

In steady state the transport will only take place in the connected pore system. During the non steady state phase the dead end pores will also contribute by acting as sinks and/sources. The dissolved solutes move by diffusion in the pore water. Sorbed species may be bound by mechanisms which make them immobile in the sorbed state and they can only move if they first are desorbed, or they may be mobile as e.g when they are attracted by diffuse electric forces which makes the water near the surface more concentrated in the "sorbed" species without actually binding them.

In steady state the transport can be described by Fick's first law

$$N = - D_p \varepsilon_t \frac{\partial C}{\partial x} \tag{6.1}$$

ε_t is the transport porosity, D_p is the diffusivity in the pore water and can be related to the diffusivity in unconfined water, D_w, by the relation

$$D_p = D_w \frac{\delta_D}{\tau^2} \tag{6.2}$$

δ_D is the constrictivity and τ is the tortuosity.

The product $\varepsilon_t . \delta_D / \tau^2$ is called the formation factor F_f.

If all solutes were influenced in the same way by the pore system, then it would suffice to measure the formation factor for one solute. This is not always the case, but F_f can still be a useful entity for comparison purposes.

When the transport is instationary and the solute accumulates, or is depleted from the pore system, Fick's second law and the law of conservation of mass is used to describe the transport and accumulation of a solute in the pore system. Assuming that transport takes place only in the water in the pores and the diffusion coefficient is constant and that the sorption is reversible, the following equation results

$$(\varepsilon + K(C)) \frac{\partial C}{\partial t} = D_p \varepsilon_t \frac{\partial^2 C}{\partial x^2} \tag{6.3}$$

ε is the total porosity including dead end pores and K(C) is the volumetric sorption coefficient which may be concentration dependent.

These equations together with the initial and boundary conditions often suffice to describe the transport and accumulation of solutes in a porous medium. For many species the sorption coefficient can be assumed to be constant.

Ion mobility in an electrical field can be used to determine diffusivity of charged solutes and is used to determine the formation factor which is directly obtained from the ratio of electrical conductivity of the solution filled sample to the conductivity of the same solution.

There are indications that some sorbed species may be mobile in the "sorbed" state (Skagius and Neretnieks 1988). This is sometimes called surface diffusion. The process is not well understood (Rasmuson and Neretnieks 1983). Then parallel to the transport in the pore water there will be transport of the sorbed species. The rate of surface transport can be written

$$N = - D_s \frac{\partial C_s}{\partial x} \tag{6.4}$$

C_S is the concentration of the sorbed substance in the solid and is in general concentration dependent. $D_s = D_s(C_s)$. As sorption is fast, equilibrium is assumed to exist between C_s and C.

$$C_s = K(C) \tag{6.5}$$

The total transport rate under steady state conditions then is the sum of the transport by pore diffusion and by surface diffusion.

$$N = N_{pore} + N_{surf} = -D_s A \frac{\partial C_s}{\partial x} - D_p \varepsilon_t A \frac{\partial C}{\partial x} \tag{6.6}$$

For instationary transport the equivalent expression to Fick's second law is

$$\varepsilon \frac{\partial C}{\partial t} + \frac{\partial C_s}{\partial t} = \frac{\partial}{\partial t} \left(D_s (C_s) \frac{\partial C_s}{\partial x} + D_p \varepsilon_t \frac{\partial C}{\partial x} \right) \tag{6.7}$$

6.1.2 Experimental approaches

Different experimental techniques are used to determine the transport properties. In the "through diffusion" experiment the rate of transport through a section of rock is monitored (Garrels et al 1974, Skagius and Neretnieks 1986a, Bradbury and Green 1985) as the solute moves from a vessel with high concentration to a receiving vessel with low concentration. The product of the pore diffusivity and the transport porosity $D_p\varepsilon_t$ is obtained. It is called the effective diffusivity D_e. The early instationary part of the experiment can be used to determine the capacity of the rock for holding the solute, $\varepsilon+K$. For nonsorbing species this is equal to the total porosity. In systems with long dead end pores, not all these are equilibrated during the early time period (Bradbury and Green 1986) This problem will decrease in thicker samples. For the time scales of interest for assessing radionuclide transport in the field, the water in the dead end pores will be in equilibrium with the transport pores.

Different solutes, both charged and uncharged and of different molecular weight have been used in the diffusion experiments. Colloids have also been used to determine their possible blocking of the pore structure (Bradbury and Green 1986). Diffusion in fracture coating materials has been measured (Skagius and Neretnieks 1984, 1986a and Bradbury and Green 1986).

The porosity can be determined by several other methods. Weighing the sample wet and dry gives the total porosity as does leaching a solute out of a previously saturated sample. Pore sizes and pore size distributions have been measured by mercury porosimetry, BET sorption and microscoping. For large samples and for sorbing solutes the through diffusion method is very time consuming and strictly instationary methods have been applied, to reduce the time. Immersion of tablets and larger pieces of rock samples in traced solutions has been used Skagius (1986). The decrease of the bath composition is then utilized to determine the transport properties and the final steady state to determine equilibrium sorption. Profiling of the samples was used by Skagius and Neretnieks (1988) to get profiles of Cesium and Strontium in granites and gneisses.

Electrical conductivity measurements of rock samples saturated with highly saline solutions have successfully been used to determine the formation factor. (Skagius and Neretnieks 1986b). This technique has been used on samples of meter lengths. (Atkinson and Titchell 1985).

Through diffusion and electrical conductivity measurements have been performed in pressure cells in the laboratory to determine the influence of stress on porosity and transport properties (Brace et al 1968, Skagius and Neretnieks 1986b, Bradbury and Green 1986 and Gilling et al 1987).

Diffusion experiments in undisturbed rock at depth under natural stress conditions have been performed in granite (Birgersson and Neretnieks 1987, Birgersson 1988) over times of more than 3 years. Attempts have also been made to measure concentration profiles of salt water intrusion in granite over time scales over 30 years in a large block immersed in salt water (Jeffries 1988).

6.2 Results from diffusion experiments with nonsorbing substances in crystalline rocks

The following section gives a more detailed description of some of the experiments with nonsorbing tracers and the results obtained.

Skagius and Neretnieks (1986a) made measurements in granites and gneisses from 8 different locations in Sweden. The samples were taken from depths down to more than 500 m. The diffusing substances used were Iodide, Cr-EDTA and Uranin. The sample thickness was 10 mm. Several of the samples were taken adjacent to fractures and had fracture coating materials.

In figure 6.1 the effective diffusivities of Iodide in the granites, gneisses and fissure coating materials are plotted versus the porosities determined by the leaching method. Results obtained by Bradbury et al (1982) for Iodide diffusion in different granites from the United Kingdom are also presented in the figures for comparison. The logarithmic mean values are marked in the figures. The effective diffusivity in the granites, logarithmic mean value = $22.0 \cdot 10^{-14}$ m^2/s and arithmetic mean value = $25.2 \cdot 10^{-14}$ m^2/s, is higher than in the gneisses, logarithmic mean value = $5.1 \cdot 10^{-14}$ m^2/s and arithmetic mean value = $9.2 \cdot 10^{-14}$ m^2/s. The mean values of the porosity determined by the leaching method are also higher for the granites, logarithmic = 0.24 % and arithmetic = 0.26 %, than for the gneisses, logarithmic = 0.13 % and arithmetic = 0.15 %.

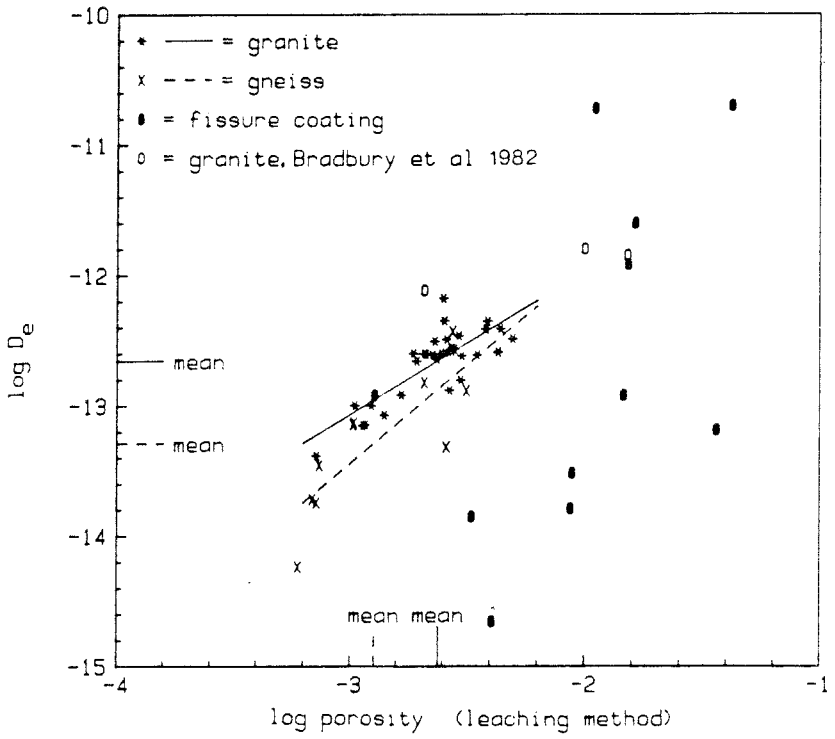

Figure 6.1 Effective diffusivity of Iodide in the rock materials versus the porosity.

Figure 6.1 also includes values for fissure coating materials. The effective diffusivity of Iodide in the fissure coating materials is of the same order of magnitude or higher than in the granites and the gneisses. Those samples that have an effective diffusivity that is of the same order of magnitude as the granites and the gneisses have, however, much higher porosity values. This could be due to a higher "storage" porosity in the fissure coating material, or to a lower pore diffusivity in the fissure coating material compared with the granites and the gneisses.

The effective diffusivities for Cr-EDTA and Uranin typically are an order of magnitude lower than those for Iodide. For Iodide, values of the formation factors were mostly in the range $1\text{-}20 \cdot 10^{-5}$, with only a few outliers, and about a factor 5 lower for the other two solutes. Skagius and Neretnieks (1986b) also measured formation factors, using the electrical conductivity method. Potassium Iodide was used as ionic conductor. Formation factors in the range $1\text{-}30 \cdot 10^{-5}$ were found with only a few outliers. Variations in porosity and diffusivity between samples taken at neighboring positions from the same core typically give values which differ by 2-3 times.

These results indicate that the electric measurement technique gives comparable results to the direct diffusivity measurements. The large difference in formation factors for Iodide on one hand and Cr-EDTA and Uranin on the other hand indicate that the latter two bulkier molecules are considerably more influenced by the pore structure.

Bradbury and Green (1985, 1986) measured diffusivities in 4 British and 1 Canadian granite using Iodide as the diffusing substance. They found effective, or in their terminology intrinsic, diffusivity values ranging from $2 \cdot 10^{-14}$ to $130 \cdot 10^{-14}$ m^2/s. Formation factors were found to lie between $1.2\text{-}\ 80 \cdot 10^{-5}$. Porosities determined from the instationary part of the diffusion experiment were between 0.06 and 1.2 %. Bradbury and Green (1985) also used technetium in the form of pertechnetate as diffusing substance and found diffusivities comparable to those for Iodide. The rock capacity factor, $\varepsilon+K$, however, was found to be considerably larger indicating that the pertechnetate sorbs or reacts somewhat in the solid.

Fracture coating materials and weathered surfaces, were found to have higher porosities and diffusivities than "good rock". The increases in diffusivity ranged from 20-200 times and the porosity from 10-100 times.

The change in transport properties with distance from the fracture surface has been measured by Skagius and Neretnieks (1986a) and Bradbury and Green (1986). In both investigations it was found that both porosity and diffusivity dropped off with increasing distance from the surface. The decrease with distance strongly depends on the degree of weathering.

Skagius (1986) measured the electrical conductivity of samples of different lengths up to 30 cm long. She found that the specific conductivity decreased by a factor of about two when the sample thickness increased from 10 mm to 50 mm and a further increase in length did not change the properties further. Atkinson and Titchell (1985) measured electrical conductivity of granite cores up to 1.25 m in length. They found very similar results.

At expected radioactive waste repository depths in the ground the rock is exposed to high stresses caused by the large overburden of rock. When drillcores are taken up from the ground this overburden no longer exists. As a result there might be an increase in the porosity of the rock samples. The effective diffusivity measured in rock samples under atmospheric pressure in the laboratory would then be higher than the effective diffusivity in the rock "in situ".

To simulate the stress that may exist in the bedrock at large depths, diffusion experiments with Iodide and electrical resistivity measurements in rock materials under mechanical stress have been performed by Skagius and Neretnieks (1986b) with stresses up to 35 MPa, and by Bradbury and Green (1986) up to 16 MPa. In the first mentioned experiment, which covered 6 different granites, the formation factor decreased 1.2 to 2 times for an increase in stress of 5 MPa and then decreased more gradually. At 30-35 MPa the formation factor has decreased by 1.6-4 times. Bradbury and Green(1986) found a faster initial decrease and a leveling off at already 5 MPa for one granite.

Figure 6.2 shows a plot of the concentration at the low concentration side versus time for Iodide diffusion through a piece from Svartboberget. The experiment was started with the piece under atmospheric pressure. After 35 days the pressure was increased to 33 MPa.

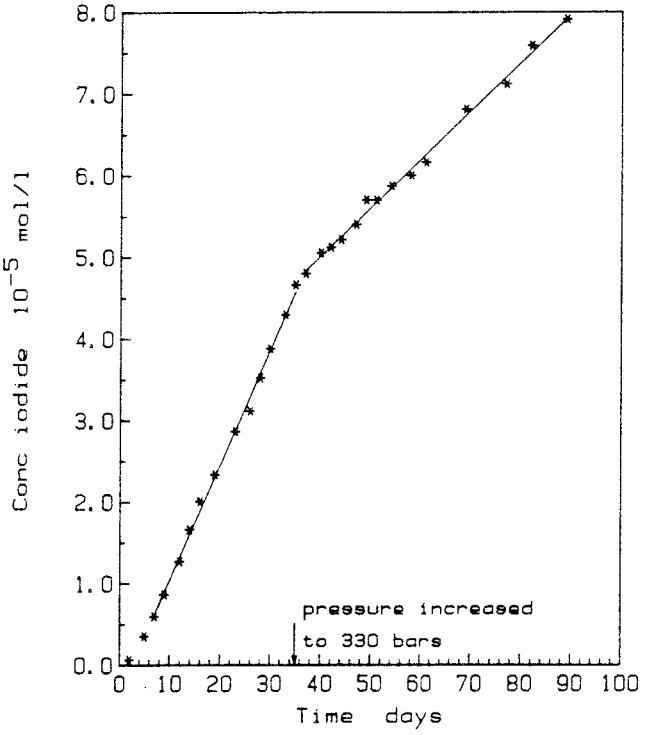

Figure 6.2 Concentration of Iodide versus time, diffusion through biotite gneiss from Svartboberget.

It is seen from the slope that there is a marked decrease in diffusivity when the pressure is increased.

In some of the electrical conductivity measurements the loading stress was cycled several times. Hystersis effects are clearly seen and both somewhat higher and somewhat lower values were found at the end of a cycle. A second cycle closely followed the first in the experiment where the cycling was repeated, figure 6.3.

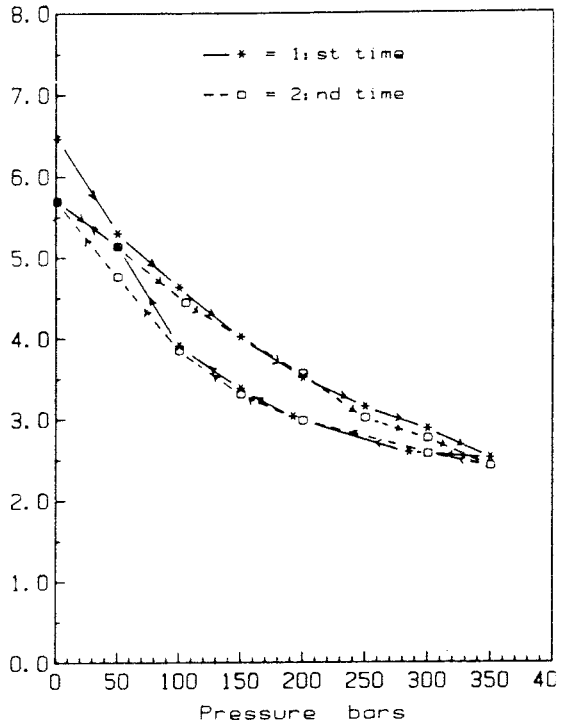

Figure 6.3 Formation factor $*10^5$ versus pressure for a granite sample from Finnsjön.

The formation factors calculated from the diffusion experiments under stress are in fair agreement with the formation factors from the resistivity measurements at higher pressures.

The results from Skagius and Neretnieks measurements are summarized in figures 6.4 and 6.5. The results from the various methods are compared. Figure 6.4 shows the diffusivities of Iodide determined in granites and figure 6.5 the diffusivities of Iodide determined in gneisses. The open bars represent the diffusivities in samples under stressed conditions and the filled bars the diffusivity in samples under atmospheric pressure.

The formation factor in samples at 30-35 MPa stress relative to the formation factor in the samples at atmospheric pressure obtained in the diffusion experiments are in fair agreement with those determined from the electrical resistivity measurements for the same rock materials. Electrical resistivity measurements can thus be used to give approximate values of the diffusivity. The advantage with electrical resistivity measurements is that the experimental time is much shorter than in the diffusion experiments.

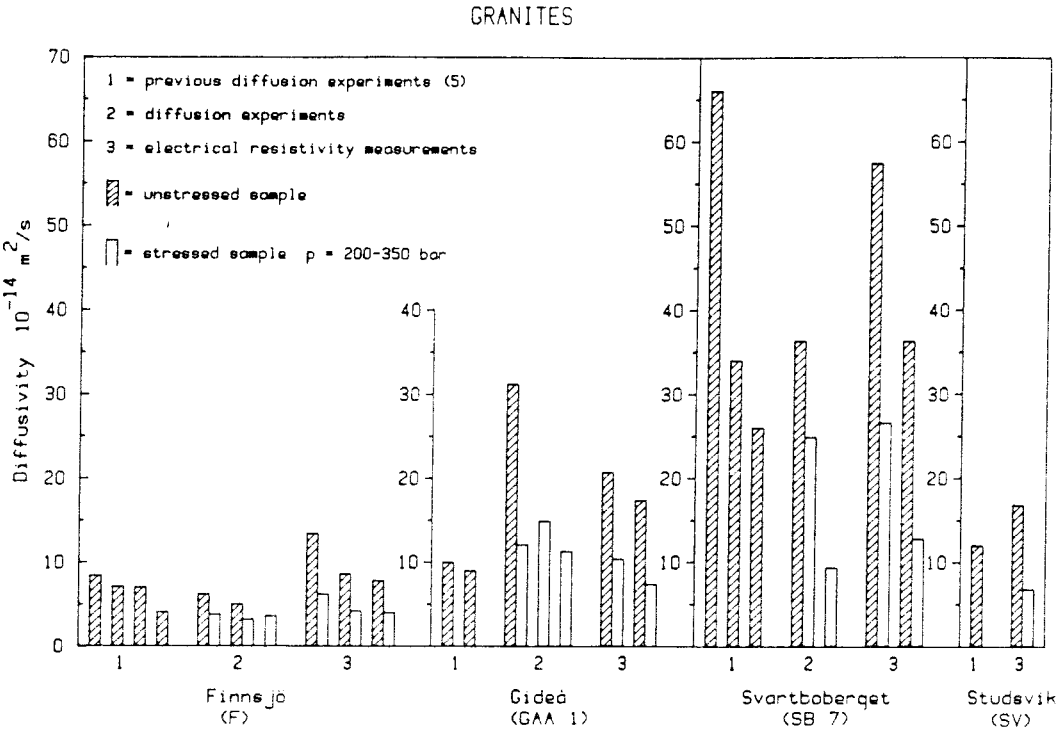

Figure 6.4 Effective diffusivities in granites.

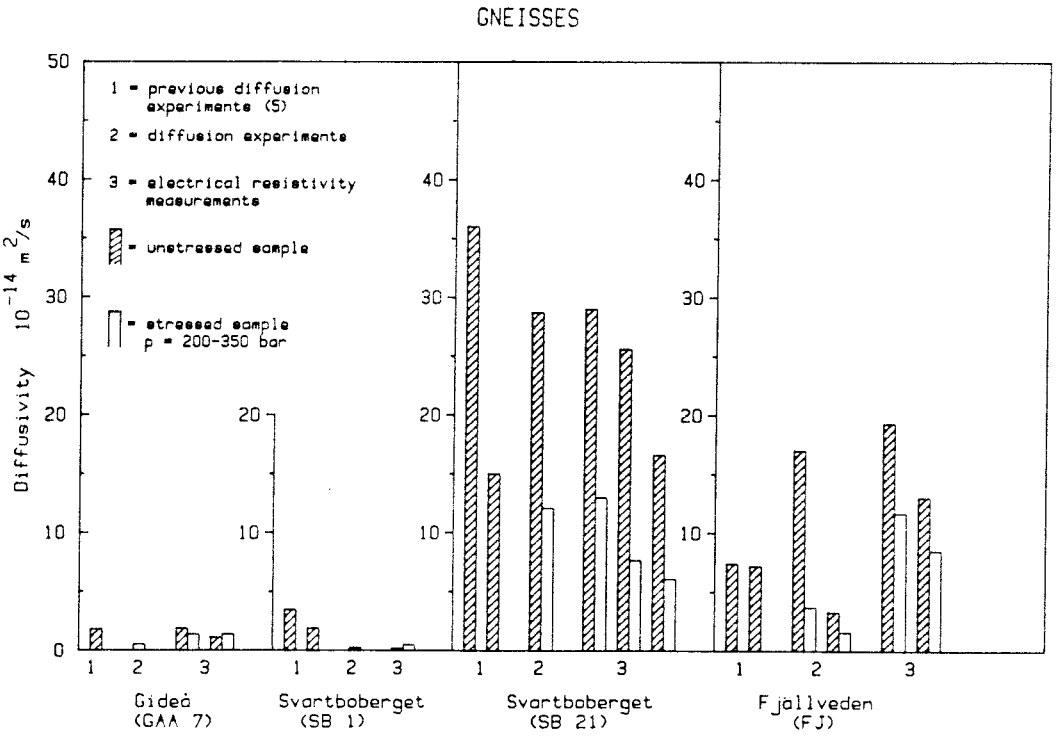

Figure 6.5 Effective diffusivities in gneisses.

The diffusivity and the formation factor in samples at 30-35 MPa was typically a factor 2 lower and in no case lower than about 1/5 of the value in unstressed samples.

6.3 Diffusion experiments with sorbing substances in crystalline rocks

In the simplest case it may be assumed that transport takes place only in the pore water and that the sorption equilibrium is reversible and linear. Equation 6.3 then simplifies to

$$\alpha \frac{\partial C}{\partial t} = D_p \varepsilon_t \frac{\partial^2 C}{\partial x^2} \qquad (6.8)$$

Where α is the rock capacity factor $\varepsilon+K$ and $K=C_S/C$, the volumetric sorption coefficient for linear sorption.

For systems where the above assumptions are valid it would be sufficient to determine the formation factor F_f, the diffusivity in water of the solute and the sorption coefficient to fully define the system.

Several experiments have set out to test the validity of these assumptions experimentally.

Bradbury and Stephen (1985) measured the effective diffusivity and sorption properties of technetium as pertechnetate, cesium and strontium in a sandstone using a through diffusion technique. The sandstone had about 10 % porosity. They found good agreement between the diffusivities for the three solutes. Sorption equilibrium measurements using a batch technique showed that the isotherms were weakly nonlinear for technetium and cesium giving a Freundlich exponents between 0.71 and 0.94. The isotherm was linear for strontium. However, It was found that the sorption capacity could be up to one to two orders of magnitude higher when determined in batch experiments with crushed rock as well as with coupons, compared to the results obtained from the through diffusion experiments on machined coupons. The reason for the differences between the results for coupons in the two different experiments is not known. The methods of evaluating the results are different, however. Batch experiments are evaluated by making a mass balance on the amount of tracer lost from the bath. The through diffusion experiments were evaluated from the time lag of the breakthrough curve. This method gives the capacity of the transport pores and does not account for the possible capacity of the "storage pores". Bradbury et al. (1982) found that for nonsorbing species storage pores had a noticeable influence on the total capacity of the rock. No investigations so far seem to have addressed the influence on storage capacity in this type of instationary experiments.

The higher sorption values for the crushed rock, with sizes <0.1 mm can be understood because the crushing will induce new microfractures and expose fresh surfaces to weathering. The sorption capacity for particles 1-2 mm was comparable to that of the coupons which were 5 mm thick.

Skagius et al (1982) made sorption and diffusion measurements on two different granites. The technique used was in-diffusion into crushed particles with 6 different size fractions ranging from 0.1 to 5 mm. The sorption isotherm for strontium was found to be linear whereas that for cesium was slightly nonlinear with Freundlich exponent of about 0.6 for both granites.

The sorption capacity was found to be practically independent on the particle size if account was taken of the larger outer surface for the smaller particles. For the smallest particle size 0.1-0.12 mm the sorption on the outer surface accounted for 11-15 % for cesium and strontium respectively on the Finnsjön granite and 40-46 % on the Stripa granite. For particle sizes larger than 1 mm the contribution from the outer surface was negligible.

The in-diffusion experiments were performed with the batch technique where the bath concentration was monitored over more than 10 000 h. Figure 6.6 shows the concentration time curve for two experiments together with the fitted curve. The fitted curve is the solution to the instationary diffusion equation (6.3) with the appropriate boundary conditions. The sorption coefficient and the effective diffusivity are obtained simultaneously from the fit.

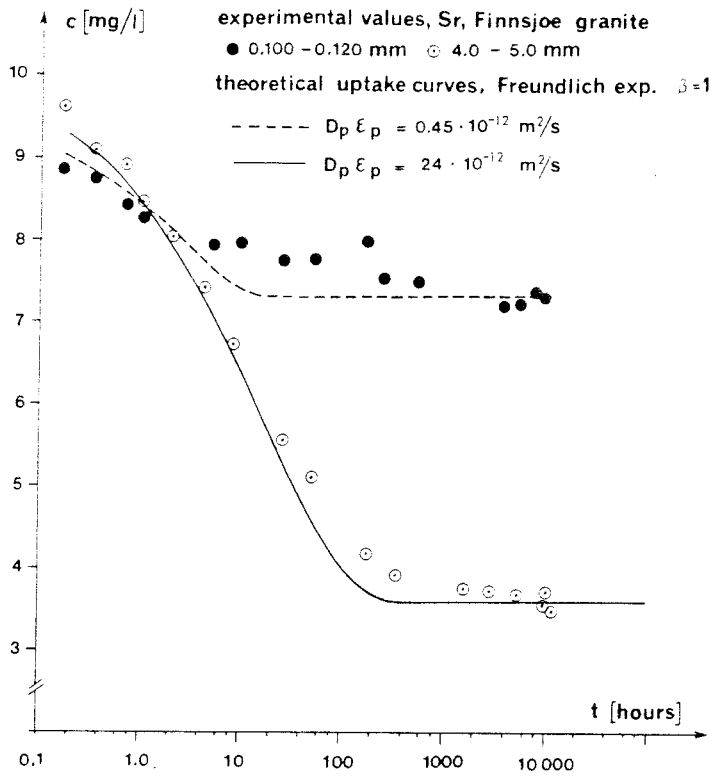

Figure 6.6 The fit of the diffusion model to the experimental uptake curve for strontium on Finnsjön granite.

Skagius (1986) made another set of batch in-diffusion experiments into 5 mm thick tablets on Finnsjön and Stripa granites. Results for Finnsjön granite are illustrated in figure 6.7. The sorption coefficients were up to three times lower in the machined tablets. The effective diffusivity was very strongly dependent on the particle size. Figure 6.8 shows the diffusivities obtained for particles.

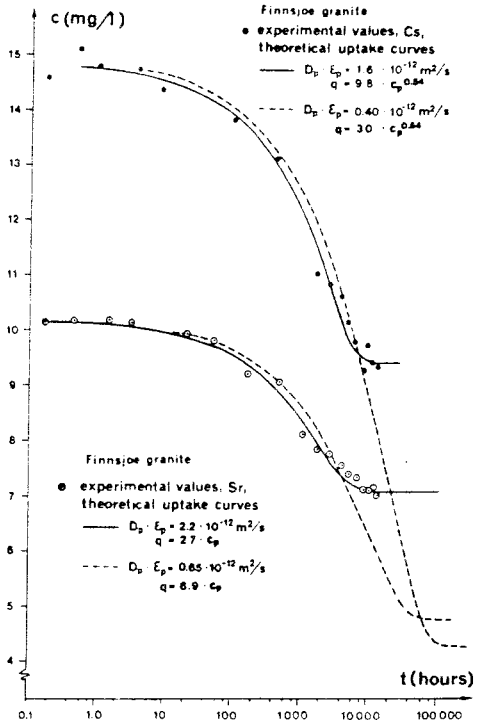

Figure 6.7 The fit of the diffusion model to the experimental uptake curve for cesium and strontium on Finnsjön granite.

Skagius and Neretnieks (1988) made sorption and diffusion measurements by the in-diffusion as well as the through diffusion method using cesium and strontium. Biotite gneiss from Fjällveden was used. After contact times of up to 1.5 years the tablets were profiled by grinding off thin sections. Sorption and diffusion values were determined both from the concentration profiles in the samples and from the time lag of the break through curves. Sorption coefficients determined from measured uptake in the rock were about half those determined from the time lag of the breakthrough curve. This contrasts strongly with the large differences obtained by Bradbury and Stephen (1985), who found up to two orders of magnitude differences.

Attempts by Skagius and Neretnieks (1988) to evaluate the effective diffusivity assuming only pore diffusion failed because the "pore diffusivity " from the slope of the breakthrough curve was much higher than can be explained by pore diffusion only. The pore diffusivity of cesium would have to be larger by at least a factor of two over the diffusivity in pure water. This is nearly hundred times more than expected from the formation factor measured with Iodide. Furthermore the experimental and theoretical breakthrough curves had distinctly different shape for early times. By assuming that part of the transport at least is by surface diffusion a good fit could be

obtained. Most of the transport must then be by surface diffusion and the transport by pore diffusion would be practically negligible.

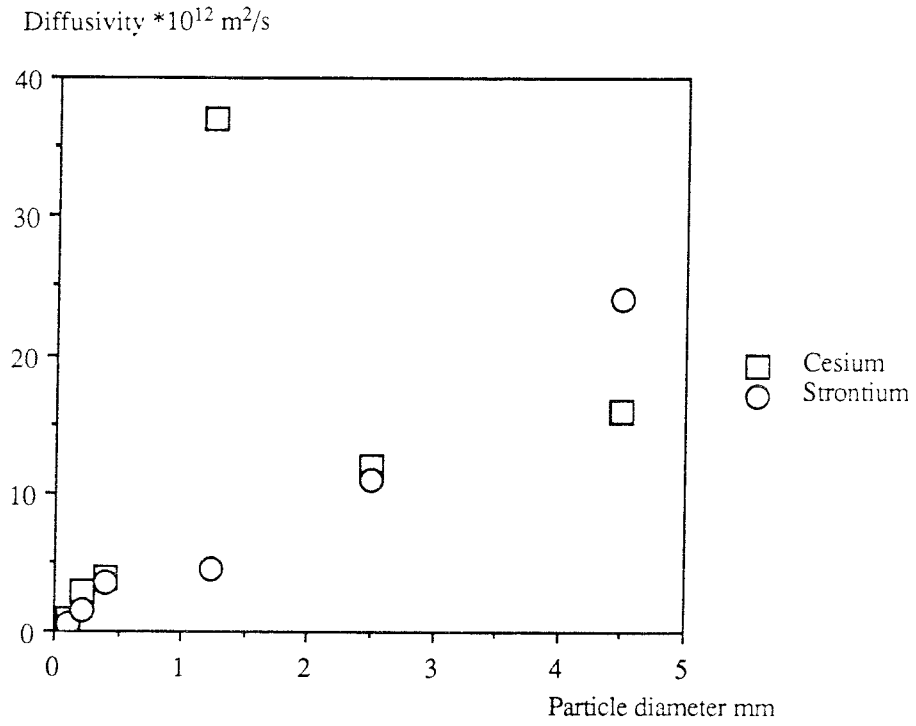

Figure 6.8 Effective diffusivity of cesium and strontium for different particle sizes.

Figure 6.9 summarizes Skagius (1986) results in the form of formation factors obtained for different solutes. It is seen that the formation factor is very much higher for cesium and strontium than values obtained from electrical conductivity measurements and from Iodide measurements. This has been interpreted as indicating the presence of a transport mechanism in addition to transport in pore water only.

6.4 Field investigations

6.4.1 A field diffusion experiment in Stripa

To test if the matrix of granites at large depths has a connected porosity, a set of three experiments has been made. The experiments have been carried out in "undisturbed" rock under its natural stress environment, at the 360 m level in the Stripa Mine (Stripa, Sweden). The rock is subject to nearly the same conditions as the rock surrounding a nuclear waste repository as proposed in the Swedish concept.

A mixture of three nonsorbing (conservative) tracers, Uranin, Cr-EDTA, and I^-, were injected into the granitic rock matrix for three different time periods: about 3 months, about 6 months, and about 3.5 years. The subsequent over-corings of the injection holes showed that the tracers had in some cases migrated at least about 400 mm

(measuring limit) into the rock matrix for the experiment with the longest injection time. It could also be seen that there were large differences in migration distance into the rock matrix for samples taken fairly close to each other.

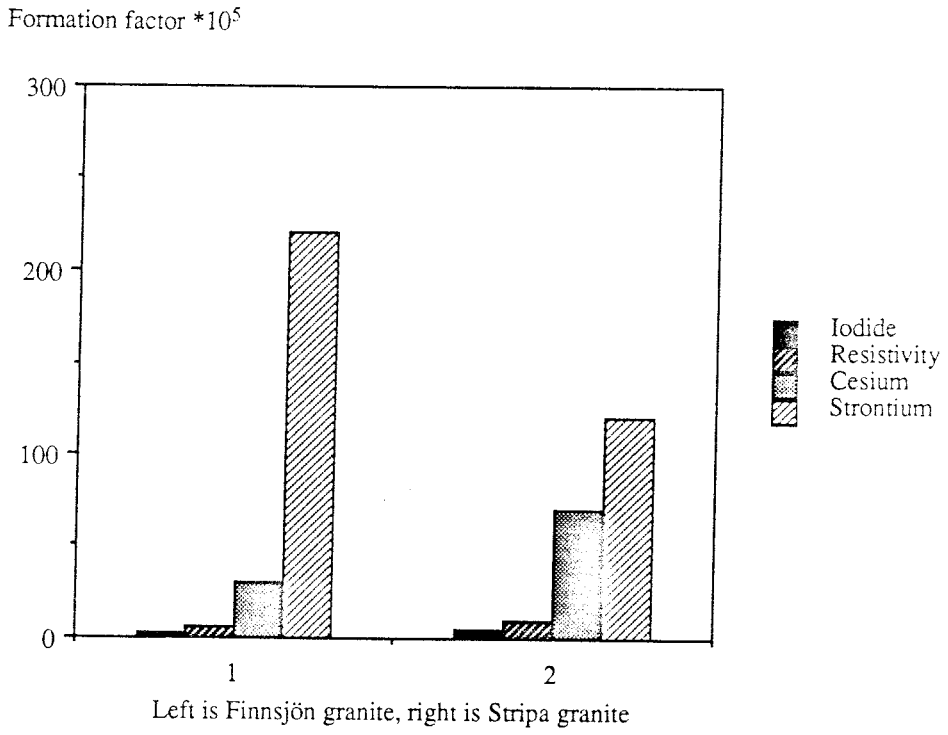

Figure 6.9 Formation factor for Finnsjö and Stripa granite.

The results from all three experiments showed that the three tracers had migrated through the disturbed zone close to the injection hole, through the fissure coating material, and a distance into the "undisturbed" rock matrix. (Birgersson 1988).

The experiment was designed in the following way. Close to a drift or a borehole the rock stresses will be considerably different from those far away from the disturbance. In order to make the experiment in undisturbed rock 3 large holes were drilled with lengths more than two tunnel diameters, > 10 m, and in the bottom of the large holes thin holes, 20 mm, extending 2-3 m were drilled, See figure 6.10. At distances larger than about 2 tunnel or hole diameters the rock is essentially undisturbed. The small holes were packed off and filled with tracer solutions which were kept under somewhat higher than ambient hydraulic pressure. The tracers flowed and diffused out into the rock surrounding the hole.

The first hole was overcored after 3 months, the second after 6 months and the third after 3.5 years. In the two longer experiments, called II and III, additional holes were drilled parallel to first after the injection period to reach rock at distances up to 40 cm from the injection hole.

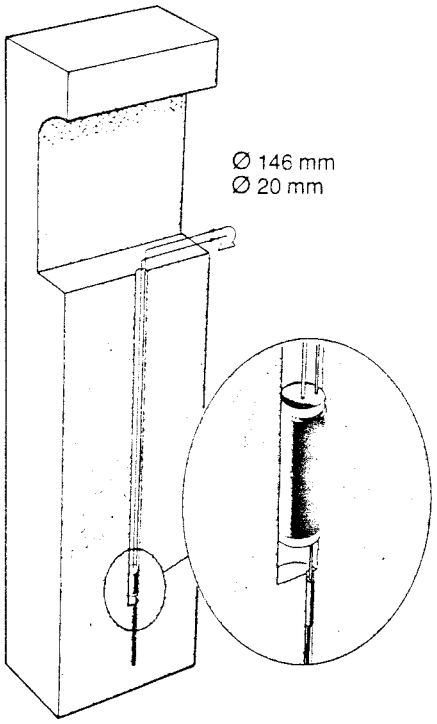

Figure 6.10 Drilling dimensions and packer positions.

Figures 6.11 shows the overcoring arrangement of experiments II. Figure 6.12 shows the coring out arrangement of experiment III. The three large holes (146 mm) made it possible to study the concentration profile as far as about 400 mm outward from the injection hole. The three additional small holes (76 mm) made it possible to study the concentrations in other directions in addition.

The cores were sectioned and sample cores were drilled from the sections. The sample cores were leached and the tracer concentrations of the leachates were determined. The number of sampling cores obtained were about 200 in experiment I, about 650 in experiment II, and about 1800 in experiment III.

Experiment I was a pilot experiment and gave only limited data on the migration distances but showed that the tracers penetrate through quite thick fracture coating materials under the natural stress conditions (Birgersson and Neretnieks 1982a,b). Experiment II has also been reported earlier (Birgersson and Neretnieks 1983, 1984).

A rock stress measurement was performed in the hole of experiment I at 15.5, 16.0, and 17.5 m depth from the floor of the drift. The stress distribution agreed well with what is regarded as natural stress in the Stripa Mine.

The porosity was measured for every individual sampling core by comparing the weight difference between wet and dry core. The porosity was found to be between 0.12-0.51 % , with an average close to 0.3 %.

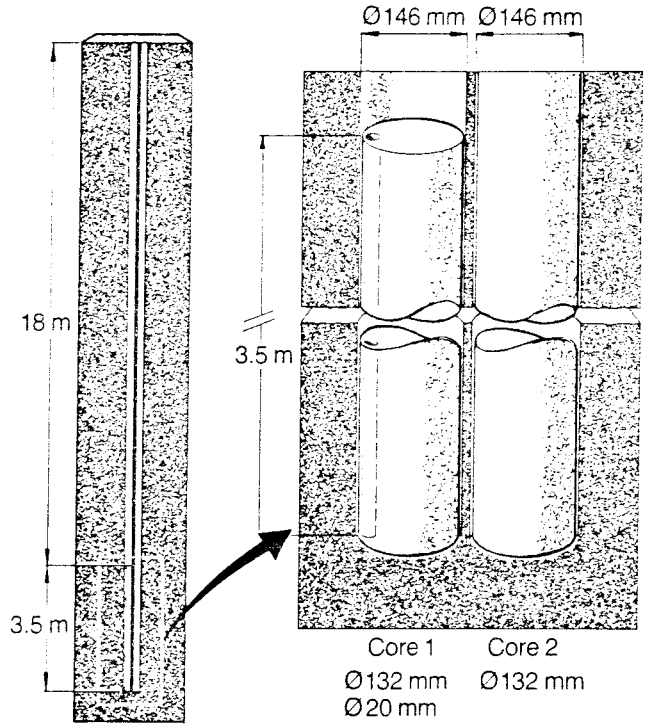

Figure 6.11 Drilling arrangement, Part II.

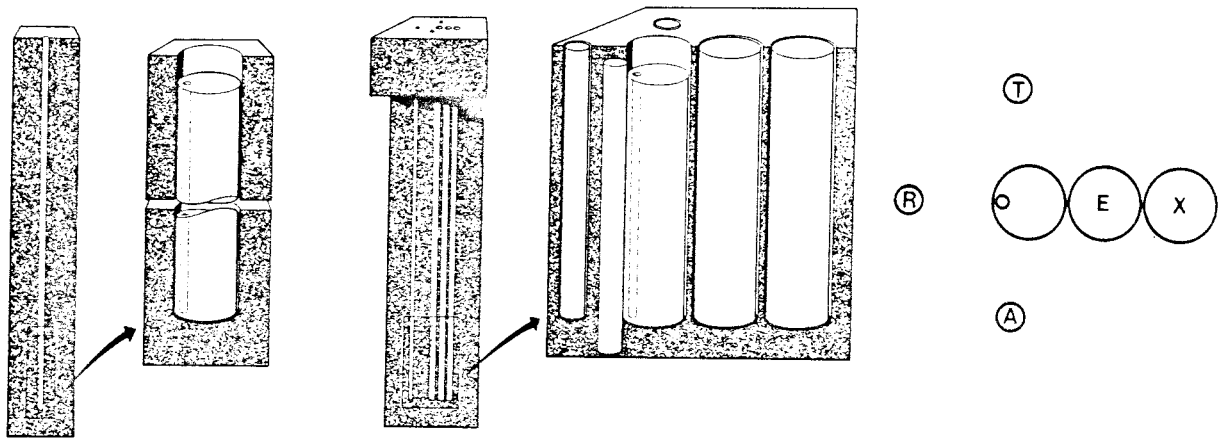

Figure 6.12 Part III. Drilling arrangement and notation of the cores.

The pore size distribution was measured using three different methods: mercury penetrometry, the BET-method (using Nitrogen gas) and by electron microscope. The pore size distribution for 5 samples were determined by this method. Figure 6.13 shows an example of the results from the electron microscope.

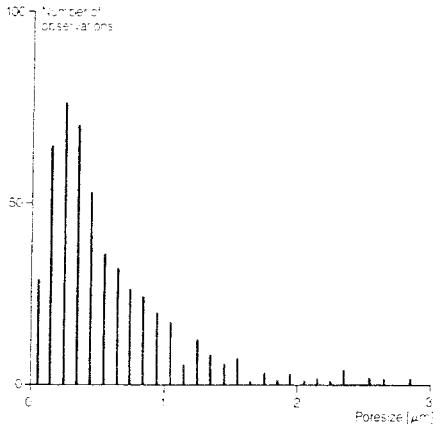

Figure 6.13 Pore size distribution for sample 25:9. Results obtained by electron microscope.

The direction of the micro fissures were determined in three samples. The method used was the DSA-method (Differential Strength Analysis). No specific micro fissure direction could be found in any of the three samples.

The diffusivity was also measured on 4 samples by the method used by Skagius and Neretnieks (1986a). Iodide pore diffusivities varied between 90 and $200 \cdot 10^{-12}$ m^2 /s and Uranin gave values of $3\text{-}10 \cdot 10^{-12}$ m^2 /s.

The hydraulic conductivity was determined for 5 samples. It was found to be $0.2\text{-}2 \cdot 10^{-13}$ m/s at confining stresses of 15-30 MPa.

Some examples of concentration profiles are shown in figures 6.14, 6.15, 6.16, 6.17, and 6.18. Together they illustrate how the penetration distances varied with tracer, with direction and with depth for experiment III. The penetration distances differ with tracer, direction and depth. Figure 6.19 illustrates the concentration of Iodide at a distance of 200-250 mm from the injection hole. This plot also shows strong variations of the migration with location.

The fact that the migration distance is different at different depths can be caused by differences in porosity (ε_p) and differences in the migration parameters (K_p and D_p).

The porosity was measured for the individual sampling cores. Figure 6.20 illustrates the mean value of the porosity (the standard deviation) for each sampling piece from core 1 and core 2 in experiment II. The variations are small and cannot alone explain the differences in migration distances.

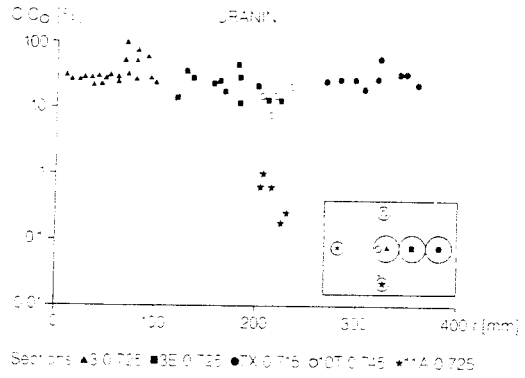

Figure 6.14 Part III. Uranin concentrations vs distance at 0.725 m depth.

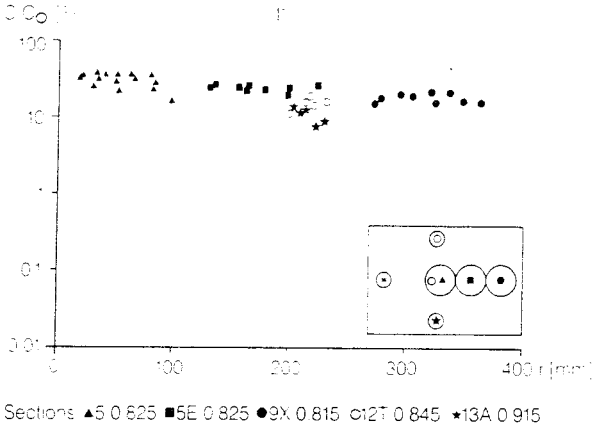

Figure 6.15 Part III. I^- concentration vs distance at 0.825 m depth.

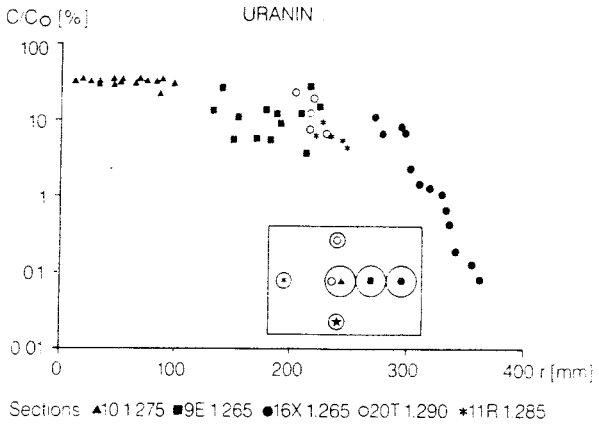

Figure 6.16 Part III. Uranin concentration vs distance at 1.275 m depth.

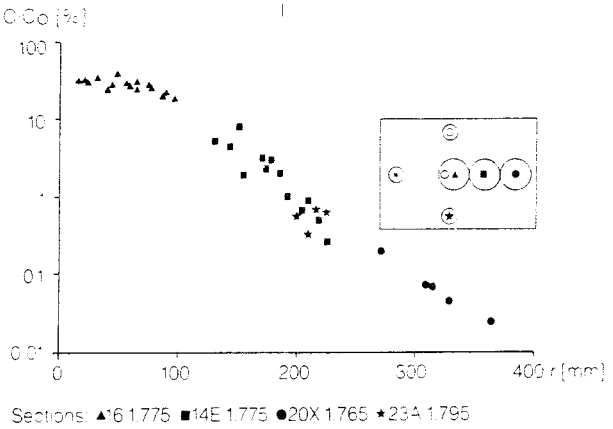

Figure 6.17 Part III. I^- concentration vs distance at 1.775 m depth.

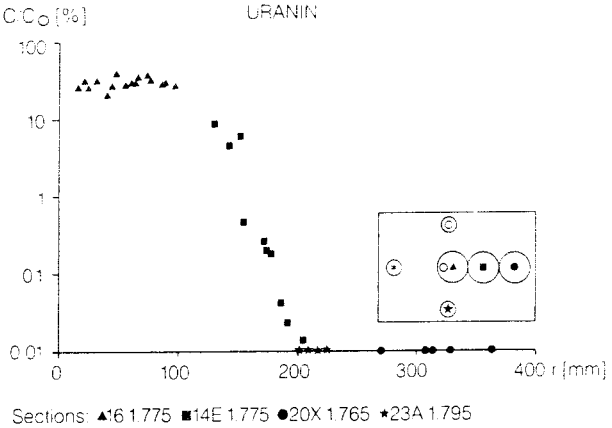

Figure 6.18 Part III. Uranin concentration vs distance at 1.775 m depth.

The values of the migration parameters have been evaluated by comparing the experimentally obtained concentration profiles with theoretical concentration profiles obtained by solving the advection-diffusion equation for the appropriate geometry (Birgersson and Neretnieks 1983). These approximate values of D_p and K_p are summarized in Table 6.1 for experiment II.

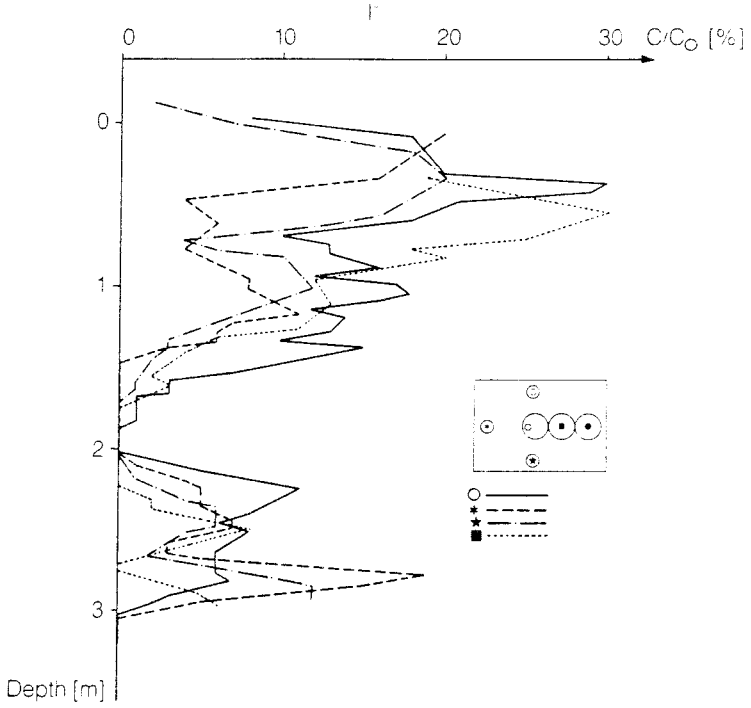

Figure 6.19 Average Iodide concentration 200-250 mm from the injection hole.

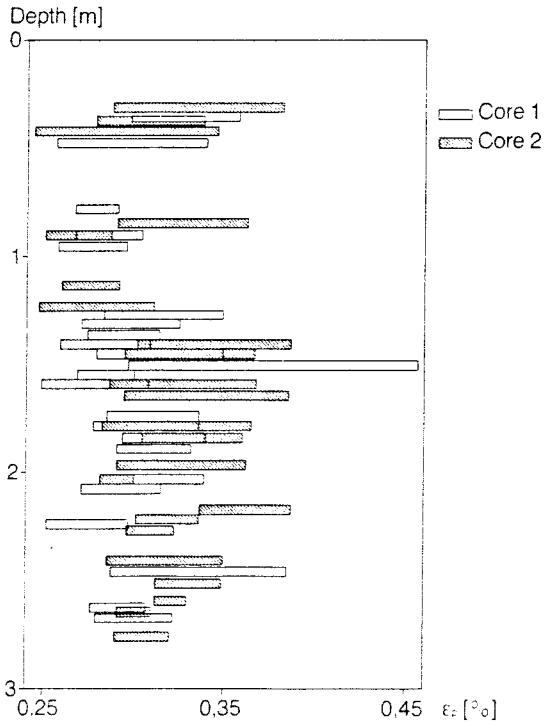

Figure 6.20 Experiment II. Core 1 and core 2. The porosity (± the standard deviation) vs depth.

Table 6.1 Approximate values on D_p and K_p for different depths.

Sampling piece	Depth (m) along little hole	D_p (m^2/s)·10^{10}	K_p (m/s)·10^{13}
1-2	0.36-0.48	>1	>2-5
3-9	0.78-1.41	0.5	0.1
10-13	1.46-1.59	0.05	<0.1
14-20	1.74-2.24	1	1
21-22	2.62-2.67	>1	>2-5

Table 6.1 shows that D_p and K_p can vary with an order of magnitude for sampling pieces separated by just a few tens of centimeters.

No obvious correlation between the penetration depths and porosity, pore size distribution or microfissure direction was found, although there was a tendency for larger penetration distances in regions where the pores were larger.

The reason for the considerable differences in migration distance for sampling pieces separated by just a few tens of centimeters in depth or at the same depth but in different directions seems to be caused by variations in the migration parameters, K_p and D_p due to inhomogeneities in the rock matrix. It was not possible to measure these properties on the individual small samples as was done for the porosity. The few measurements of diffusivity and hydraulic conductivity made from the same cores show a considerable variation.

The diffusivity and hydraulic conductivity were evaluated at the locations illustrated in figures 6.21 and 6.22. The evaluation was made by fitting the obtained concentration profiles to the advection-diffusion equation for radially symmetric migration. It was not possible to follow the concentration profile as far out into the rock matrix as needed for the evaluation of D_p and K_p at the other locations. The difference in behavior between the tracers is also clearly illustrated. Iodide has diffusivity values that are one to two orders of magnitude larger than Cr-EDTA, while the diffusivity for Uranin is somewhere between these two tracers. The pore diffusivities vary between $2 \cdot 10^{-12}$ to $5 \cdot 10^{-10}$ m^2/s.

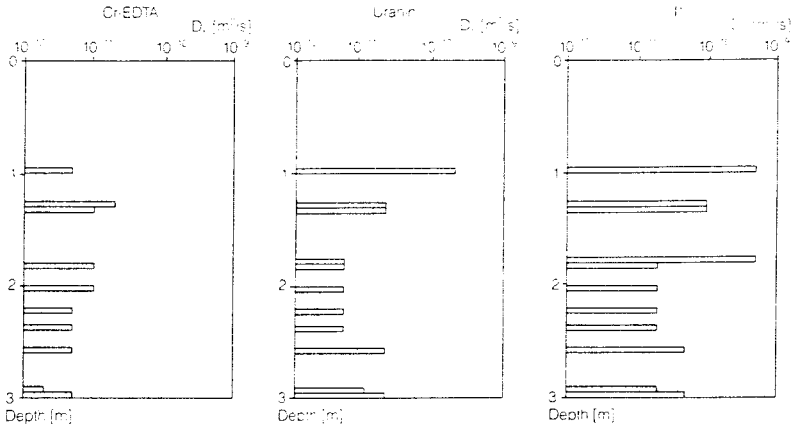

Figure 6.21 Experiment III. D_p vs depth in the cores for the three tracers.

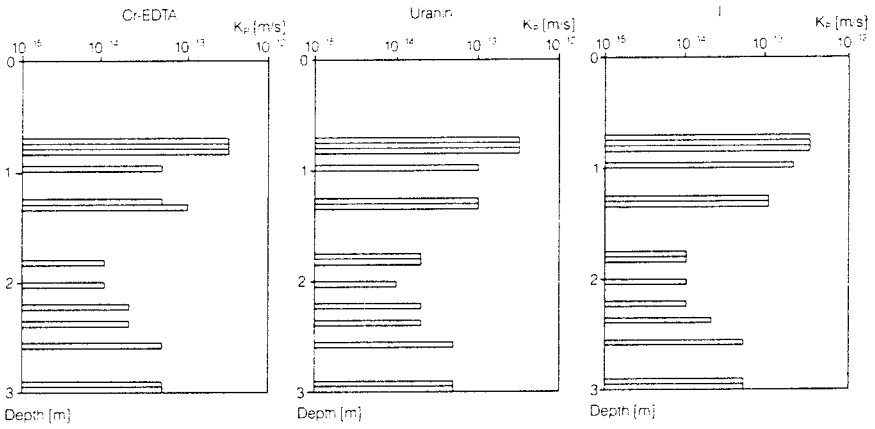

Figure 6.22 Experiment III. K_p vs depths in the cores for the three tracers.

This difference between the tracers was also seen in the laboratory experiment. These values are of the same order of magnitude as those obtained in situ and are illustrated in figure 6.23. The difference in stress levels between the laboratory and the in situ measurements are expected to make the laboratory data about a factor 2 higher (Skagius and Neretnieks 1986b).

The hydraulic conductivities obtained in situ and those obtained in the laboratory experiment are of the same order of magnitude, see figure 6.24.

It was concluded from the investigations that the pore system in virgin undisturbed rock is open and connected. This was found to be the case for at least 40 cm. The diffusive and hydraulic properties vary by order to orders of magnitude even at close locations.

The changes in migration properties at different locations and in different directions could not be explained by the laboratory experiments performed concerning porosity, pore size distribution or direction of microfissures.

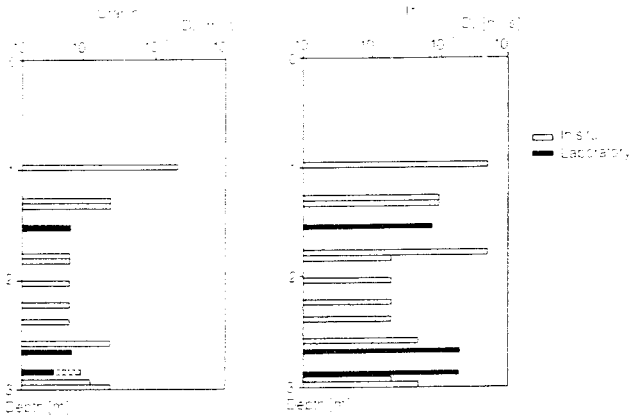

Figure 6.23 Comparison between diffusivities obtained in the laboratory and in situ.

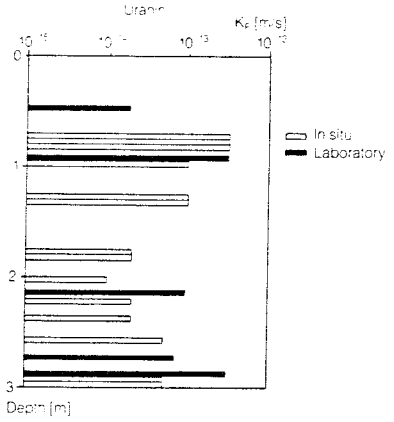

Figure 6.24 Hydraulic conductivity vs depth in core. From in situ conditions and laboratory experiments.

The diffusivities and hydraulic conductivities obtained in situ compared well with those obtained in the laboratory experiments.

6.4.2 Salt water diffusion profiles in a granite block

Jeffries (1988) has reported on the investigation of a salt water profile in a block of granite rock which was immersed in salt water 30 years ago. The block of granite was 1.5*1*0.6 m and was taken from the Carnmenellis pluton in Cornwall. It was used to construct a water break in Falmouth 1956. After 30 years of immersion in salt water it was retrieved and samples were taken by coring through the block in the shortest direction.

The core was sectioned and leached of its dissolved anions, Cl^-, Br^- SO_4^{2-}, and F^-. The concentration of the ions in the leachates were measured and concentration profiles were obtained. Cl^- and Br^- concentrations were 15 to 40 times higher than those in fresh granite samples obtained from the same quarry. The profiles were flat

and only lower bounds of the diffusivities could be determined. The pore diffusivity was estimated to be larger than $9 \cdot 10^{-11}$ m^2/s. Measured values on samples of fresh unweathered rock were found to be at least 3 times lower.

The SO_4^{2-} and F^- profiles had sharp concentration peaks about 10 cm from the surface which were interpreted to be caused by weathering of the rock which contains minerals with these species. It was suggested that these species are slightly sorbed on the mineral surfaces and that the movement of these species is slightly retarded in relation to non-interacting species. Diffusivities and sorption coefficients could not be determined unequivocally from the data but the assessed apparent diffusivities were found not to be unreasonable.

7 FLOW AND TRANSPORT IN INDIVIDUAL FRACTURES

7.1 Laboratory experiments

A set of laboratory tracer experiment have been performed using natural fractures. The aim of the experiments was to study sorbing tracer retardation by sorption and matrix diffusion in natural fractures.

Nonsorbing tracers - tritiated water and a large organic molecule, lignosulphonate, were used to evaluate the fracture aperture and dispersive properties. The sorbing tracers cesium and strontium were used to study the retardation effects.

In the first set of experiments (Neretnieks et al 1982) the rock used was a 30-cm-long granitic drill core 20 cm in diameter taken from the Stripa mine at a depth of 360 m below ground level. The core has a natural fracture which runs parallel to the axis. The cylindrical surface of the drill core was sealed to prevent any water leaving the rock except through the outlet end of the fissure. The granite cylinder was mounted between two end plates containing inlet and outlet channels (Figure 7.1).

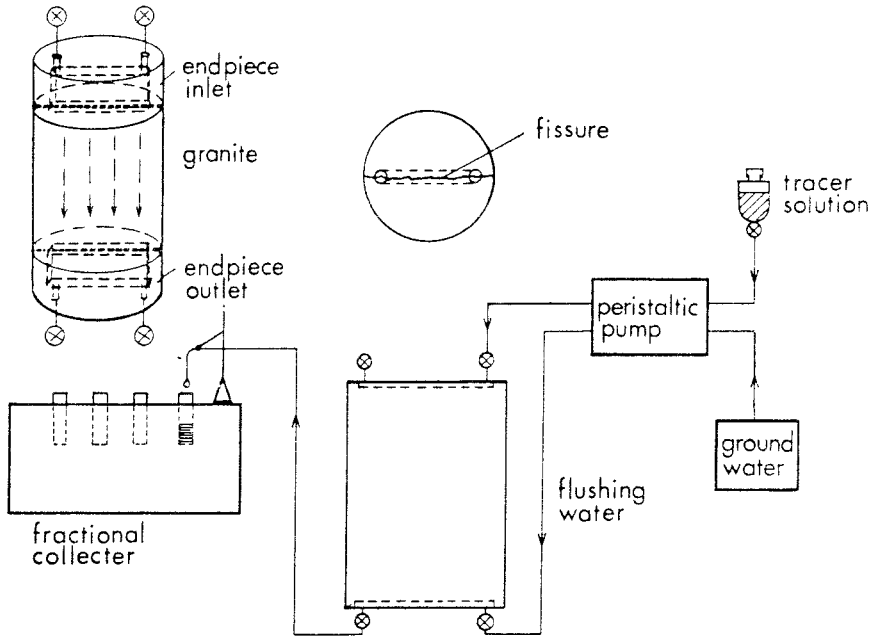

Figure 7.1 Experimental setup.

Artificial groundwater with a tracer was fed to the upper channel. The effluent was analyzed for tracer concentrations. The tracers were introduced, either as a step up or as a step up followed by a step down, after a suitable amount of tracer had been introduced.

Figure 7.2 shows the breakthrough curves for tritiated water for different flow rates.

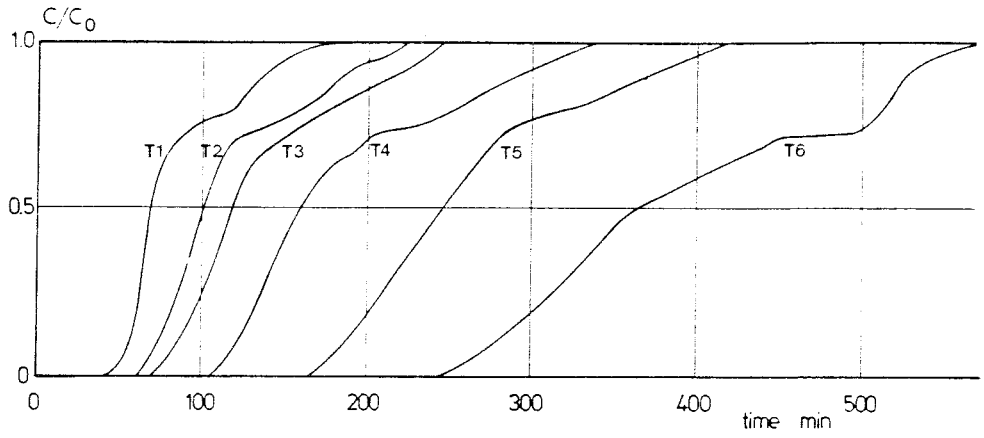

Figure 7.2 Experimental breakthrough curves for THO.

The figure shows plateaus at C/C_0 = 0.7-0.8 indicating that there are at least two channels. Similar curves were obtained with the other nonsorbing tracer - the negatively charged lignosulphonate ion. Neglecting the presence of two channels the best fit to the advection-dispersion equation gives Peclet numbers ranging between 8 and 27 with an average of 14.2. The dispersion length was 25 mm. The average fracture aperture calculated from the residence time was 0.18 mm. The same data were also analyzed with the advection-channeling model, assuming that the breakthrough curve is caused by different velocities in a multitude of independent channels. With a log normal (base 10) distribution the logarithmic standard deviation was found to be 0.094 on the average.

Strontium and cesium were run in the same core. A typical breakthrough-curve for strontium is shown in Figure 7.3.

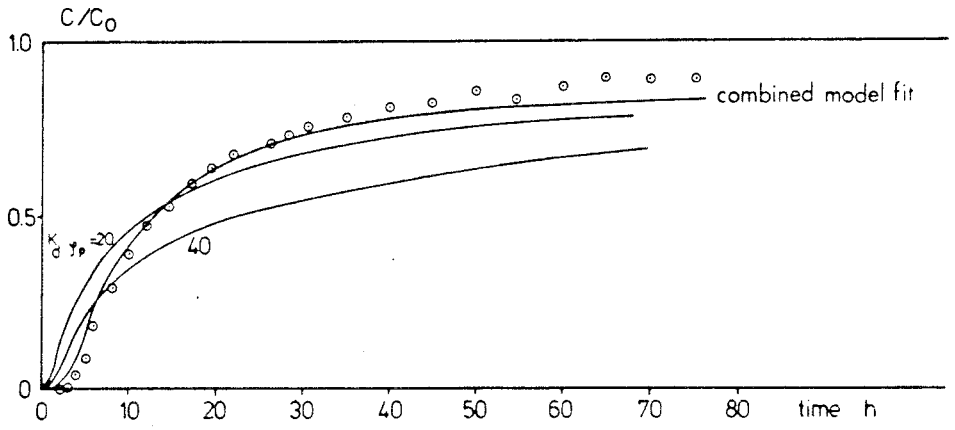

Figure 7.3 Experimental strontium breakthrough curve and curve predicted by advection-channeling-matrix diffusion model.

Whereas the tritiated water and the lignosulphonate ion were predicted and found to show negligible effects of penetration of the matrix, strontium and cesium were predicted to be strongly influenced by sorption within the rock matrix and by sorption on the surface of the fracture. The predicted and the experimental results compare reasonably well in all 13 runs with sorbing tracers. Figure 7.3 gives one example. Attempts to fit the experiment with only surface sorption, only matrix diffusion and inner sorption in the rock matrix were not successful. Simultaneous surface sorption and matrix diffusion with sorption in the rock matrix had to be assumed to account for the experimental results. The two curves with $K_d\rho_p$=20 and 40 in figure 7.3 show attempts to fit only with matrix diffusion.

In a later set of experiments (Moreno et al 1985) two more cores were used, 18.5 and 27 cm long. More refined models were used which also account for the dispersion effects of the inlet and outlet end pieces. Peclet numbers of 20 and 15 and fracture apertures of 0.14 and 0.13 mm were found. Predicted and experimental results on diffusivities and sorption equilibria for strontium differed much more for these cores than for the first core. The obtained results are, however, within the large range of diffusivities and sorption data found for crystalline rocks and coating and alteration materials (Skagius and Neretnieks 1985a).

The diffusion and sorption data obtained $D_e=10^{-12}$ m^2/s and $K_d\rho_p$=10 and 135 for strontium and cesium respectively agree with independent measurements (Skagius et al 1982).

Table 7.1 summarizes the fracture properties and the data obtained for the sorbing species. The cores were obtained from the Stripa mine.

Table 7.1 Fracture properties and the data obtained for the sorbing species on Stripa granite

Reference	Core 1 Neretnieks et al 1982	Core 2 Moreno et al 1985	Core 3
l length cm	30	18.5	27
W width cm	20.0	10.0	10.0
δ Aperture mm	0.18	0.14	0.13
Pe Peclet number	12	20	15
STRONTIUM			
K_a Surface sorption coeff mm	1	0.12-0.31	0.14
$D_eK_d\rho_p$ m^2/s	$135\cdot10^{-12}$	$10\text{-}101\cdot10^{-12}$	$16\cdot10^{-12}$
CESIUM			
K_a Surface sorption coeff mm	1		
$D_eK_d\rho_p$ m^2/s	$10\cdot10^{-12}$		

Skagius et al 1982 obtained values of K_a for both strontium and cesium on crushed rock pieces of 1 mm. For strontium Skagius (1986) obtained values of $D_e K_d \rho_p$ = $1\text{-}2 \cdot 10^{-12}$ m^2/s for tablets.

These investigations indicate that the transport of sorbing species in natural fractures is influenced by both surface sorption and by diffusion into the rock matrix. The fractures used were natural fractures with a thin coating and this may influence the transport. The values obtained for the sorption coefficients and diffusivities are in the range of values obtained by other measurements.

7.2 Field experiments

7.2.1 Stripa 2D experiment

This experiment was aimed at investigating the flow and transport in a natural fracture in situ with migration distances of 5 and 10 m. This is more than one order of magnitude larger than the distances used in laboratory experiments. The experiment was done by injecting tracers in the naturally flowing water in a fracture and by collecting the tracers as they emerge in the drift. In addition the fracture was excavated after the experiment and its surfaces monitored for the sorbing tracers.The experiment was performed in the Stripa mine in central Sweden at a depth of 360 m.

Figure 7.4 shows a schematic illustration of the fracture with one of the injection holes and several sampling holes. Figure 7.5 shows the two main fractures in the actual site. Fracture 2 was used for the test.

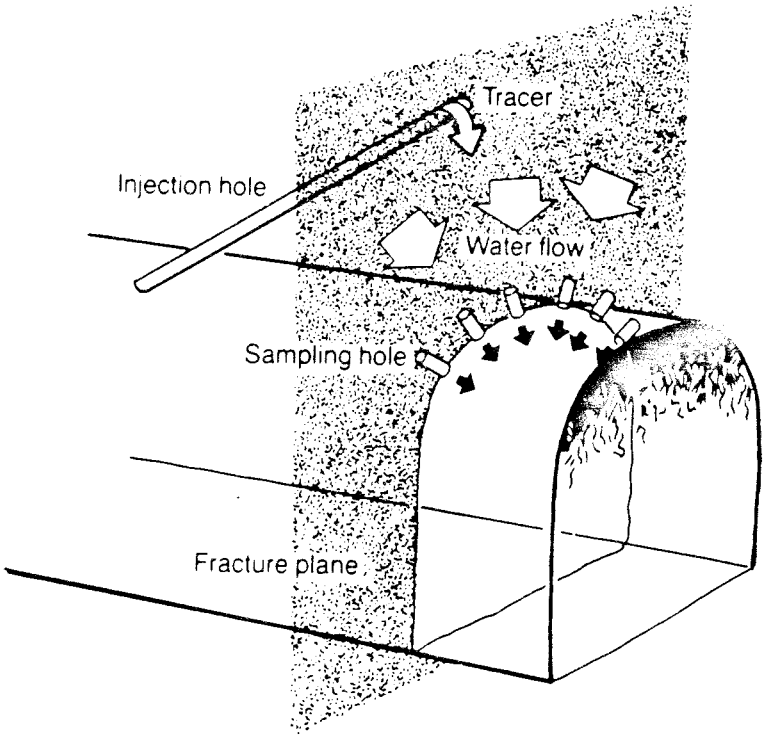

Figure 7.4 Schematic illustration of tracer injection.

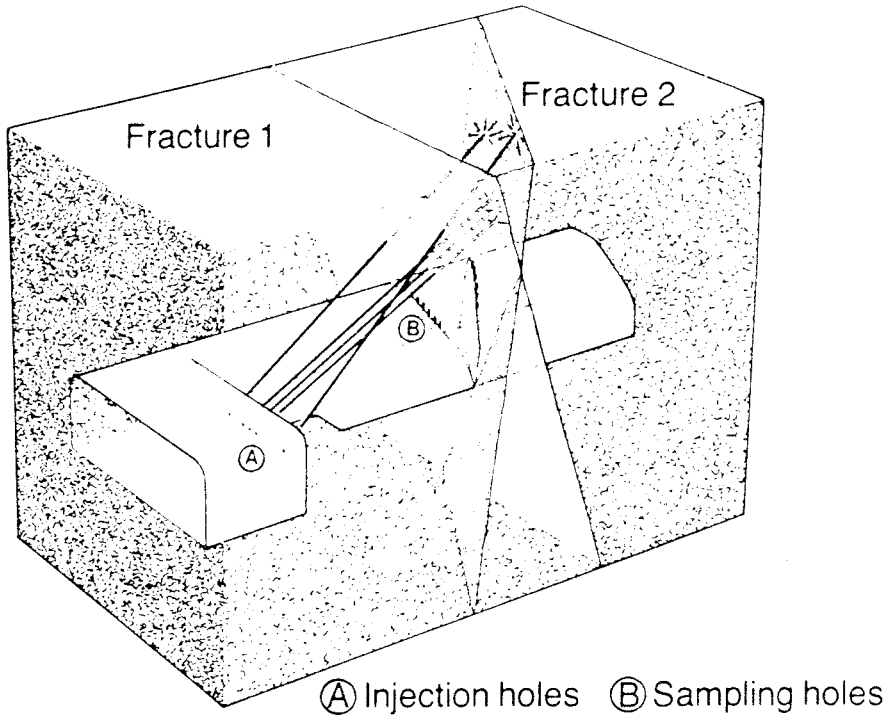

Figure 7.5 Schematic illustration of the two fractures intersecting the drift.

The fracture was characterized hydraulically by pressure pulse tests in 5 holes intersecting the fracture and by measurements of natural flowrates and hydraulic heads. Figure 7.6 shows the location of the injection holes.

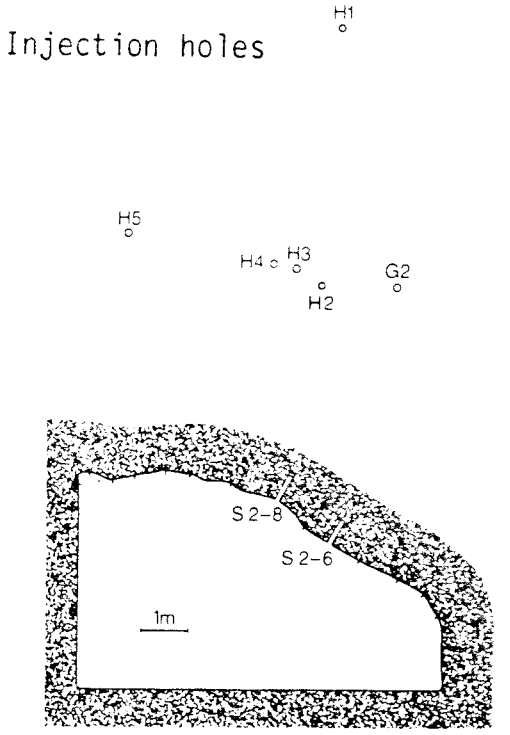

Figure 7.6 Location of injection and some collecting holes in fracture No. 2.

Figure 7.7 shows the natural flowrates into the collection holes of fractures no 1 and no 2. Water flow rates and hydraulic heads were also measured in the fracture of the pilot investigation.

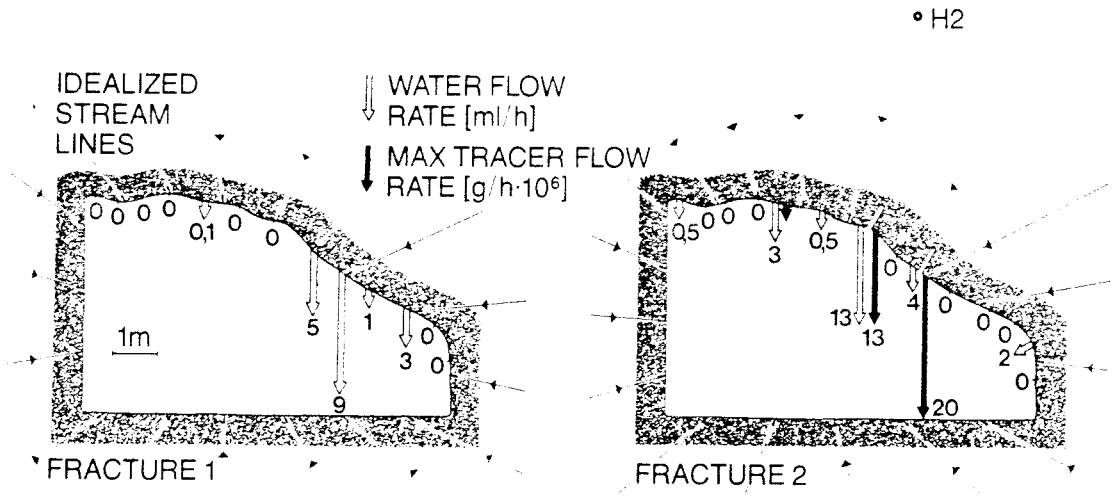

Figure 7.7 Water flowrates in fractures No. 1 and No. 2.

Tracers were injected over a 6 month period. Four different injection points were used. In one of the injection points, sorbing tracers, Cs, Sr, Eu, Nd, Th, U, as well as nonsorbing tracers, Iodide and Uranin, were injected simultaneously.

All water emerging from the fracture was collected under anoxic conditions to reduce the risk of precipitation of ferric iron hydroxides and other redox sensitive elements.

After the injection stopped the fracture was excavated. Small sample cores were drilled perpendicular to and into the fracture surface. These small cores were ground off in sections and each section analyzed for sorbed tracers.

The 7 nonsorbing tracers injected at the four different points H1, H2, H3 and H5 were monitored in the waters collected from the different collection points. See figures 7.6 and 7.7.

In hole H2 the tracers Iodide and Uranin were injected, the latter on two different occasions. Both Uranin and Iodide were found in collection holes S2-6 and S2-8. Uranin was also found in very small amounts in S2-9 and S2-10, two sampling points to the right of S2-8 at 0.7 and 1.4 m distance. See figure 7.7. Eosin from H3 was found in S2-6 and S2-8 whereas Albumin also from H3 was not found at all.

The sorbing tracers were injected in hole H2 continuously for 6 months. None of the sorbing tracers were found in the collected waters. This was expected except for Sr which had been predicted to have a fair chance of arriving within the year long monitoring period.

A total of 210 sample cores were drilled into the excavated fracture surface. The small sample cores were ground down in thin sections of approximately 0.2 mm starting from the surface of the fracture. The ground off samples were analyzed for the sorbing tracers.

Figure 7.8 gives Cs concentrations on the fracture near the injection hole. The increased concentration can be traced to a distance of about 0.5 m, which is the end of the cored out fracture in this direction.

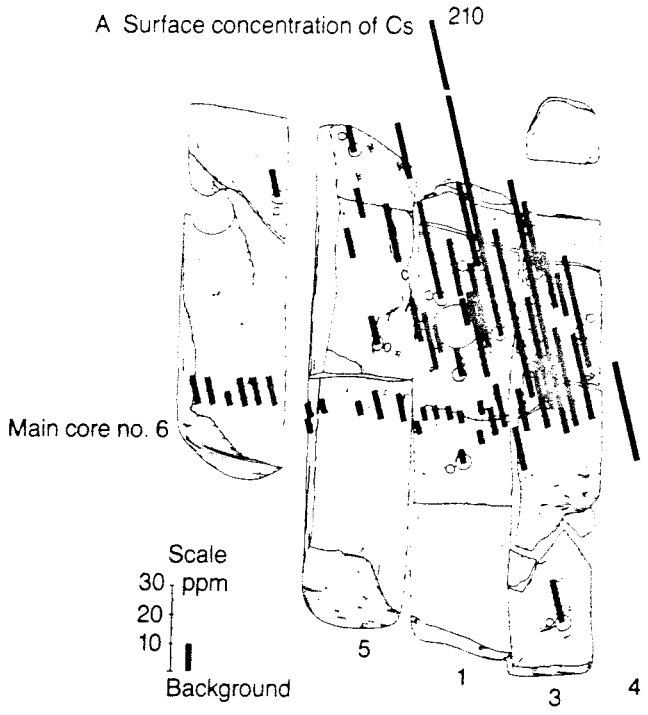

Figure 7.8 Examples of surface concentrations of Cesium and on fracture A. The injection hole is seen in core 1, a third from above.

Figure 7.9 shows the Cs concentration varying with depth at the different locations.

Figure 7.10 shows an example of the variation with depth of Cs, Eu, Nd, Th and U at a point about 50 cm "below" the injection point.

The data available made it possible to determine the fracture aperture in three different ways. By mass balance, by the laminar flow assumptions in a slit using pressure drop and flow rate data and from laminar flow and residence time data.

For the ideal parallel smooth fracture with laminar flow the three apertures should be the same.

The results will depend on if the tracer solution migrates without mixing or if it is mixed with the naturally flowing water at the injection point. If the injected tracer stream is carried by and flows with the velocity of the water in the fracture the tracer residence time will be the same as that of the water. This case is called the mixing case. If on the other hand the tracer solution is injected in a flow path where it moves more or less independently of the water in the rest of the fracture the tracer residence time may not reflect the residence time of the water. This is called the non mixing case. If the widths of the pathways in both cases are the same the fracture aperture for the much smaller tracer stream will be much smaller than that needed for all the water. Both radial and linear flow assumptions were tested in the analysis of the experiments.

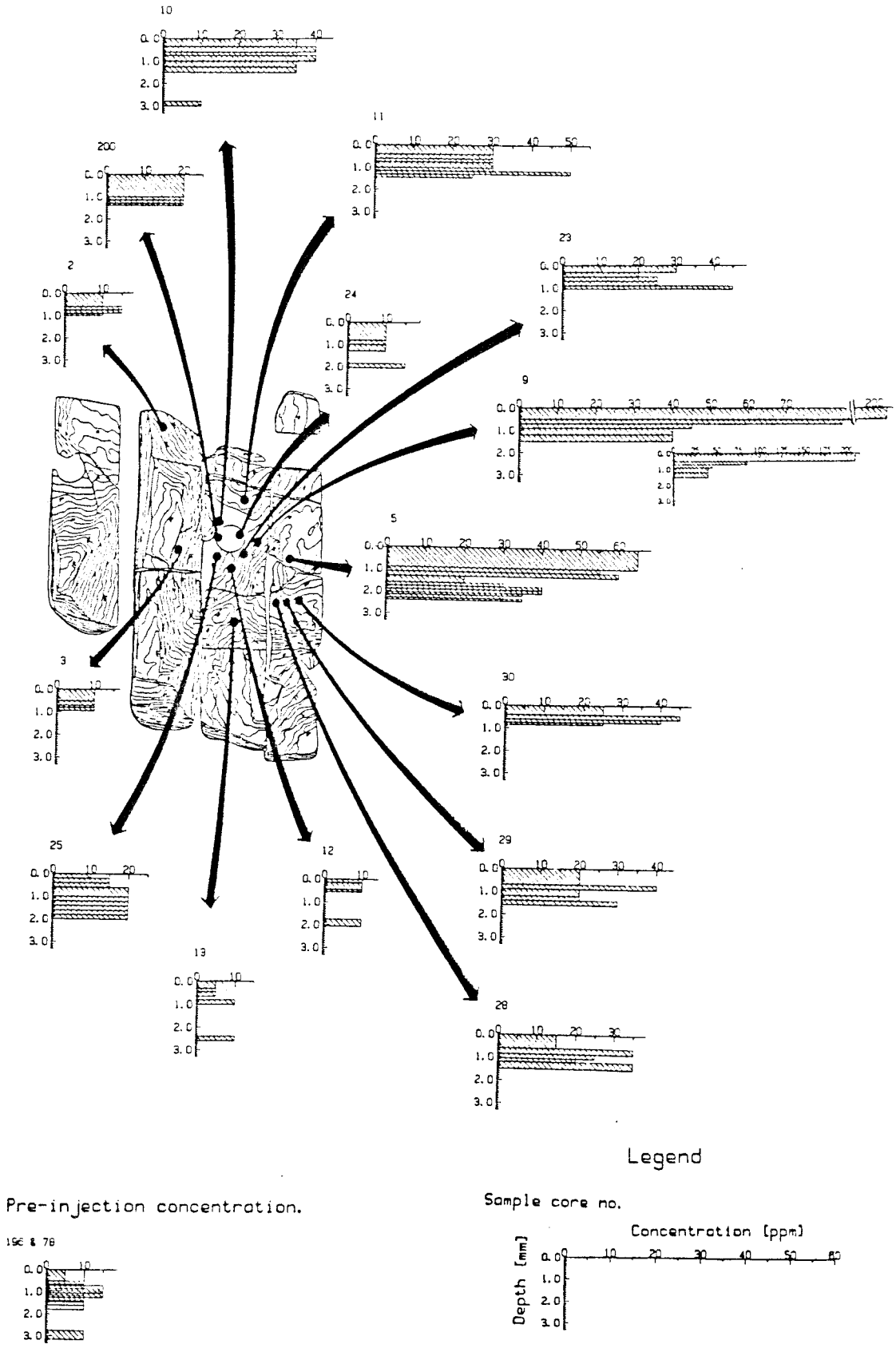

Figure 7.9 Variation of Cesium with depth at different locations in fracture A.

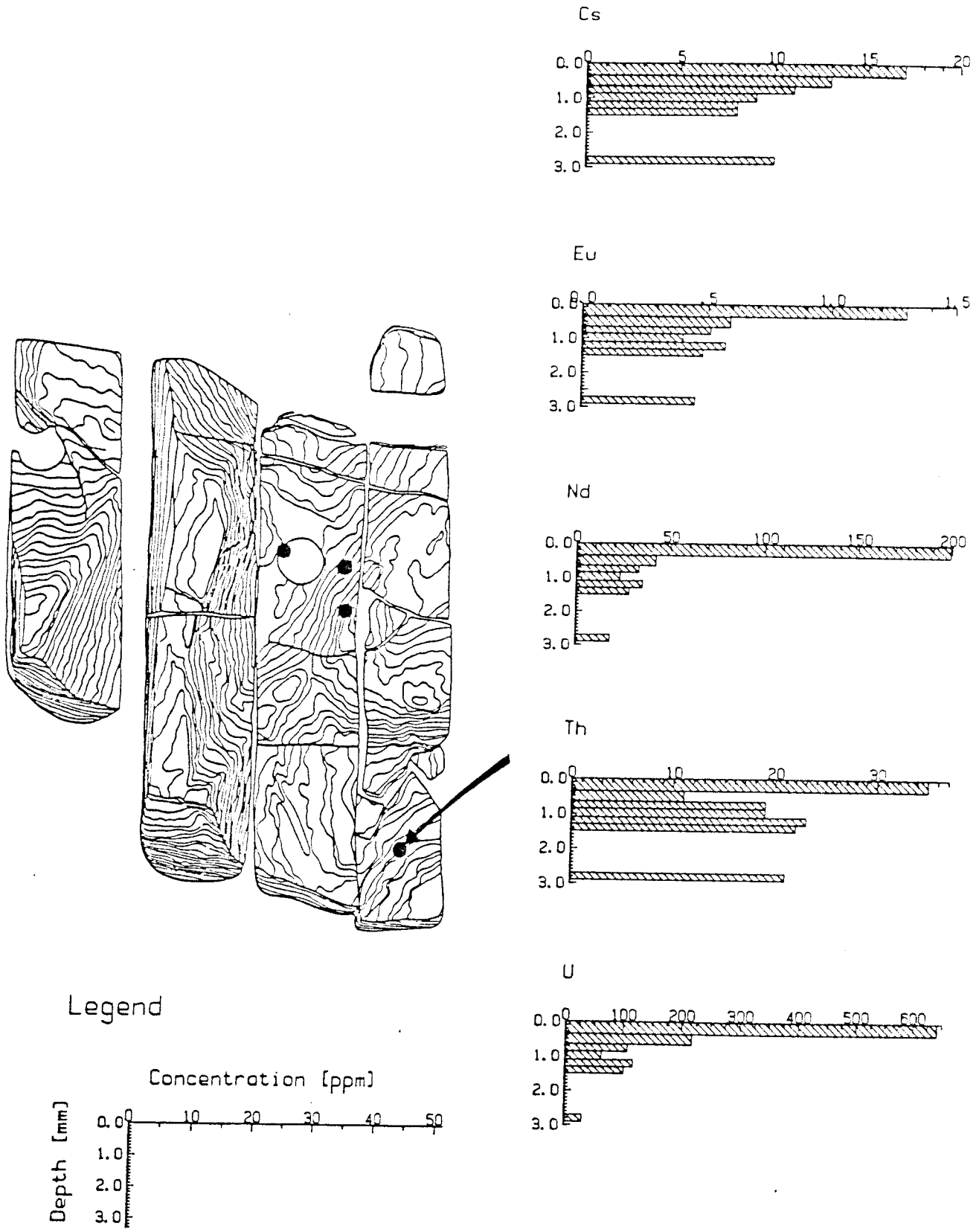

Figure 7.10 Variation of tracer concentration with depth in sample core no 142 in fracture A.

The results are given in tables 7.2 and 7.3.

Table 7.2 Fracture apertures (μm) assuming mixing at injection point.

Sampling hole	linear			radial		
	δ_f	δ_l	δ_c	δ_f	δ_l	δ_c
	mass bal	friction	cubic law	mass bal	friction	cubic law
S2-6	240	1.1	6.7	130	1.2	5.5
S2-8 (100)	280	2.0	10	150	2.1	8.5
S2-8 (500)	1400	0.9	10	750	0.9	8.5
4*	2200	1.3	16	1200	1.4	13
5*	1500	0.9	11	820	0.96	9.1

* Two sampling holes used in a pilot investigation in another fracture.

Table 7.3 Fracture apertures (μm) assuming mixing at collection point.

Sampling hole	linear			radial		
	δ_f	δ_l	δ_c	δ_f	δ_l	δ_c
	mass bal	friction	cubic law	mass bal	friction	cubic law
S2-6	60	1.1	4.7	43	1.2	3.8
S2-8 (100)	28	2.0	4.6	15	2.1	4.0
S2-8 (500)	140	0.9	4.6	75	0.9	4.0
4*	20	1.3	3.2	10	1.4	2.6
5*	90	0.9	4.3	50	0.96	3.6

* Two sampling holes used in the pilot investigation

A single fracture with an aperture corresponding to the one calculated from the frictional losses (δ_l) could not carry all the water entering the sampling holes. There have to be several of these fractures within the fracture plane to obtain water flow rates equal to those measured at sampling holes S2-6 and S2-8. The actual number is obtained by dividing the mass balance aperture and the frictional loss aperture δ_f/δ_l.

Three different model concepts were tested against experimental data: the advection-dispersion surface sorption model, the advection-dispersion matrix diffusion model, and the channeling model with no intermixing between channels.

Fitting of the actual models to the experimental breakthrough curves for the nonsorbing tracers was done to obtain residence times and dispersion information. The residence times for the pathway emerging at collection hole S2-6 was found to be 280-350 h for all threes models fitted. For the pathway to S2-8 the residence times

were between 530-710h. An extremely low value of 45 h was found in one fitting attempt where the effect of matrix diffusion was unrealistically large. Dispersion values corresponding to Peclet Numbers of 1-3 were typical resulting from the very long tails.

Figures 7.11 and 7.12 show the fit between the three different models and the experimental data. As can be seen in the figures it is possible to get a good fit with all the models. It is not possible to select between the models with the results from this experiment only. Some of the mechanisms and their parameters have to be determined independently.

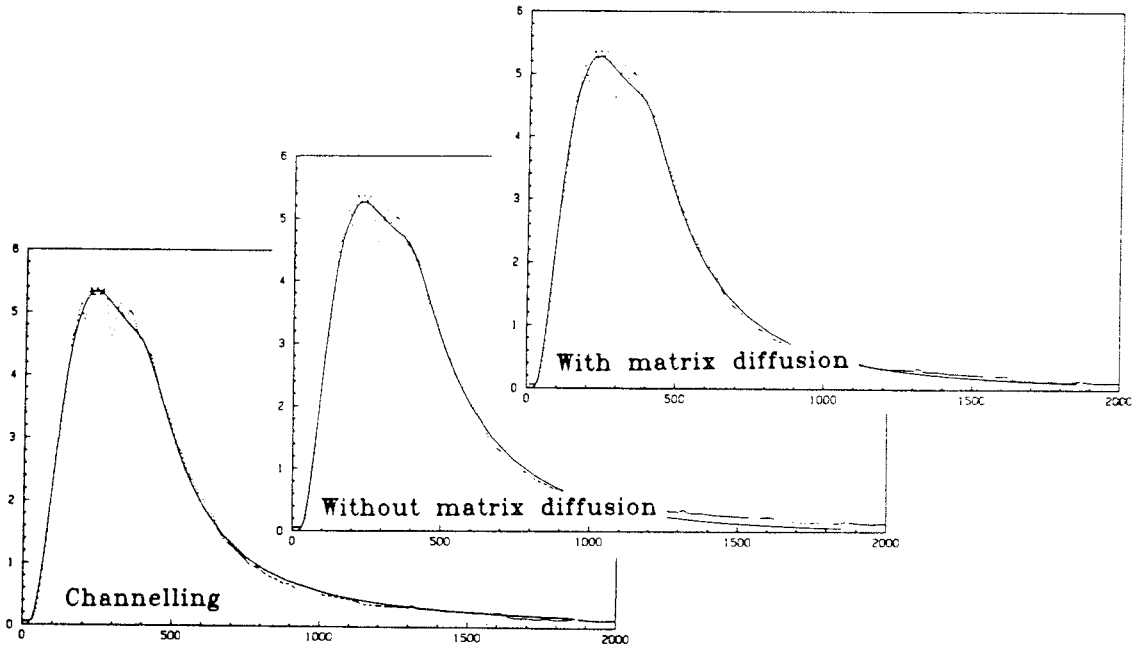

Figure 7.11 Best fit between models and experimental data at sampling hole S2-6 Left figure: channeling without matrix diffusion. Middle figure: advection-dispersion. Right figure: advection-dispersion with matrix diffusion.

Uranin injected in hole H2 gave the highest concentrations and the shortest residence times, on the order of 300-700 h depending on model. The other tracers arrived in very low concentration and after longer times. Elbenyl injected in hole H1 at about 9.5 m distance just reached the detection limit after 1 500 h when the experiment was closing down.

Iodide injected in hole H2 together with Uranin behaved very similarly to Uranin.

Eosin injected in the hole H3 was found in both S2-6 and S2-8. The breakthrough curves showed two peaks indicating at least two different pathways. The residence times were longer from H 3 than from H 2. Figure 7.13 shows the breakthrough curves of Uranin and Eosin plotted in the same diagram. It should be noted that the two injection holes are at practically the same distance from the collection point S2-8. This observation together with the fact that hardly any tracer could be injected in hole H4 strongly suggests that the hydraulic and transport properties are very variable within a fracture.

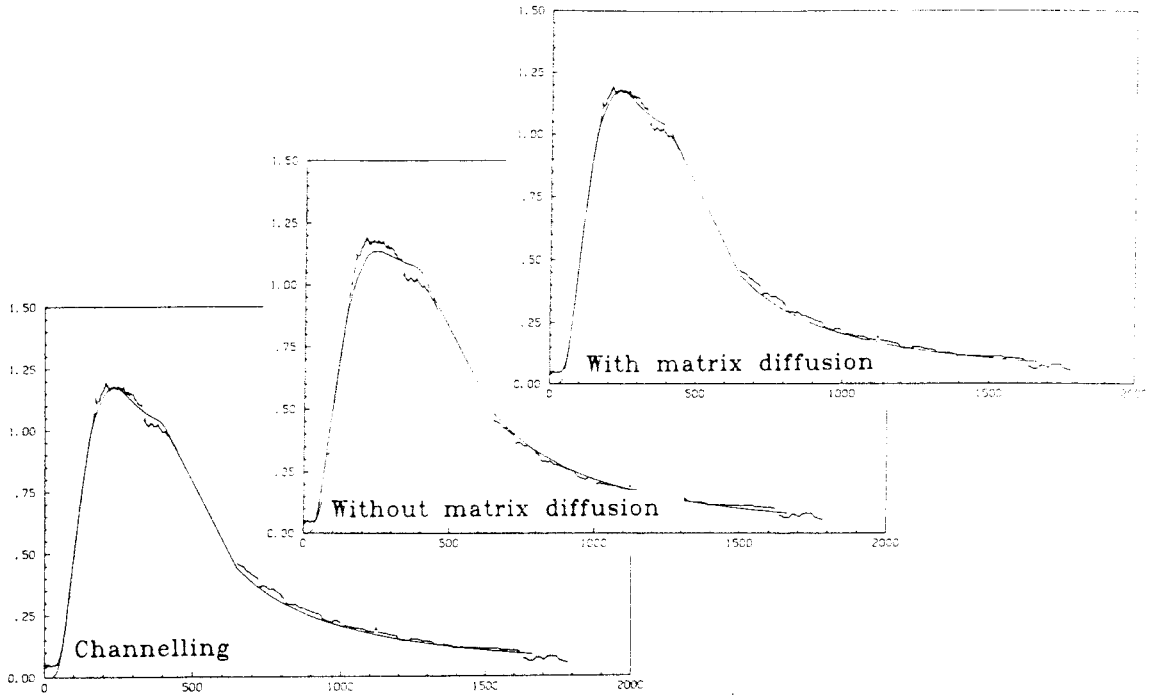

Figure 7.12 Fit between models and experimental data at sampling hole 2-8.

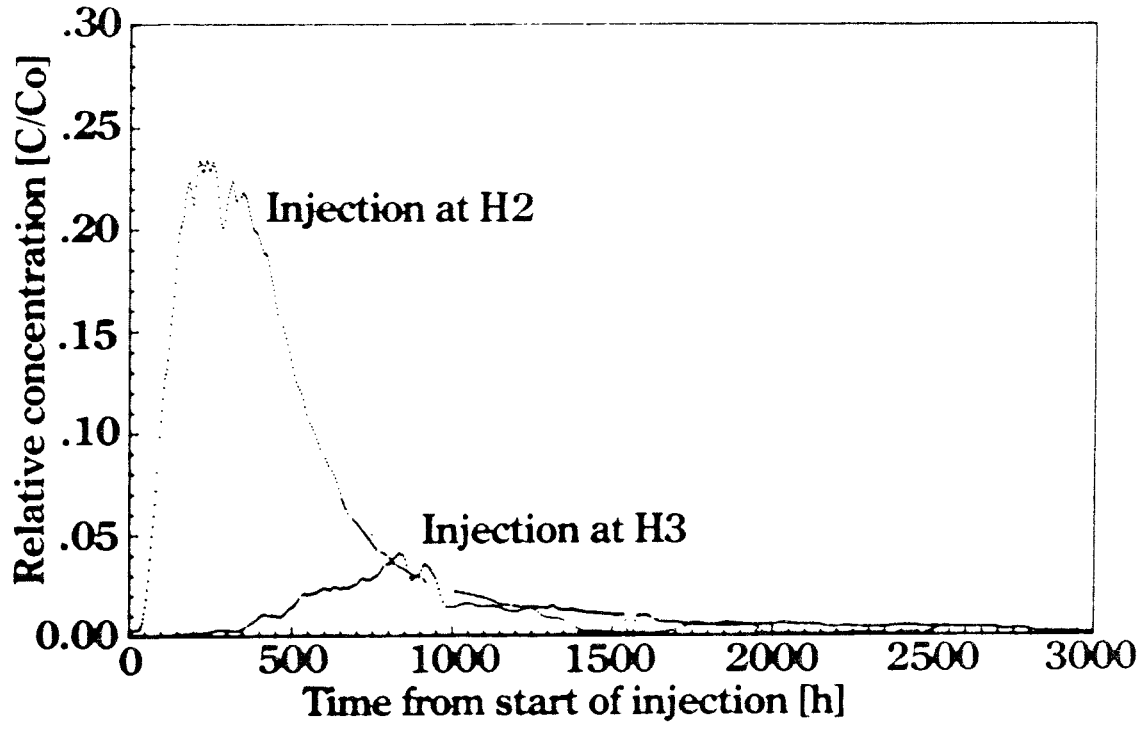

Figure 7.13 Breakthrough curves at sampling hole S2-8 for injection at point H2 and point H3

The results of the fitting show that the spreading of the tracer pulses is very large. If it is interpreted as hydrodynamic dispersion as in the advection-dispersion model, Peclet numbers of on the order of 1-2 are obtained. This means that the dispersion length is between half and up to the full travel distance.

The attempt to fit the advection-dispersion-matrix diffusion model gave similar results when laboratory data on the diffusivity was used. The matrix diffusion may have been noticeable in the pathway H2 to S2-6 but not in the pathway H2 to S2-8. The fitting of the channeling model gave similar results.

It is clear from the results that none of the models give a unique interpretation of the experiments. There are indications as for the Eosin runs from H3 that there are at least a few different major flowpaths. In such circumstances attempts to fit models which basically assume one flowpath will lead to bad fits and seemingly high dispersion numbers.

The results show that the assumption of where the tracer enters the main stream of the water is crucial to the interpretation of the fracture aperture (mass balance). This assumption cannot be checked with the information available.

Whichever mixing case is the more correct it is evident that the aperture estimated by the cubic law cannot give a good estimate of the aperture which determines the residence time (the mass balance aperture).

The sorbing tracers Cs, Sr, Eu, Nd, Th, U were injected in hole H2 together with the Uranin. These stable nuclides already exist in the rock and groundwater and the added concentrations will be superimposed on those in the system. Both water samples and rock samples were therefore taken before the injection started.

The sorbing tracer concentrations on the fracture surface show a very scattered picture, figures 7.9 and 7.10.

It was not possible to reconcile this information with the assumption of smooth even pathways.

In this field experiment it was attempted to investigate flow and tracer behavior in a natural fracture in granitic rock. The experiment was designed on the basis that the fracture would have a variable water flow in different parts, so called channeling effects. A considerable number of injection and collection points were therefore used. It was envisaged that the sorbing tracers would not arrive to the collection points and that the fracture must be excavated after the experiment. The variability of flowrate in the fracture was clearly seen and was found to be more important than originally anticipated. It was found that the volumetric fracture aperture was very different from that calculated from the transmissivity. This may be caused by fracture filling materials in a natural fracture. It was concluded that the fractures investigated did not by far behave as parallel walled fractures either from the pressure drop point of view or as to the uneven flow. Channeling was very pronounced.

The sorbing tracers were found to be strongly retarded and to have penetrated the matrix of the rock as anticipated from laboratory experiments. Due to channeling effects which made it impossible to monitor all possible surfaces for the sorbing tracers no mass balance for these was possible. The concentration profiles into the rock matrix of the sorbing tracers near the injection point had concentrations and penetration depths which are within the expected ranges.

7.2.2 Chalk river experiments

A set of tracer experiments have been performed in a single fracture in a monzonitic gneiss rock body at Chalk River in Canada. In one radially diverging test the distance was 50 m and covered several pathways (Novakowski et al. 1985a). Hydraulic tests were made and resulted in cubic law apertures of 16-61μm. The estimates from the tracer tests gave similar apertures.

Another experiment in the same location, but involving only one fracture, was run as injection withdrawal tests over a distance of 10.6 m. Novakowski et al (1985b) analysed these tests using an advection diffusion model and the assumption that the flow field was a dipole. The hydraulic formation gave cubic law apertures of 60 μm and the tracer tests gave values of 510 μm. Dispersion lengths obtained by curve fitting were found to be 1.4 m.

In a third experiment in the same rock body, 5 test were made. four of them as injection withdrawal tests and one as a radially converging test. The distances were 12.7 and 29.8 m. Both injection- withdrawal tests and radially converging tests were made with pulse injection of tracer. In the latter test the non sorbing tracers $^{82}Br^-$ and a dye, sodium Fluorescein were used. The fracture was located at about 35 m depth (Raven et al 1988).

The breakthrough curves had peak arrival times between 2 and 6 hours for the shorter distance and about 60 h for the longer distance using hydraulic head differences for the injection withdrawal tests of 2.35 to 4.90 m and 5.95 m for the short and long paths respectively.

These tests were analysed using both the conventional advection-dispersion model and dipole flow field, when appropriate, but also with a model which accounts for exchange of solute with stagnant water volumes adjacent to the mobile water. The transfer rate between the mobile and the stagnant water was assumed to be proportional to the concentration difference and the volume of stagnant water was assumed to be finite. The model was called "the transient solute storage model". Two additional fitting parameters were needed, the transfer coefficient and the volume of stagnant water. Because of the short residence times the effects of matrix diffusion were ruled out.

The advection-dispersion model gave very bad fits to the experimental data especially in the tails. The transient solute storage model gave excellent fits with the fraction of mobile water ranging between 0.35 and 0.65 for the shorter flow path. For the longer flow path where the residence times was more than one order of magnitude larger, all the water could be modelled as mobile. This was interpreted as all stagnant water having been equilibrated with the mobile water.

Cubic law apertures ranging between 110 and 190 μm were obtained from hydraulic tests and the tracer tests gave values of 95-115μm. This is somewhat surprising because hydraulic (cubic law) apertures tend to be smaller than residence time apertures. The reported apertures do not seem to include the presence of the stagnant water volume and as this was found to be about as large as the mobile water volume, the total volume available for a solute will be about twice as large once the solute has accessed it. Accounting for this effect the residence time aperture will be larger than hydraulic aperture.

8 LARGE SCALE FLOW AND TRACER EXPERIMENTS

8.1 Stripa 3D investigation

8.1.1 Overview

In the Stripa experimental mine a drift was excavated at the 360 m level below the ground in order to study water flow and tracer migration in low permeability fractured granite. The broader aim was to understand and quantify transport processes relevant to the safety of a final repository for high level radioactive waste (Abelin et al. 1987).

The drift, which is located in water saturated rock, has a natural inflow of water. The water flowrate to the totally 100 m long drift was monitored by collecting the water in about 375 plastic sheets which were glued onto the ceiling and upper part of the walls. More than 700 m^2 of the drift was covered. This is half the total surface of the drift. In addition the water inflow to the lower part of the drift was measured by a ventilation test. The water inflow to the 140 m long access tunnel was also measured by a ventilation experiment. Hydraulic heads were measured in three vertical 70 m long holes extending upwards from the drift. Water flows were monitored for more than 2 years.

The three vertical holes were completely sealed off except in a total of nine 2.5 m long sections at distances varying from 10 to 55 m from the drift. Nine different tracers were injected for nearly two years into these sections. Later two more tracers were added to the injected water in one of the previous locations.

The tracers were monitored in all sheets carrying water and in some locations in the floor of the drift where water was seeping out. Many of the tracers were strongly colored dyes and were looked for in other nearby drifts and galleries as well as in waters sampled in other places in the mine. Six of the tracers arrived in measurable concentrations in many of the water bearing sheets. In all 167 tracer breakthrough curves suitable for interpretation were obtained. Average travel times were between 2000 and 7000 hours. Tritium was also looked for in some sheets and was found in two of them.

The recovery of the tracers varied between 2.8 % and 65 % for 5 of the tracers. One of the tracers had a recovery of 0.002 %, four were not found at all, and one was recovered in a considerable but unknown quantity. The tracers which were not found were, as a rule, injected at the farthest distances.

Very few investigations have been made regarding flow and transport properties in deep lying crystalline rocks. There are no well developed techniques available to investigate the properties of interest. The flow patterns and mechanisms are not well known and the investigative techniques must be developed so that many conceivable results can be accommodated with the experiments.

The flowrates, velocities, channeling frequencies and geometry of pathways were not known before the experiment to within several orders of magnitude. Nor were the possible variations in the properties known or could be reasonably assessed. To accommodate possible large variations of these properties some special techniques were developed. The basis for the whole experiment was the development of the large scale plastic sheeting technique which permitted a very detailed monitoring of the

water flowrate and tracer path distribution. Another special aspect of the experiment was to use as many different tracers as possible, 9+2 tracers, in order to investigate variations in the transport properties of the rock. The choice of different injection distances was made with dual purposes. First, because of the a priori unknown water velocity a large difference in the migration distance would ensure that at least some of the tracers would arrive during the duration of the experiment. Second, different migration distances along essentially the same flow path may give information on how the dispersivity is influenced by the migration distance. This is an open question of some importance.

The size of the wetted surfaces is unknown. If it is large, small molecular weight tracers might diffuse into the micropores of the matrix and to a large extent be withdrawn from the mobile water (Neretnieks 1980). This might cause the tracers to be retarded and diluted to such an extent that detection in the collected water in the drift may be difficult. Tracers of different molecular weight were used and a high molecular weight tracer was synthesized especially for this purpose.

8.1.2 Experimental

The experimental drift was excavated starting about 100 m from the nearest drifts and extending 75 m due north further into the undisturbed granite. Figure 8.1 shows an overview of the mine adjacent to the experimental drift. Figure 8.2 shows the plastic sheeting arrangement.

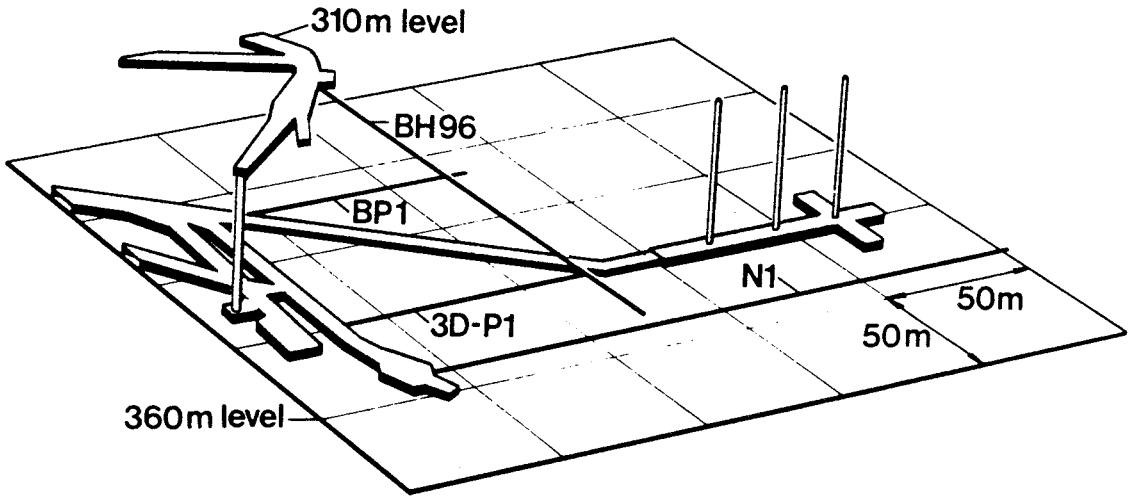

Figure 8.1 Overview of the mine adjacent to the 3-D test site.

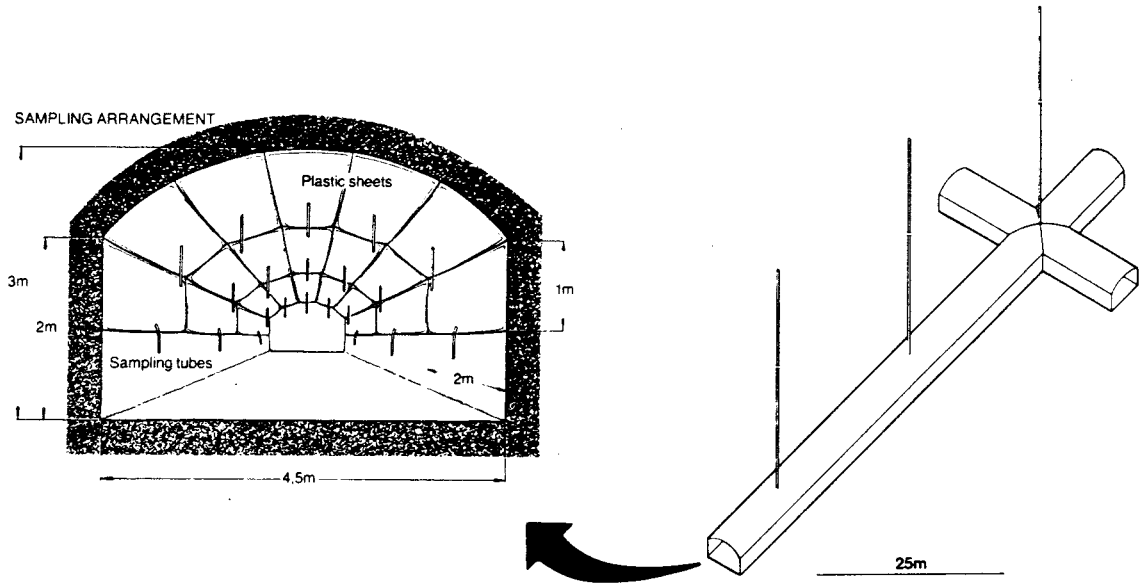

Figure 8.2 Dimensions of the 3-D test site.

Monitoring of water flowrates was performed at different locations and during different time periods. In a pilot hole which was drilled into the region where the test was to be located, water inflow rates were measured over 7.5 m intervals. As soon as the site had been fracture mapped and photographed, the upper part was covered with plastic sheets which allowed a high resolution in water inflow and tracer monitoring. The water inflow monitoring continued for 26 months. During this time period the injection holes were drilled, measured, sealed, and the injection of tracers was completed. The water inflow rates to the three vertical injection holes were measured in 2 m sections. In addition to the detailed inflow rate in each sheet the total water inflow rate has been monitored by a "ventilation experiment." In this experiment the total inflow rate to the access drift was also monitored.

Water samples were collected in test tubes every 16 hour from all sampling sheets with a high enough water flowrate. Data exist on the breakthrough from 7 of the 11 injected tracers that were found in about 65 different sampling sheets. Tritium analysis has been performed on water samples from both the site and from the injection holes.

8.1.3 Results

The upper part of the test site, approximately 700 m^2 (which is half the surface area of the test site) was divided into about 350 sampling areas each with an area of 2 m^2. As more sheets were added during the experiment at potential points of interest there were approximately 375 sheets at the end of the experiment. Each sampling area was covered with a plastic sheet. The total water inflow to the covered area was 0.7 l/h. Of the 375 sampling sheets 145 gave measurable amounts of water, 50 % of the total inflow came from approximately 3 % of the covered area. The wettest sheet carried

about 10 % of the total inflow. The water inflow rate distribution from the "undisturbed" rock (prior to the drilling of the three injection holes) was monitored for 6 weeks. The results from these measurements are presented in figure 8.3 where it can be seen that the water inflow is concentrated in a few areas with large dry areas in between.

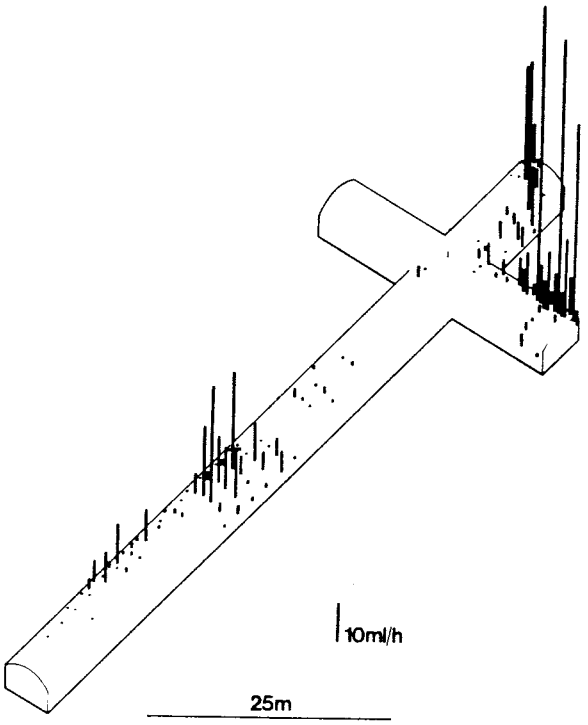

Figure 8.3 Water inflow rates into the test site before drilling of the injection holes.

The duration of the ventilation experiment was half a year. The total water inflow rate into the uncovered part of the test site and access drift was found to be 4 l/h. Of this measured total water inflow 2 l/h came from the uncovered part of the test site. Summing up all the measured inflow into the test site gives a total measured inflow of 3.1 l/h, which compares well with the water inflow rate into the corresponding part of the pilot hole, 3 l/h, which was drilled prior to excavating the drift.

The water flowrates and tracer occurrences along the two drifts were compared with the following fracture characteristics per surface area within 2 m sections, along the two drifts:

- Total fracture lengths
- Total zone lengths
- Number of fracture intersections
- Presence of different fracture filling materials
- Fracture length within the 4 fracture sets.

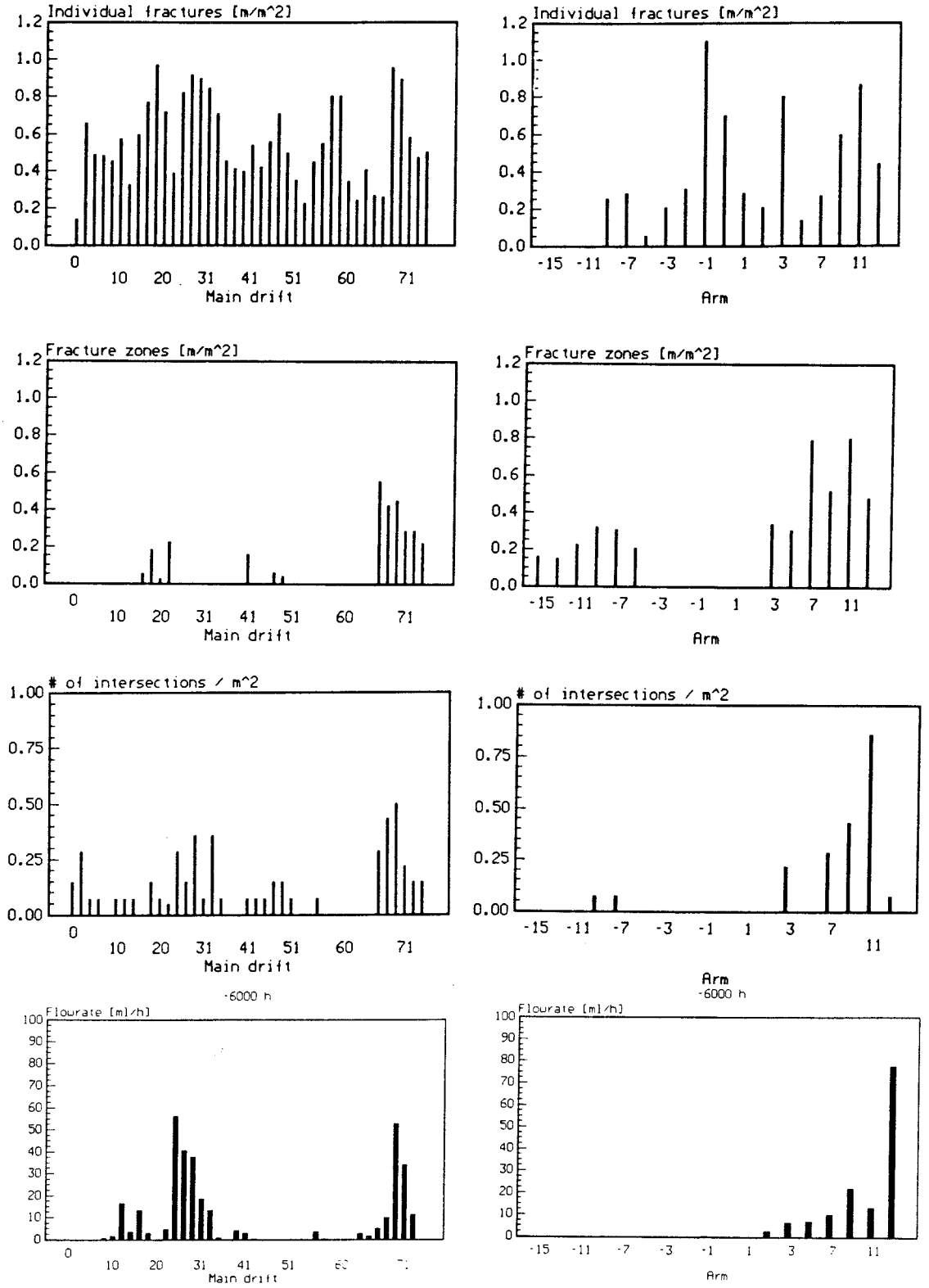

Figure 8.4 Fracture length, fracture zone length, and number of single fracture intersections per m for main drift and arm. Water flowrates for main drift and arm before drilling of the injection holes.

The first three fracture characteristics for both the individual fractures and fracture zones are given and can be compared with the water flowrates for the main drift and the arm given in figure 8.4 and can be compared with the water flowrates for the main drift and the arm given in the same figure. In the histograms for the number of intersections only the intersections concerning individual fractures and not zones are included. Comparisons between the flowrates and histograms for individual fractures and fracture zones for the four fracture sets and fracture fillings were also attempted. No obvious correlation between these fracture characteristics and the measured water flowrates is evident. On the other hand the areas which have a higher number of fracture intersections have higher water flowrates. This was thought to be a significant finding and it is in accordance with observations in another investigated site in Sweden.

The tracers were injected continuously at distances ranging from 12 to more than 55 m for more than 20 months. Water entering the test site was sampled for tracers during the time of injection plus an extra 6 months after the end of injection. Injection flowrates varied between 1 and 20 ml/h.

An overview of tracer breakthrough is given in the following figures. Figure 8.5 shows the test site from the side and to which parts of the test site the different tracers have migrated.

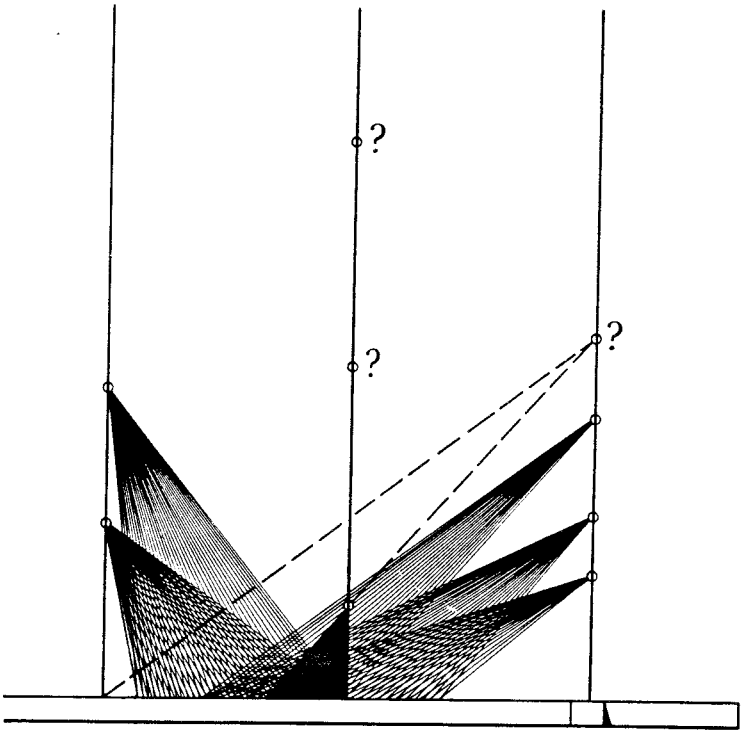

Figure 8.5 Areas in the test site where the different tracers have emerged.

It can be seen in figure 8.5 that tracers from 6 of the 9 zones have emerged into the test site. During the last period of reduced sampling a seventh tracer was found which is illustrated with dashed lines in figure 8.5. This occurrence might be due to the preparations for Stripa Project Phase III.

No tracers were found in the right part of the arm which is the area with the highest water inflow rates. The right arm is also closest to the injection zones in hole III, but the tracers injected at these zones emerged at the central part of the main drift.

Figure 8.6 shows a view from above of where tracers were found. Only those sampling areas with "high" water flowrates i.e. connected to fractional collectors, are included in the figure. Figure 8.7 shows the locations where the individual tracer emerged. As can be seen in figure 8.7 all tracers emerge in the central part of the main drift over a length of 35 meters.

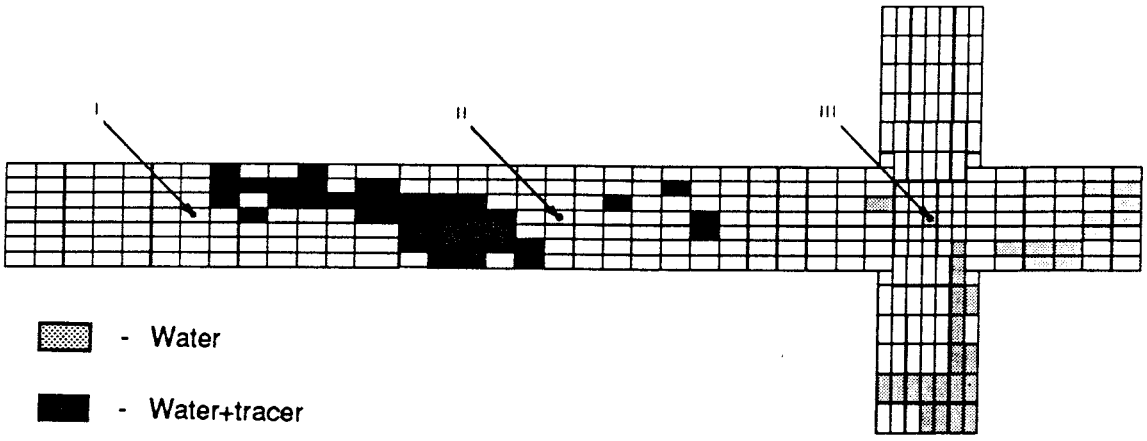

Figure 8.6 Areas where tracers have been found in the test site.

Figure 8.8 gives an example of breakthrough curves for the different tracers. More than 160 such curves were obtained with up to a thousand individual measurements each.

Tritium is often used as an environmental tracer. Infiltrating rain water contains about 10-20 TU (Tritium Units), at present. During the nuclear bomb tests in the 1950's and 1960's considerable amounts of Tritium were released to the atmosphere. The Tritium content of the rain was increased considerably and peak values of more than 500 TU were measured in the period 1963-1967. The Tritium content of water before the bomb tests was on the order of 5 TU. Tritium has a half-life of 12.3 years. Therefore "pre-bomb" Tritium should have decayed to about a tenth of the initial concentration of those times i.e. to values below 1 TU. If values higher than this are found, then it is an indication that the surface water has reached the sampling points in less than about 30 years.

Tritium samples were taken in May 1985 and in June 1986 at some locations in the drifts and in two of the injection zones in hole III.

The result indicate that in at least two sheets where the tritium concentration was 5.1 and 5.7-7.3 TU, the surface water has had a residence time of less than 30 years.

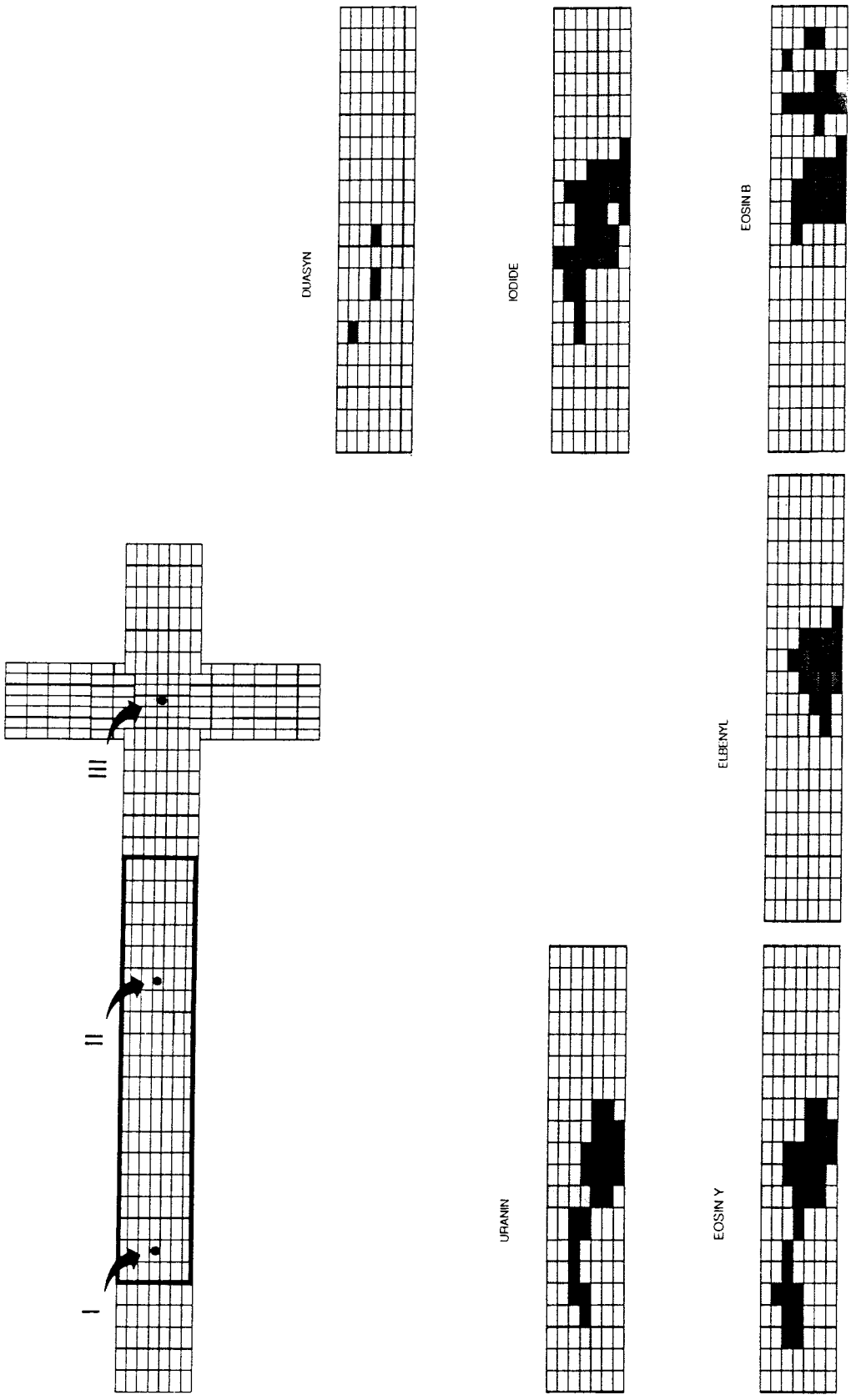

Figure 8.7 Tracer occurrence in the main drift for the individual tracers.

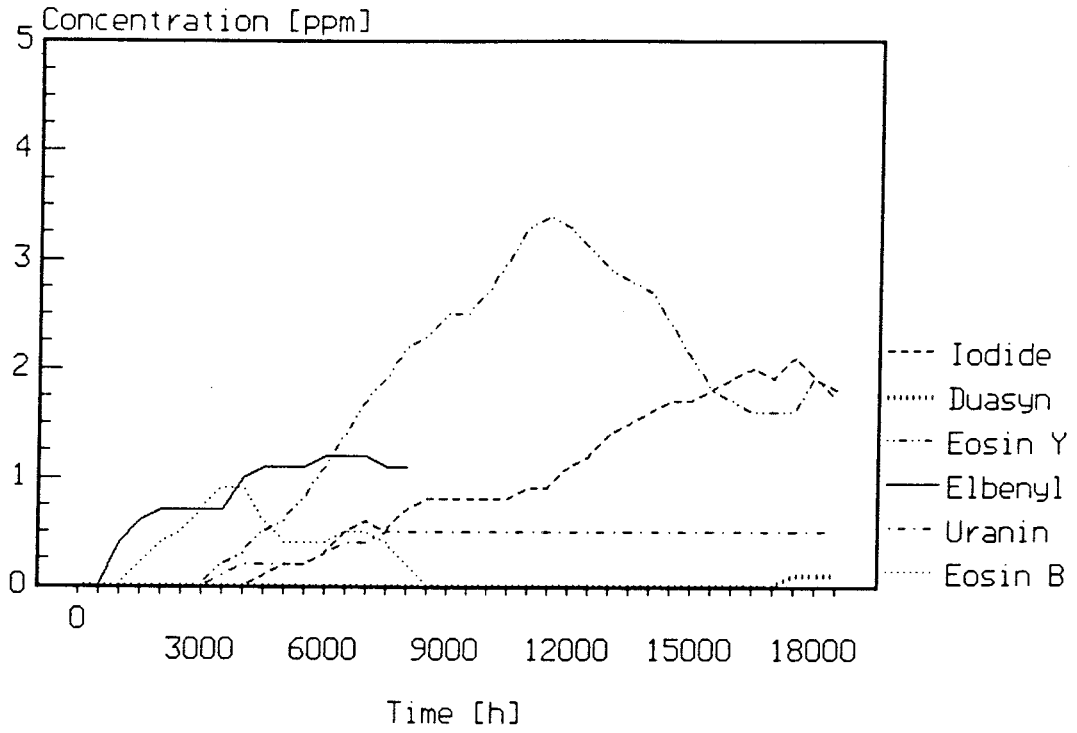

Figure 8.8 Example of different breakthrough curves.

8.1.4 Evaluation and interpretation of experimental results

The tracer tests were analyzed using different models, see table 8.1.

Listed are some items that are of special interest in evaluating the different models:

- Water travel time (flow porosity)
- Dispersion length
- Matrix diffusion effects
- Wetted area
- Channeling characteristics.

Models which have more parameters may describe more mechanisms and thus may give better agreement with the experimental results. Of the models used, the simplest models contain only three parameters, e.g. travel time, dispersivity and dilution factor, and the more complex models include four independent parameters. By including more parameters it is easier to obtain better fits without actually increasing the physical meaning of the obtained parameter values. However, a good fit does not imply that the mechanisms which the model is based on actually are active at all. Therefore several models have been analyzed with different mechanisms which may give similar results, e.g. the spreading of a tracer pulse may be caused by hydrodynamic dispersion, channeling, matrix diffusion, or some other causes which are not included in the model. The three mentioned mechanisms will in many circumstances lead to a similar spreading of a pulse and cannot be distinguished from one another by just fitting one or a few experimental curves in a model. In order to separate out the various mechanisms, independent information is needed.

Models used for fitting tracer concentration curves

Table 8.1 below summarizes the models used and the parameters which are obtained with each model.

Table 8.1 Models used and parameter values determined.

Model	Parameters
Advection-Dispersion (AD)	t_w, Pe, DF
Advection-Channeling (AC)	t_w, σ_l, DF
Advection-Dispersion-Matrix Diff. (ADD)	t_w, Pe, A, DF
Advection-Channeling-Matrix Diff. (ACD)	t_w, σ_l, D_D, DF

The theoretical models were fitted to the experimental results by a least squares nonlinear fitting process.

First, all the selected individual curves were fitted with the AD model (Advection-Dispersion Model). Of the nearly 170 different curves fitted many had high dilution factors and contain very small amounts of the tracer in comparison to the other curves.

After fitting "all" the tracer breakthrough curves, a set of 5 selected curves were chosen for each tracer. The selected curves accounted for a significant amount of the tracer. These curves were studied in more detail with the ADD model and AC model.

The results from the model fits indicate that the dispersion for many of the breakthrough curves was very high. There are many conceivable reasons for high dispersion values. One is the spreading of the tracer pulse by diffusion of the tracer into and out of stagnant or nearly stagnant volumes of water. Such volumes of water are known to exist in the porous matrix of the rock as well as in the fracture itself. They can be accessed by molecular diffusion from the flowing water in the channels. The ADD model was used to investigate this possible cause of dispersion and also to investigate the matrix diffusion. The matrix diffusion mechanism may be an important cause of withdrawing the tracer from the flowing water and into the rock, thus causing a less than full recovery to be obtained even after very long collecting time periods.

The injection flow varied with time and for this reason a mean value for the injection flow (or mass of tracer injected in a given time) could not be used. The breakthrough curve of variable injection can be calculated using the convolution theorem which requires an integration over time.

The breakthrough curves were first fitted using the Advection- Dispersion Model. The curves which were near the detection limit were often erratic and were not used. Curves in which a plateau was not reached were not used either. In total 167 individual breakthrough curves were fitted. In these nonlinear least square fits three parameters were fitted: the Peclet number, the residence time, and a dilution factor. Preliminary results showed that most of the curves have a very low Peclet number (high dispersion). The model used was not valid for Peclet numbers less than three

(Sauty, 1980). For this reason the Peclet number was limited to values greater than 4.0. It was observed that the dispersion was low for the runs with the tracer Iodide. The runs with the tracers Eosin B and Uranin showed high dispersion. The agreement between the fitted curves and the experimental data was good for the runs with the tracers Eosin Y and Iodide. The agreement was very bad for the runs with the tracer Uranin. Figures 8.9-8.13 show some typical results of the fitting.

In figure 8.9 it is shown that the theoretical curve does not reproduce the form of the experimental points very well. There are two distinct dips in the experimental points at 5000 h and at 15000 h which are not seen in the fitted curve. The fit gives a residence time of 7045 h and a Peclet number of 5.1. A visual observation of the experimental points shows that the fitted curve cuts over the two early peaks. Inspection of the other curves for Eosin B shows that the form of the response curves are quite different in some cases. This indicates that there is more than just advection and hydrodynamic dispersion occurring which influences the responses along these pathways.

Because a large number of the curves available contributed to a very small amount of the total recovered tracer, five curves for each tracer were chosen for continued analysis. These curves were chosen because they represented an important part of the tracer recovered during the observation time or because they represented the different zones where the tracer was found.

From these results representative values for the transport parameters are determined and are shown in table 8.2. The tracers Eosin B and Uranin show a very high dispersion. The Peclet numbers for the tracer Iodide were about 30.

Table 8.2 Representative values for the parameters obtained from the Advection-Dispersion model.

Tracer	Peclet number	Residence time [hours]	Distance from injection [m]
Eosin B	4.0	6 000	31
Uranin	4.0	5 000	35
Elbenyl	5.0	2 000	11
Eosin Y	5.0	7 000	24
Iodide	30	8 000	41

The ADD Model requires the determination of four parameters: the Peclet number, the water residence time, a parameter which takes into account the diffusion into the rock matrix, and the dilution factor. It was found that the parameter which accounts for the matrix diffusion effects could not be determined in this way because it influences the curves in a similar way as does the dispersion and the two processes could not be distinguished sufficiently well with the data available. Another approach to determine matrix diffusion effects is discussed later.

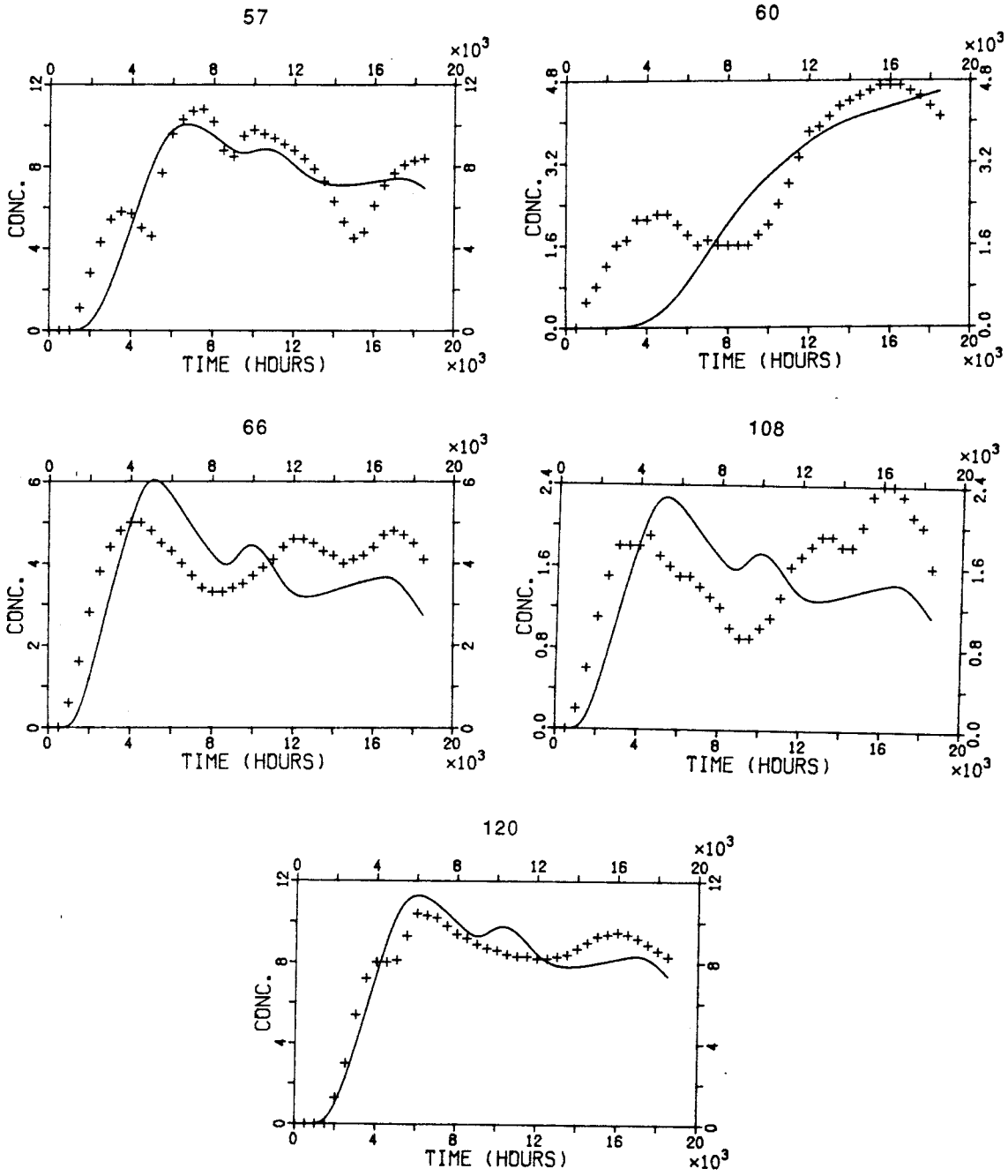

Figures 8.9-13 Eosin B breakthrough curves from selected sheets. The full line gives a fitted curve by the AD model and the crosses show selected experimental points. The figures are numbered from left to right, starting in the upper left corner.

When the flowrate, the residence time, and the travel distance are known, the flow porosity may be evaluated. This is done by using the assumption that the flow is radially converging.

Other assumptions also had to be made. Only the flowrate of the water with the tracer was said to have the residence time of that tracer. The flow area was taken to that section of the covered drift where tracer was found. The pathlength was taken to be the shortest distance between drift and injection hole. The uncertainties involved in these assumption can easily lead to uncertainties in the determined "average" porosity of a factor of two. It may even be questioned if it is meaningful to try to assign an average porosity to so limited a portion of a heterogeneous rock at all.

Figure 8.14 shows a plot of the porosity as a function of the distance to the injection point. There is a tendency for the porosity to decrease with increasing distance.

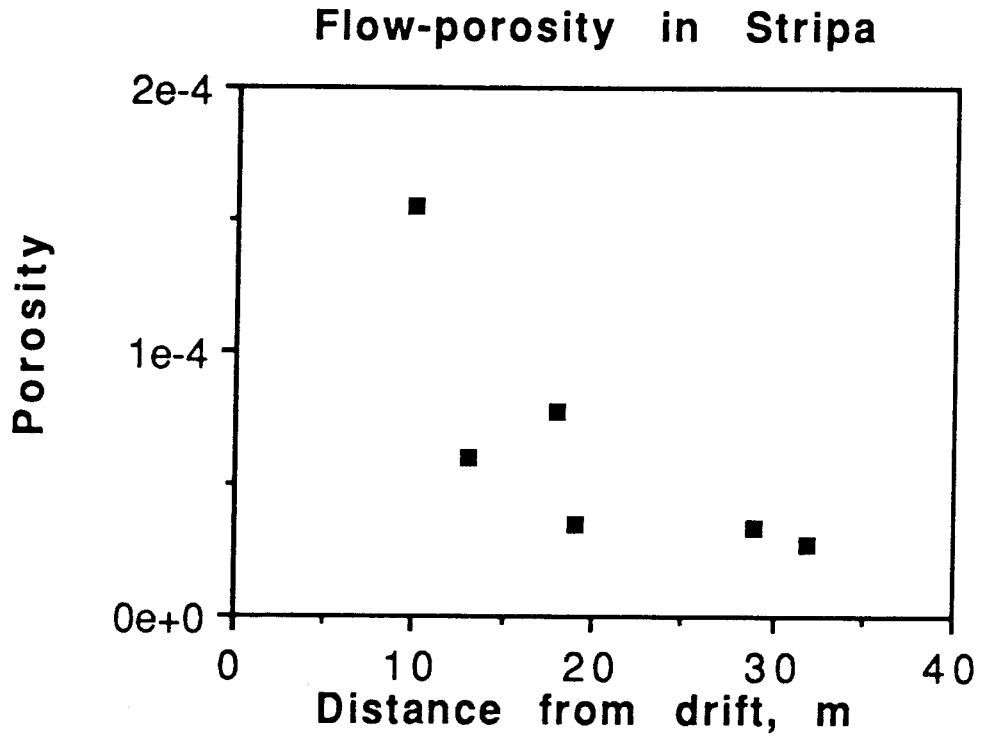

Figure 8.14 Porosity versus distance from drift.

In the determination of the porosity there is an underlying assumption that the residence time measured with the tracers represents that of the main flow in which the tracers were subsequently found as they emerged in the drift. The average individual injection flowrates are in the range 0.45 to 8.94 ml/h for the six tracers. The sum of the flowrates for these six recovered traces is 24.4 ml/h. This may be compared to the total flowrate to the covered part of the drift ranging from 600-700 ml/h. The injection flowrates of these tracers made up 3-4 % of the flowrate to the drift. The tracers were recovered in the flow to the central part of the drift where the flow was only about 150-200 ml/h. The dilution of the individual tracers is then between 22 and 396.

The paths for the tracers may not be representative for those waters where the tracers were found if the mixing of the tracer solution with the main water flow has occurred near the drift. In the extreme the porosity of the rock where the tracers have migrated might be smaller by a factor equal to the dilution factor.

The recovery for the different tracers was calculated by integrating the breakthrough curves multiplied by the respective flowrates. The cumulative amount of tracer that reached the drift as a function of time was also calculated, see figure 8.15. The recoveries of the tracer varied from 2.8 % for Uranin to 65.8 % for Elbenyl. The tracers Rose Bengal and Phloxine were not found at all. Only 0.002 % of Duasyn was recovered. The low value for Duasyn was because its first arrival time was about 15,000 hours. Bromide showed a recovery of 153 %. This impossible value for Bromide was caused by errors in the analysis due to the presence of Iodide. Therefore the Bromide data are not used in recovery calculation.

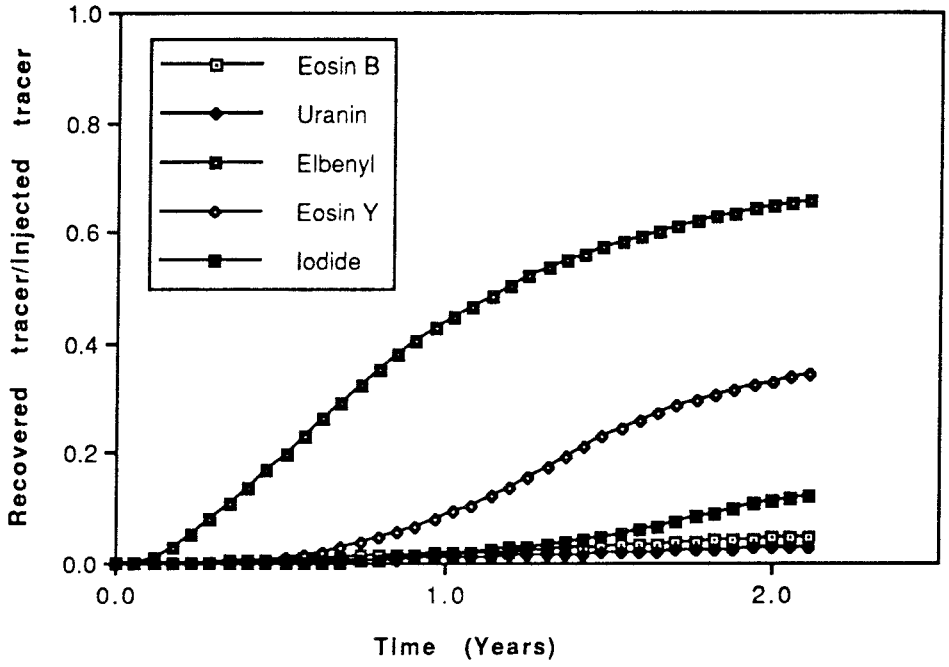

Figure 8.15 Recovered tracer/total injected tracer versus time.

The results do not indicate that the distance from the injection point to the sampling area was the sole factor influencing the recovery. For example, Iodide had a recovery higher than Eosin B even though Eosin B was injected at a shorter distance.

Table 8.3 Some data on tracer residence times and recoveries.

Tracer	Injection distance [m]	Residence time* [h]	Porosity $*10^5$	Section length [m]	Recovery [%]
Elbenyl(II)	9-11	2000	15.5	10	65.8
Bromide(III)	12-14	2500	4.5	31	-
Eosin Y(I)	17-19	6000	6.9	27	34.2
Eosin B(III)	18-20	3000	3.4	22	4.8
Iodide(III)	28-30	7000	3.0	31	12.4
Rose Bengal(II)	33-35	-	-	-	-
Uranin(I)	31-33	5500	2.0	23	2.8
Duasyn(III)	36-38	>15000	-	-	0.002
Phloxine(II)	55-57	-	-	-	0
STR7(I)	31-33	-	-	-	0
Fluoride(I)	31-33	-	-	-	0

*Approximate average values estimated from the fits with AD, AC and ADD models.
**Determined from flowrate and residence time.

It is seen in table 8.3 that there is a trend that the recovery of the tracers decreases with increasing injection distance.

There may be several causes for a less than full recovery of the tracers. Some of the causes are listed below:

1. The tracer has partly moved into pathways that do not lead to the experimental drift
2. The tracer is still travelling in the mobile water
3. The tracer has reacted "irreversibly" or been degraded
4. The tracer has moved into stagnant volumes of water by molecular diffusion.

Cause 1 is known to have occurred for one tracer, Eosin Y, which has been found in a drift 150 m distant. All tracers have been looked for in nearby drifts and holes but only the one mentioned has been found. The probability and extent of cause 1 can therefore not be assessed at present. Cause 2 is certainly true to some degree but can be accounted for. Cause 3 is not probable because extensive sorption tests in the laboratory over long times have not revealed that the tracers react or degrade. Cause 4 is known to take place as diffusion into the stagnant water in the matrix in the rock and is also suspected to take place into the stagnant water in the fractures.

In the following the possibility of matrix diffusion as a cause for the low recovery is explored.

It was projected (Neretnieks, 1980) that small readily mobile molecules, dissolved in the water, would migrate into the water in the micropores of the matrix and thereby withdraw the molecules from the moving water. There have subsequently been a series of measurements performed on the porosity and diffusivity of small molecules in granites and gneisses in the laboratory. Typical values of the porosity are 0.05-0.5 % for intact rock. Higher values are often found near fracture surfaces. Effective

diffusivities, D_e, are typically in the range 10^{-14} to 10^{-12} m^2/s. Pore diffusivities are higher by two to three orders of magnitude in comparison to the effective diffusivities ($D_e = D_p \varepsilon_p$, where ε_p is the matrix porosity). To illustrate the potential capacity and accessibility of the matrix water to the molecules, it may be noted that the water volume contained in a fracture of thickness 0.05 mm is as large as the water volume in a 100 mm thick slab of rock adjacent to the fracture if the rock has a porosity of 0.05 %. Consider the possible dilution effect as follows: if the fracture was filled with a tracer solution with concentration "C" and the solution was given time to equilibrate with the non-contaminated water in the pores of a 50 mm thick rock slab on either side of the fracture (total rock slab on both sides of the fracture is 100 mm), then the concentration in the fracture and in the pores would be 0.5*C. If the fracture was emptied of the water, the recovery would be 50 % and the rest of the tracers would reside in the porous rock matrix. The time for this process can also be estimated. From the diffusion equation (Bird et al., 1960) it is found that the penetration thickness η for this case can be determined by

$$\bar{\eta} = \sqrt{D_p t} \tag{8.1}$$

For a pore diffusivity D_p of 10^{-10} m^2/s the time to completely penetrate 50 mm is 0.8 years. The duration of the experiment was more than 2 years and the water residence times for the tracers were in the time interval 0.2 to 0.8 years or more. It thus seems reasonable that this effect may be of importance if the fracture apertures are small enough.

The fracture apertures can be estimated if the flow porosity and the fracture frequency is known. The flow porosity was estimated from data on residence times and total flowrates. The porosities ranged between $2 \cdot 10^{-5}$ and $15 \cdot 10^{-5}$. For a given fracture spacing (parallel fully open fractures), the flow porosity ε_f is δ/S (the aperture divided by the fracture spacing). For a flow porosity of $5 \cdot 10^{-5}$ and a fracture aperture of 0.05 mm, the spacing is 1 m.

The above data are in the range of possible values. It thus seems worthwhile to explore this possibility further.

The specific surface a' was determined by comparing the experimental recovery and the recovery obtained from model calculations. Calculations were made using the Advection-Dispersion-Matrix Diffusion model to fit the recovery. The obtained range of values are given in table 8.4 column 3 using the matrix porosity and diffusivity data obtained in the laboratory diffusion measurements (Abelin et al. 1987). The porosity obtained from the diffusivity measurements is about 10 times lower than that obtained by weighing a wet and dry sample. The higher values may be more appropriate for the long contact times in the tracer experiment. If the higher values are used about a factor of three smaller surface a' is obtained. It should be noted that the matrix porosity and diffusivity measurements were made on samples of rock not directly adjacent to a fracture with flowing water. Skagius and Neretnieks (1986a) found that the rock, directly adjacent to fractures practically always has considerably higher porosity and diffusivity than rock further from the fracture. Porosities of 1 to more than 7 % were found in the rock adjacent to the fracture. Diffusivities were mostly larger and

sometimes several orders of magnitude larger in the rock adjacent to the fracture than in rock at some distance from the fracture surface. If the fractures in contact with the tracers in the field experiment have 2% porosity and a diffusivity of $5 \cdot 10^{-14}$ m^2/s. the specific surface needed to account for the non recovery of tracers is much smaller. Column 4 gives these values of a'.

Table 8.4 Compilation of obtained specific surfaces.

Tracer	Injection distance [m]		Specific surface [m^2/m^3]
Column 1	2	3	4
Eosin B	19	14-27	1.4-2.7
Uranin	32	5.1-12	0.5-1.2
Elbenyl	10	15-20	1.5-2.0
Eosin Y	18	4.7-7.7	0.5-0.8
Iodide	29	0.49-1.1	0.22-0.5

The large specific surfaces for diffusion into the rock matrix, a' in column 3, which were obtained for the dyes are not reasonable because they imply that there should be spacing of conducting fractures 2/a' m. For Iodide this would mean spacing of 1-2 meters and for the dyes 0.07-0.4 meters. This seems to contradict the observations in the drift where, considerably less than 100 large water conducting fractures were observed over a length of 100 m. Since only a fraction of the fractures conduct water this means that the fracture spacing must be larger than 1 m in the rock near the drift. Unless the diffusivity and porosity of the rock adjacent to the water conducting channels is considerably larger corresponding to the values to generate column 4, matrix diffusion effects alone cannot explain the low recoveries if only the large fractures are assumed to carry most of the flow.

In a recent mapping of fractures along 5 boreholes near the experimental drift, with a total hole length of about 900 m, Gale (1988) found values of typically 2-4 fractures per m on the average. Locally 10 or more fractures per m were found. These observations include all visible fractures in the bore cores also, very short fractures. Trace length measurements showed that most of the fractures have trace lengths less than 1.5 m. This would give specific surfaces 4-8 m^2/m^2 and more than 20 m^2/m^2 locally if a parallel pattern is assumed. For a cubic or random pattern 3 times higher values are obtained.

It is possible that the effects of matrix diffusion can account for most or even all of the non recovery of the tracers if the rock adjacent to the fracture surfaces with flowing water is more porous than rock further in or if a large fraction of the fractures are conducting.

It cannot be resolved at present which are the more correct values for the diffusivity and the porosity. A much more extensive sampling of rock near fracture surfaces is needed to do this.

Another possible cause for the low recovery of tracers is also explored. It is based on the concept that the water flows in channels that are in contact with practically stagnant pools of water. The tracer in the flowing water in the channel may diffuse into the nearby stagnant water and thus be withdrawn from the mobile water. Figure 8.16 illustrates this process.

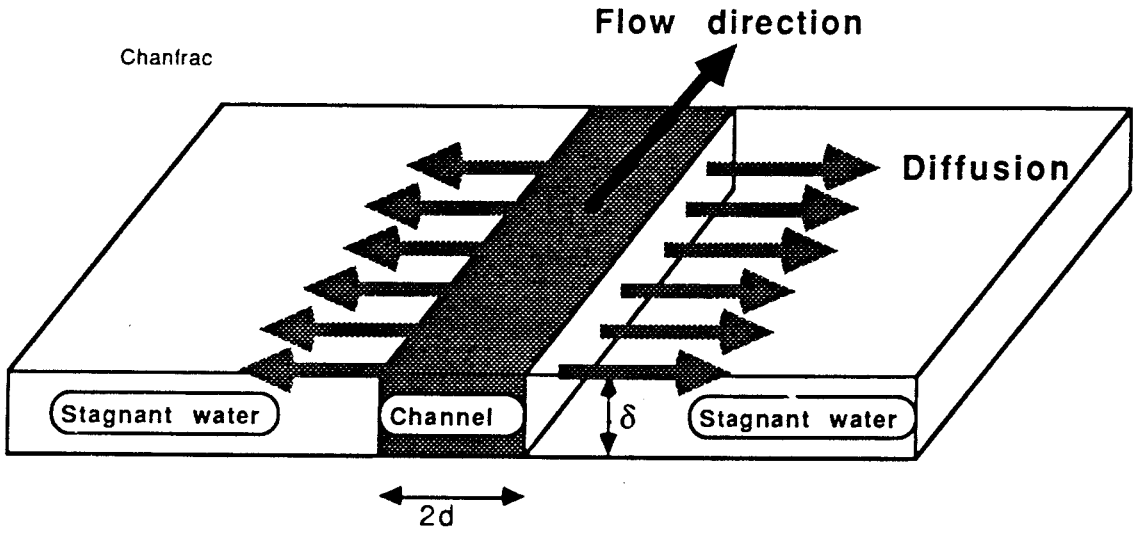

Figure 8.16 A fracture cross section with a channel containing flowing water is shown. In contact with the flowing water are stagnant volumes of water into which the tracer is carried by diffusion.

The aperture of the channel is δ and the width of the channel is 2d. The species diffuse into the stagnant water. For a channel with a small width, in comparison to the diffusion distance, it may be assumed that the concentration of the species across the width of the channel is constant. Therefore, the previously used equation for diffusion into stagnant water in the rock matrix can also be used to describe this case. The effective diffusivity will then be equal to the diffusivity in unconfined water ($D_e=D_w$) and the equivalent of the matrix porosity is equal to unity.

The diffusivity D_w of the dyes in water is on the order of 10^{-9} m^2 /s and for Iodide it is $4 \cdot 10^{-9}$ m^2 /s (Skagius 1986). The obtained channel widths, 2d, are summarized in table 8.5. They are based on an average value of a' from the previous calculations.

Table 8.5 Estimated equivalent channel widths 2d.

Tracer	ε_f flow porosity $\cdot 10^5$	a' (central value) [m^{-1}]	$D_e \varepsilon_p$ 10^{16} [m /s]	Channel width (2d) [m]	Sum of apertures ($\Sigma\delta$) [m]
Eosin B	3.4	20	0.1	0.034	0.154
Uranin	2.0	8	0.1	0.050	0.064
Elbenyl	15.5	17	0.1	0.182	0.060
Eosin Y	6.9	6	0.1	0.023	0.567
Iodide	3.0	0.8	2	0.335	0.019

The channel widths obtained are smaller or, at most, of the same magnitude as the penetration depths into the stagnant water for one year contact time. Therefore, the assumption that the concentration over the channel width is evened out is thus not grossly violated.

The above analysis gives no indications of how large the apertures of the channels are. An estimate of the sum of the apertures of the channels, assuming that they all have the same widths, can be made in the following way. The sum of all the cross section areas of the channels is denoted as 2d ($\Sigma\delta$). The total cross section area of rock, A_O, that these channels intersect at the face of the drift was utilized to evaluate the flow porosity , ε_f. The porosity is the ratio of the cross section of the channels to the cross section of the area containing the channels

$$\varepsilon_f = (\Sigma\delta)*2d/A_O \qquad (8.2)$$

From the above expression the sum of the channel aperture ($\Sigma\delta$) can be obtained. The values range from 19 mm to 567 mm and are given in table 8.5.

The tracers arrived in many of the sheets. If every sheet on the average had a few channels, several tens of channels would determine the sum of apertures ($\Sigma\delta$). So for 50 channels this would mean a 3 mm individual channel aperture for Eosin B, slightly more than 1 mm for Uranin and Elbenyl, more than 10 mm for Eosin Y, and a 0.4 mm aperture for Iodide. Most of these values are considerably larger than what the visual observations indicated.

These results are based on the assumption of straight flowpaths and that tracers mix into the main flow of water. Flowpaths may easily be up to 2 times larger and as discussed in relation to dilution factors the uncertainties as to where mixing takes place can cause more than one order of magnitude overestimation at the porosity and thus the sum of channel apertures.

The diffusion into stagnant pools of water cannot unequivocally alone explain the loss of tracer. The diffusion into the rock matrix may also not be the sole cause for the loss of tracer. The tracers may have taken paths which are directed to some other drifts in the mine although they are much further away. There is one such observation.

Eosin Y was found to have migrated in substantial quantities to a gallery about 150 m away from the injection point although the sheeted drift was located only 18 m away. This indicates that the assumption that all the injected tracer mass moves towards the experimental drift is not true for one tracer and may not be true for the other tracers either. In that case the analysis based on this assumption may determine too large specific surfaces and channel widths.

If most of the tracer moved in the direction of the drift the results of the calculations indicate that both matrix diffusion and diffusion into stagnant pools of water may play a role. There are probably other mechanisms which could cause the recovery to be small. One such possible cause is that the injection, although small, compared to the total flowrate may be large when viewed on a local scale. A dipole type of flow may then develop where some of the flow moves away from the drift for some distance before returning to the drift. This would produce a lengthening of the concentration curve tails and a lowering of the tracer recovery during a certain observation time.

Determination of hydraulic conductivity.

The hydraulic conductivity of the rock adjacent to the drift is evaluated based on the assumption that the rock mass may be described as a homogeneous porous medium and that Darcy's law is valid. Some simplifying assumptions needed to be introduced because the head boundary conditions are not known exactly due to the presence of drifts and tunnels in the old mine. For a homogeneous porous medium the simplifying assumptions would introduce only minor errors and are generally accepted in most other cases which study the properties of fractured rocks.

The hydraulic head was measured in the three vertical injection holes. Flowrates were measured in about 375 sheets in the upper half of the drift. In addition, ventilation experiments were conducted to measure the inflow to the lower half of the drift and to the access drift.

Table 8.6 gives the flowrates in the different parts of the drifts.

Table 8.6 Flowrates in the different parts of the drifts.

Part of drift	Flowrate l/h	Length of drift m
Plastic sheets	0.7	100
Bottom part	2.4*	100
Access drift	2	115

* Covered parts of floor + ventilation

Using the above flowrate and head data the hydraulic conductivities of the different parts of drifts are obtained. These values are summarized in table 8.7.

Table 8.7 Hydraulic conductivities in the Stripa 3-D drifts.

Location	Conductivity*10^{11} m/s	
	Steep gradient	Low gradient
Experimental drift		
Ceiling + upper sides	0.56	1.07
Floor + lower sides	1.9	3.6
Average	1.3	2.3
Access drift	0.7	1.3

The flowrates varied considerably over the length of the drift and so did the hydraulic conductivities. The data in table 8.7 were averaged over more than 100 m of drift. The variations within the experimental drift are shown in figure 8.17 where 10 m averages are shown. It is observed that on a 10 m scale the hydraulic properties of the rock are far from constant. The difference of the hydraulic conductivity between the access drift and the experimental drift is a factor of 2. This may indicate that the 100 m scale is not large enough to obtain reasonably constant average values.

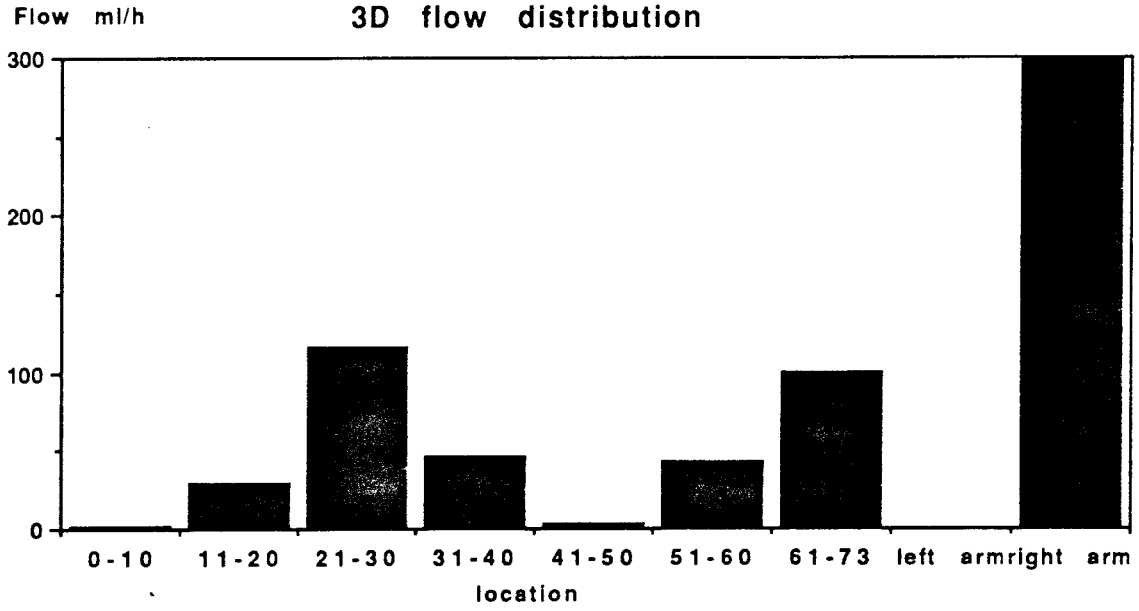

Figure 8.17 Flowrate in the experimental drift averaged over 10 m.

Flowrate and tracer distribution

The tracers arrived in very varying rates, concentrations and in water flows to the different sheets. The mass flowrate to a sheet is determined by the product of the flowrate and concentration. The differences in mass flowrates to the different sheets show if any preferential paths may exist. Figures 8.18 - 8.22 show how the tracer recovery is divided among different sheets for the five tracers Eosin B, Uranin, Elbenyl, Eosin Y, and Iodide. The bars in the histograms show how much of a tracer was recovered in a given range of mass recovery. The right hand bar in Figure 8.18 shows that there were four sheets (the figure above the bar) which had a tracer recovery in the range 400-800 mg. The sum of the tracer that arrived to these four sheets is given by the height of the bar.

It is seen that for all the tracers 3 to 5 sheets out of 27 to 52 sheets carried more than half the tracer.

The distribution of flowrates in the different sheets show that a few spots carried most of the water. This is an indication of channeling. The dimensions of the channels are not known from these observations but figure 8.4 indicates that the larger flowrates are observed in those parts of the drift where many fracture intersections exist. This may be an indication that the water flows along fracture intersections where the channels are very narrow.

The tracers were spread out among many sheets. It is clear that the tracers were not confined entirely to one or a few channels but spread considerably. However, a small fraction of the sheets carried a large fraction of the tracer.

The flowrate distribution over the experimental drift shows clearly that adjacent sheets may carry very varying flowrates. One of the 375 sheets carried 10 % of the water. Often the sheets adjacent to a sheet that carried a considerable flowrate was dry or nearly dry. The size of the channels in the fractures were not measured in the experimental drift but observations in other tunnels and drifts in Sweden indicate that channels widths vary from a few centimeters to many tens of centimeters or even a meter or more (Neretnieks, 1987).

The distribution of tracers over the different sheets showed a similar behavior as the flowrate distribution. One tracer Duasyn, which was injected in hole III at 37 m distance from the drift, was first detected in a sheet at the opposite end of the drift. The water where it was found contained very little or none of the other tracers. One conclusion is that Duasyn must have passed over the main area of sheets, where the other tracers were found, without being drawn down into those sheets. The sheets where this tracer was subsequently found had another pattern of travel than that of the other tracers. Duasyn must have traveled in a pathway(s) which bypassed the system of pathways that the other tracers traveled. Eosin Y which was injected in hole I at 18 m from the drift had a recovery of 34 %. Neither this tracer nor any other tracers were found in any other waters in the mine area that were sampled at intervals during the experimental time. After the sampling was finished in December 1986 and the mining operations were starting for the next phase of the Stripa program, Eosin Y was found in a newly excavated gallery about 150 m away from the injection point. The amounts found were estimated to be on the order of several tens of percent of the total injected mass of this tracer. There were no indications either in the hydraulic head measurements or by any other observations that the tracer should travel in this direction.

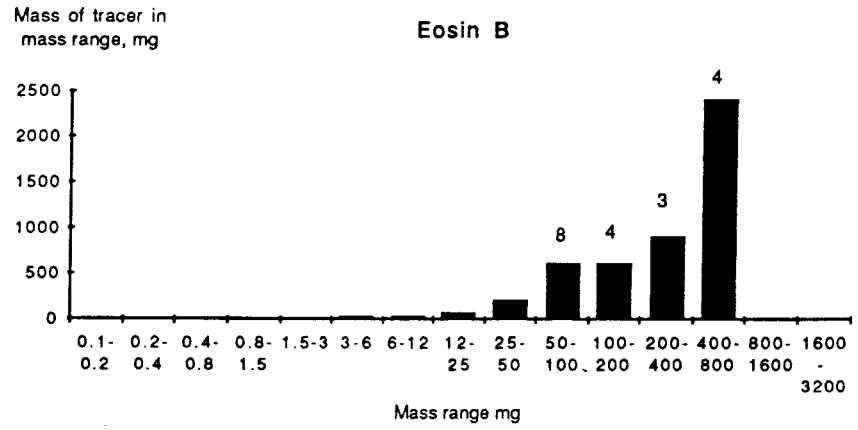

Figure 8.18 Histogram over the recovery of Eosin B in different mass ranges. 43 sheets carried this tracer in measurable quantities.

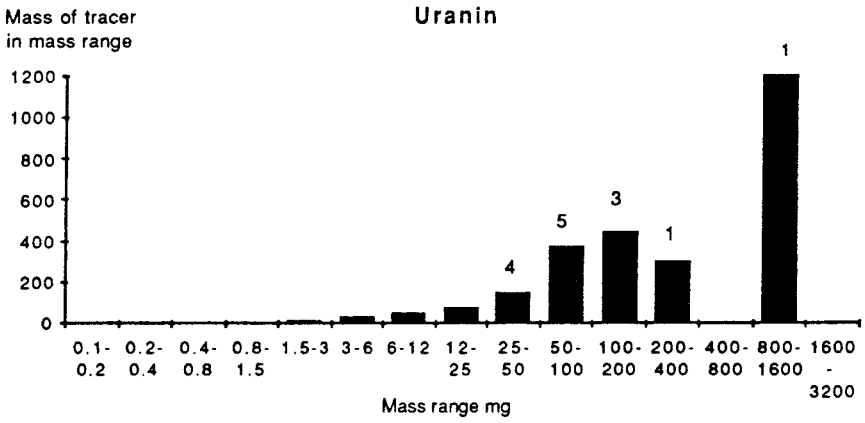

Figure 8.19 Histogram over the recovery of Uranin in different mass ranges. 45 sheets carried this tracer in measurable quantities.

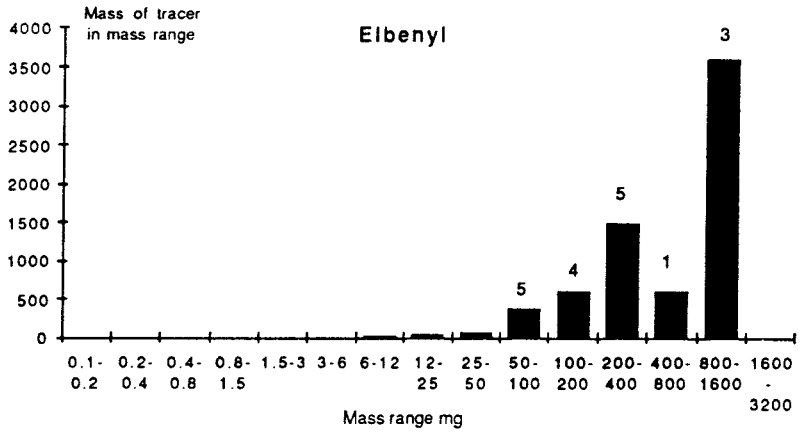

Figure 8.20 Histogram over the recovery of Elbenyl in different mass ranges. 27 sheets carried this tracer in measurable quantities.

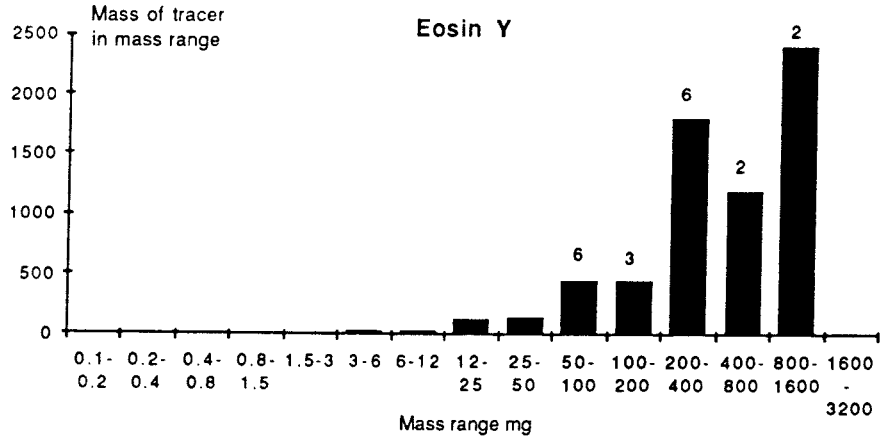

Figure 8.21 Histogram over the recovery of Eosin Y in different mass ranges. 46 sheets carried this tracer in measurable quantities.

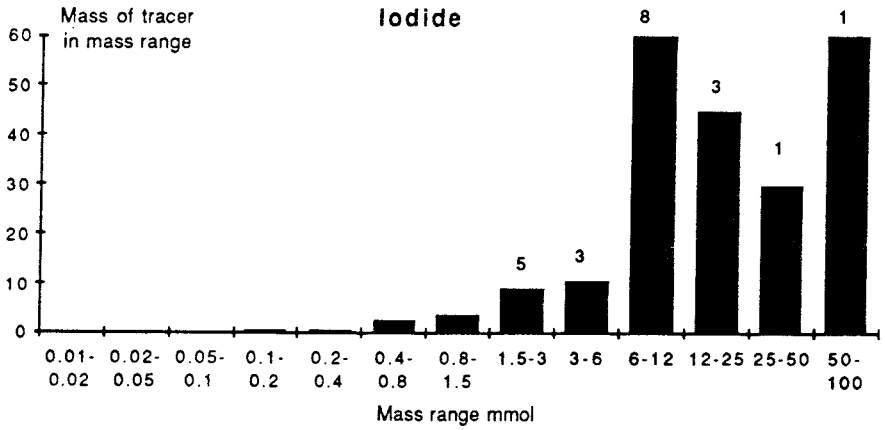

Figure 8.22 Histogram over the recovery of Iodide in different mass ranges. 52 sheets carried this tracer in measurable quantities.

8.1.5 Summary of main results, discussion and conclusions

The single most prominent feature of this investigation was the use of a multitude of plastic sheets in a long underground drift. The use of a drift located well below the water table ensured that the water flow would mainly be directed towards the drift from practically all the tracer injection points. The use of a 100 m long drift with about 375 plastic sheets made it possible to monitor the flowrate and tracer transport in detail which cannot be done by other known techniques such as "between hole tracer tests." Most of the information obtained with the present technique, e.g. variability of conductivity and channeling, is difficult, if at all possible, to obtain with other methods.

Samples were taken for Tritium analysis in several sheets and at other locations on two occasions. Tritium was found to be present in two of the six sampled sheets. Had the samples instead been taken from the mixed water of the sheets, the Tritium

concentration would have been below the detection limit. The presence of Tritium in the waters indicate the presence of fast nearly isolated channels of small extent. Probably such channels would have gone unnoticed had not the plastic sheeting technique been used.

The porosity was found to decrease with distance from the drift. The values for the rock far from the drift were found to be on the order of $2 \cdot 10^{-5}$ -$7 \cdot 10^{-5}$, the porosity in the 10 m nearest the drift was found to be $15.5 \cdot 10^{-5}$ which indicates that the presence of the drift has increased the porosity.

The water residence times which were used to estimate the porosity varied considerably between sheets. Also the residence times for major flow paths and averaged flow paths were quite variable. These and other observations indicate the presence of channeling. This adds further the need to use the average properties with considerable caution. The presence of Tritium in some sheets, for example, indicates that there is some part of the porosity which is not well connected to other parts of the rock porosity.

The models used do not describe some of the important causes of dispersion and attempt to force the parameter values to account for processes which they cannot do. This is clearly seen in the fitted concentration curves. The model results cannot describe the several ups and downs in the experimental curves. Furthermore the experimental curves in adjacent sheets with the same tracer in many cases are quite dissimilar. This indicates that there either must be very large differences in the values of the dispersivities and velocities in the different pathways to the different sheets or that there are mechanisms which cause these variations that have not been modeled. If the former is true then there are strong differences between adjacent pathways, which would be termed channeling. If there are un-modelled processes, then one of them may be the transport in several pathways. This is supported by other information such as the presence of Tritium in some sheets and the very large variations in the ratios between tracers in adjacent sheets. If there was a regular mixing constantly occurring then this is the basis for the concept of hydrodynamic dispersion the curve forms and the ratios in adjacent sheets would behave in a much more regular way.

The results show that for the tracers to have been taken up by the rock matrix, fracture spacings (equivalent water carrying fractures) for the dyes of between 7 to 40 cm and for Iodide between 50 and 100 cm are needed. These values are probably much too small if only the 100 prominent fractures visible in the drift of 100 m are assumed to be active conductors. The number of fractures with lengths of a few meters or less is orders of magnitude larger and if these actively participate in the conduction of the flow the loss of tracer is easily accounted for by matrix diffusion effects. The diffusivity data used were for intact rock. It is known from other measurements that the rock and fracture coating or alteration materials adjacent to water conducting fractures may be much more porous and have much higher diffusivities. If this is the case then the fracture spacings needed are between 1-10 m and the matrix diffusion effects may have played an important role in these experiments also if only the larger fractures conduct most of the flow.

The diffusion into stagnant water in the fracture was also explored. For Uranin, Elbenyl, and Iodide this effect may contribute noticeably but it probably has a small effect for Eosin B and Eosin Y. This latter effect is more speculative than the matrix diffusion because many assumptions must be made regarding the geometry and quantity of the stagnant water zones.

Similar effects may be caused by the slow flow into semi-stagnant pools of water. There is even less information available for speculations on this process.

The results of the tracer experiments and the Tritium measurements give strong support to the notion that a non-negligible portion of the flow takes place in channels which have little contact with other main channels. This cannot be treated by the models which have been applied in the analysis of the experiment. A probably fruitful avenue would be to try to incorporate the variability in the models. So called stochastic models are available for porous media and some attempts to apply them to this type of rock have been made recently (Gelhar 1987b, Moreno et al., 1987a,b, Tsang et al., 1987). These models need considerable amounts of data to obtain the statistic properties. They also must be made to incorporate the correct processes.

The mechanisms of diffusion into stagnant pools of water, matrix diffusion, and the frequency of mixing and especially that of the non-mixing of channels will have to be studied more.

8.2 Fannay Augere investigation

8.2.1 Overview

A large scale flow and tracer experiment has been performed in fractured granite in France at Fannay-Augeres (Cacas et al 1990a, b). The fractured structure of the rock and observations that flow and solute transport is strongly channeled globally as well as in the fractured planes, has led to the development and application of a model whose structure should be able to account for these observations. The model is a stochastic network model where the flow in every fracture is assumed to follow one dimensional channels from fracture to fracture. The geometric properties of the fractures such as sizes, orientations and frequencies are determined from local observations on walls, cores and in drillholes. Hydraulic properties are determined from short interval injection tests by calibrating the injections to a sufficiently large number of simulated realizations. A set of assumptions as to the form of the conductivity distribution, placement of channels in the fracture plane, volume of the channels, dispersion in the channels, mixing at channel intersections and more, must be made. Some of the assumptions can be and have been tested.

8.2.2 Experimental

The flow and tracer experiments were performed in a 100 long part of a tunnel in granite in Fannay Augeres in central France. The tunnel is located at a depth of 150 m. The rock is highly fractured and there is a steady flow of water into the drift. Water flowrate into the drift was measured continuously both before and after the ten 50 m long measurement holes were drilled. The flowrate varied from 5.1 to $11 \cdot 10^{-5}$ m^3/s

before the drilling of the holes and dropped to $3.7 \cdot 10^{-5}$ m^3/s after the holes were drilled. The decrease in flowrate was attributed to partial de-saturation. The holes were located in three planes as shown in figure 8.23. From the holes and the cores fracture orientation and fracture density data were obtained. Fracture trace lengths were obtained from a survey of the eastern wall of the tunnel section. Hydraulic injection tests were made in all holes using packed off lengths of 50 m, 10 m (50 sections) and 2.5 m (185). The flowrates in the 2.5 m sections were found to be well described by a log normal distribution. Piezometric heads were monitored in 685 m long sections in the 10 boreholes at distances from 5.5 to 47.5 m.

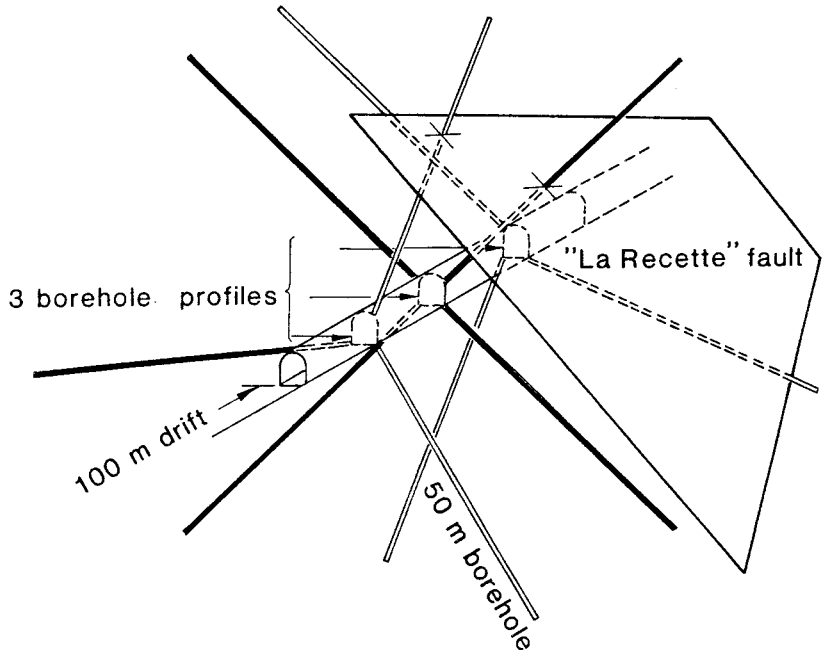

Figure 8.23 Position of drift and boreholes.

Out of the injection tests in holes, one third were below the detection limit $3 \cdot 10^{-7}$ m^3/s.

Tracer tests were performed by injecting 6 different tracers in 10 different locations divided among two of the boreholes. The tracers were collected in three different locations. One location was at the ceiling below the two injection holes. The other two locations were in the drainage ditch 25 and 50 m downstream from the injection holes. Tracers were collected for up to 150 days. Of the 10 injected tracers 2 did not arrive in the drift in measurable concentrations, one had a multi-modal breakthrough curve, two injections failed. Five tracers were thus successfully recovered and could be used for model comparisons.

Some samples which were taken in two other boreholes at distances of 5, 12 and 18 m from the drift showed that the tracers had a component of movement which was parallel to the drift. The recovery of the 5 successful tracers varied between 5 and 45 %. First arrival times were 2.5 and 3.5 h to the nearest collection point in the ceiling and up to 570 h to the furthest collection point. One tracer moved a longer distance in a 3 to 6 times shorter time than another tracer injected in the same hole but at less than half the distance. It was found that the tracers emerged into the drift at three main locations.

At this scale the medium and pathways are very heterogeneous and cannot be described by a homogeneous continuum.

8.2.3 Conceptual model

The basis of the model is that the flow and transport takes place in a network of fractures. The fracture locations, size and orientations are assumed to be random although the fractures are allowed to be grouped in different sets. In this specific model it is assumed that the fractures are circular disks. In most fracture network models (Roleau 1984, Robinson 1984 and Andersson 1987, Long and Billaux 1987) it is assumed that the fractures can be modelled as parallel plates and thus have a uniform conductivity in the fracture plane. There are several observations which go contrary to this assumption (Gentier 1986, Neretnieks 1987, Tsang 1987, Bourke 1987) indicating channeling.

In this model it is assumed that the flow takes place in a channel from the center of the fracture to the line of intersection with the next fracture. The channel in a fracture plane is connected with the channel in the intersecting fracture. A fracture will then have as many channels connecting its center to the other fractures as the number of intersecting fractures. The hydraulic resistance of a path connecting the center of two fractures will be the sum of its two channels. For simulations of steady state flowrates this information is sufficient.

For the simulation of the transport of non reactive tracers additional information on the volume and dispersive properties of channels is needed. The volume will be the sum the volumes of the channels. Further it is necessary to make some assumption on the mixing of intersecting streams. The dispersion in an individual channel is modelled by a diffusion like random process. Full mixing is assumed to occur at intersections. Tracers are assumed to be non reactive and it is further assumed that there is no diffusion into the rock matrix or into other stagnant waters.

From the computation point of view the model structure reduces to a 3 dimensional network of resistances and volumes. The length of the channels is obtained from the stochastically generated network of fracture planes and the hydraulic properties of the channels in the fracture planes are obtained from an independent stochastic process. In this application of the model it has been assumed that the volume of a channel is determined by its conductivity, using the assumption of a circular channel and that there is Poiseuille flow. The latter assumption gives a direct relation between the radius of a tube and its hydraulic resistance.

With the fracture sizes and densities measured it was found in the simulations that every fracture on average was connected to 5 other fractures.

8.2.4 Interpretation of hydraulic information

The interpretation of the experiments was done in a stepwise manner. First the local scale measurements were used to evaluate the stochastic properties of the fractures, then an intermediate scale was selected which was as large as could practically be handled in the computations. Finally a global scale was used to compare the results with the all over inflow to the tunnel section.

The geometric information was assumed to be correct and relevant. The fracture conductivities were assumed to be log-normally distributed and the distribution was assumed to be ergodic. The mean and standard deviation of the the distribution was determined by generating 200 networks in each of which 2.5 m packer tests were simulated. The simulated tests were also found to be log normally distributed. By fitting the simulations to the the experiments the standard deviation of the PDF for the fractures was found to be 7.4 on the natural logarithm scale or 3.2 on the 10-base logarithm scale. This is a very wide distribution and implies that there is an 8 order of magnitude difference between the first 10 % and the last 10 % of the conductivities. It was shown in simulations that almost all the flow occurs in a limited number of pathways and that the less conductive fractures can be neglected in the calculations. It was found possible to reduce the number of fractures by half in the simulations if those of the lower end of the distribution were left out.

These simulation results seem to explain the large scale channeling obtained in the Stripa experiment (Neretnieks 1987).

It was not possible to simulate the whole region of interest with one single fracture network model because of computer limitations. Instead the notion was introduced that at some intermediate scale, it might be possible to assign a block in the region with a value of the hydraulic conductivity and if need be with anisotropy properties. The punctual values of the intermediate scale can then be used to assess the properties of an equivalent continuum on the global scale although some anisotropy was found on the intermediate scale.

Using the previously obtained values for the PDF of the fractures, 17 simulations of 10 m cubes, were made. They showed that the medium appears to be isotropic on the global scale. For a porous medium with linear flow the global conductivity should lie between the geometric mean and the arithmetic mean of the intermediate scale values. Based on the simulated results the global conductivity can be expected to lie between $1.5 \cdot 10^{-8}$ and $2.3 \cdot 10^{-8}$ m/s. This is then essentially a prediction of the global conductivity using only geometric and small scale hydraulic data.

The comparison of the predicted global conductivity and that obtained from the global inflow measurements was done. The experimental global conductivity was obtained from inflow and detailed hydraulic head measurements in the boreholes, using the porous media model. The analysis was complicated by the fact that the rock had been partially de-watered when the holes were drilled, which reduced the inflow by a factor of 2.6. The obtained average value of the global conductivity was found to be $1.8 \cdot 10^{-8}$ m/s. This is within the expected range.

One important question addressed was if the local scale injection test values could be used to estimate the global conductivity. It should be expected to fall between the geometric and arithmetic mean which were $3 \cdot 10^{-8}$ and $1.1 \cdot 10^{-6}$ m/s. This is a far to wide range to be useful.

8.2.5 Interpretation of tracer information

Simulations of the tracer movement are done by the particle tracking method. Robinson (1984). The crucial information on the volume of the flow channels is not available. In this application of the conceptual model, the volume of each channel was assumed to be directly related to the hydraulic conductivity by the relation of Poiseuille flow in a circular tube. The actual volume of all channels was assumed to be directly proportional to the Poiseuille volume. The proportionality factor, called a slowing down factor, was subsequently found by calibration to be 32.

The model was used to study the sensitivity of some assumptions and parameters before proceeding to comparisons with the real tracer results. It was found that the dispersion in the individual channels contributed very little to the dispersion in the network. The slowing down factor has only the effect of scaling the time.

The calibration of the slowing down factor was done by making 20 simulations for each of four tracer tests. The so obtaining histograms of peak residence times for each test were then scaled by one and the same slowing down factor to obtain the best overall value. The histograms obtained and the experimental value are shown in figure 8.24 the scaling factor is 32. Other values a factor of three higher or lower would also have been reasonable. Only four test could be simulated because the fifth tracer required a to large simulation region.

It should be noted that the only additional information beyond the model calibrated by the hydraulic tests is the information on the volume of the channels. The dispersion data do not influence the results. The mean and standard deviation of the hydraulic conductivities obtained from the calibration of hydraulic data were used in these simulations.

The average radius of the pipes is 0.031 mm to attain the conductivity and it is 5.5 time larger, i.e. 0.171 mm (0.32 mm diameter), to account for the volume needed for the residence time. If the average flow channel were not a circular pipe but a ribbon with the same hydraulic conductivity and volume, the aperture and the width of the ribbon would be = 0.006 mm and 15 mm respectively. Whatever the geometry, this implies that only a very small part, a few % or less, of the fracture is in contact with the flowing water.

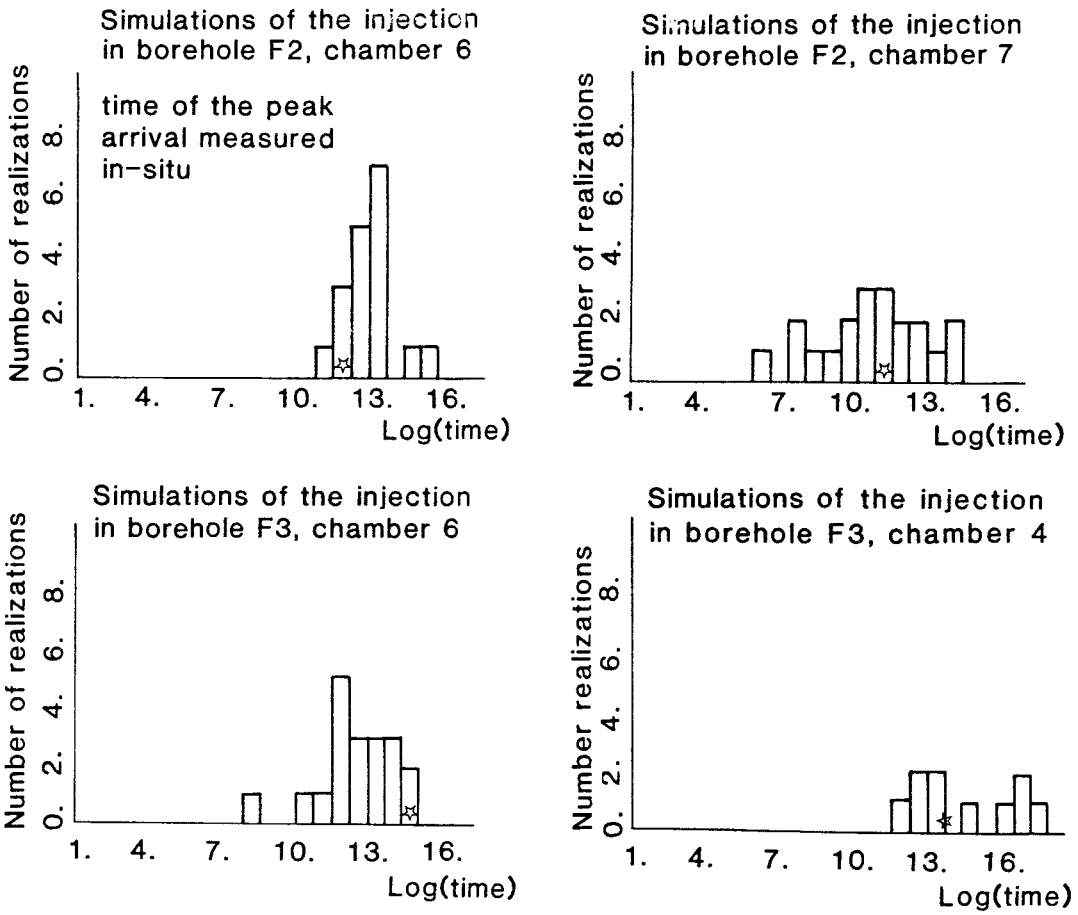

Figure 8.24 Histograms of simulated peak arrival times for 4 tracer paths and the experimentally obtained value. Scaling factor is 32.

So far only the peak arrival times times and not the residence time distribution nor the spatial distribution of the tracers have been addressed. The residence time distribution, RTD, is strongly influenced by the variation of the flowrates among the different channels, i.e. the PDF of the conductivities as well as on the volumes which in this application of the model is obtained from the conductivity. It is expected that the larger the standard deviation σ in the PDF is, the wider will be the RTD, and the more pronounced the channeling. The natural logarithm standard deviation of the radii obtained from the hydraulic calibrations was σ_r=1.85. (This is equivalent to σ=3.2 for logarithm of base 10 for the conductivities for circular tubes.) Simulations were also made with σ_r= 0.1, 1.0 and 1.85 to find the locations of the effluent points in the drift. For the larger value of σ_r, one location accounted for 60 % of the recovery and also for σ= 1.0 the channeling was pronounced.

Further simulations were made to study the residence time distribution. This was done by determining the "breakthrough duration", which was arbitrarily defined as the time for 90 % of the injected tracer pulse to arrive. For 15 linear flow simulations the breakthrough duration values were on the average about 50 to 100 times larger than

the peak arrival times for a σ_r =1.85. This indicates a very large dispersion but is nearly one order of magnitude larger than the values obtained in the experiments. The latter may however be underestimated because they have been determined without having access to the whole tail of the breakthrough curves and because the overall recovery was so low. Further simulations of the tracer tests to the tunnel, where the flow is essentially radial, showed that the breakthrough duration values agreed with the experimental if scaled by the same factor of 32 as the peak residence times. Because the variations in the simulated times typically span a range of a factor of 500, the value of the slowing down factor could vary considerably.

The simulations of the recovery of the tracers spanned the same range as the experimental values, 2-70 %, but the comparison is complicated by the fact that the boundary conditions in the model are not quite comparable to those of the drift from the recovery point of view.

8.2.6 Discussion and conclusions

The use of the stochastic network approach to the flow and tracer results in Fannay-Augere has made it possible to use geometric information on fracture densities, orientations and lengths together with small scale measurements on hydraulic conductivity to predict global scale conductivity. The model also accounts for recent observations on strong channeling over large areas as well as for the observations that water does not flow evenly in fractures. It has been possible to predict some characteristic properties of the residence time distribution of tracers. The model also accounts for the observations in Fannay-Augere and Stripa that tracers arrive preferentially in a few regions.

Several assumptions made in the model have not been possible to validate with the data available. The assumption of the conducting channels being circular tubes has no impact on the hydraulic model but the there to coupled assumption that the volume of the conduits can be related to conductivity by the assumption of Poiseuille flow may have an impact on the transport of non reacting tracers. Other reasonable and possible assumptions have not been tested in this study.

One important aspect of the model is that it proposes that only a small part of a fracture conducts water. The area of a fracture wetted by the mobile water is much smaller than the total area of the fracture surfaces. The simulations indicate that only at most a few percent of the fractures are open to flow. For reacting solutes this will have a very large impact because they will see much less rock to react with. This aspect of the model has not been tested yet.

9 REFERENCES

Abelin H. Migration in a single fracture. An in situ experiment in a natural fracture, Ph. D. Thesis, Dep. Chemical Engineering, Royal Institute of Technology, Stockholm, Sweden 1986

Abelin H., Neretnieks I., Tunbrant S., Moreno L. Final Report of the Migration in a Single Fracture - Experimental Results and Evaluation, Stripa Project Report 85-03, OECD/NEA, SKB 1985

Abelin H., Birgersson L., Gidlund J., Moreno L., Neretnieks I., Widén H., Ågren T. 3-D migration experiment - Report 3, Part I, Performed experiments, Results and Evaluation, Stripa Project Technical Report 87-21, Stockholm Nov. 1987

Abelin H., Birgersson L., Neretnieks I., Ågren T. A channeling experiment to study flow and transport in natural fractures, In Scientific Basis for Nuclear Waste Management XII, Berlin Nov 1988, Proceedings, p 661-668, 1989

Ahlbom K., Smellie J.A.T. Characterization of fracture zone 2, Finnsjön study-site, SKB TR 89-12, 1989

Andersson J., Dverstorp B. Conditional simulation of fluid flow in three-dimensional networks of discrete fractures, Water Resources Research **23,** p 1876-1886, 1987

Atkinson A., Titchell I. Diffusive transport in granite studied using ionic conductivity, UK Atomic Energy Authority Report AERE R 11827, 1985

Bear J. Hydrodynamic dispersion, in flow through porous media, edited by R.J.M. de Wiest, Academic, New York, 1969

Bird R.B., Stewart W. E., Lightfoot E.N. Transport Phenomena, Wiley 1960

Birgersson L. Diffusion in the matrix of granitic rock, Field test in the Stripa mine. M.S. Thesis Dep. Chemical Engineering, Royal Institute of Technology, Stockholm, Sweden, May 1988

Birgersson L., Neretnieks I. Diffusion in the matrix of granitic rock, Field test in the Stripa mine. Part 1, SKBF/KBS Technical Report 82-08, July 1982a

Birgersson L., Neretnieks I. Diffusion in the matrix of granitic rock, Field test in the Stripa mine, In: Scientific basis for nuclear waste management V, Berlin, June 1982, Elsevier, p 519, 1982b

Birgersson L., Neretnieks I. Diffusion in the matrix of granitic rock. Field test in the Stripa mine, Part 2, SKBF/KBS Technical Report 83-39, March 1983

Birgersson L., Neretnieks I. Diffusion in the matrix of granitic rock. Field test in the Stripa mine, In: Scientific basis for nuclear waste management VII, Boston, Nov. 1983, Elsevier, p 247, 1984

Birgersson L., Neretnieks I. Diffusion in the matrix of granitic rock. Field test in the Stripa mine, Scientific Basis for Nuclear Waste Management, Boston, Nov. 1987, Proceedings, p 189-198, 1987

Black J., Holmes D., Brightman M. Cross hole investigations - Hydrological results and interpretations, Stripa project report 87-17 OECD/NEA, SKB Nov 1987

Bourke P. Channeling of flow through fractures in rock, Proceedings of GEOVAL-87, International Symposium, Stockholm, Sweden, April 7-9, p 167-177, 1987

Brace W.F., Walsh J.B., Frangos W.I. Permeability of granite under high pressure, J. Geophys. Res. 73, p 2225, 1968

Bradbury M.H., Lever D., Kinsey D. Aqueous phase diffusion in crystalline rock, In: Scientific basis for nuclear waste management V, Berlin 1982, Elsevier, p 569-578, 1982

Bradbury M.H., Green A. Measurements of important parameters determining aqueous phase diffusion rates through crystalline rock matrices, J. Hydrology **82**, p 39-55, 1985

Bradbury M.H., Stephen I.G. Diffusion and permeability based sorption measurements in intact rock samples, Materials Res. Soc. Symp. Proc **50**, p 81-90, 1985

Bradbury M.H., Green A. Investigations into factors influencing long range matrix diffusion rates and pore space accessibility at depth in granite, J. Hydrology **89**, p 123-139, 1986

Cacas M.C., de Marsily G., Tillie B., Barbreau A., Durand E., Feuga B., Peaudecerf P. Modelling fracture flow with a stochastic discrete fracture network: calibration and validation - 1 The flow model, Water Resources Research, in print, 1990a

Cacas M.C., Ledoux E., de Marsily G., Barbreau A., Calmels P., Gaillard B., Margritta R. Modelling fracture flow with a stochastic discrete fracture network: calibration and validation - 2 The transport model, Water Resources Res., in print, 1990b

Cathles L.M., Spedden H.R., Malouf E.E. A tracer technique to measure the diffusional accessibility of matrix block mineralization, Paper presented at the 103rd annual meeting, Amer. Inst Mining Eng., Dallas Tex., 1974

Dershowitz W.S., Gordon B.M., Kafritsas J.C. A new Three Dimensional Model for Flow in Fractured Rock, IAH Conference Jan 7-12, 1985, Tucson Arizona, Volume XVII Proceedings published by a Committee of USA Members of the International Association of Hydrologists, p 449-462, 1985

Gale J., Stråhle A. Site characterization and Validation Drift and Borehole Fracture Data. Stage 1, Stripa Project Internal Report 88-10, Sept 1988

Garrels R.M., Dreyer R.M., Howland A.L. Diffusion of ions through intergranular space in pore water saturated rocks, Bull. Geol. Soc. Am. **60**, p 1809-1828, 1949

Gelhar L.W. Applications of Stochastic Models to Solute Transport in Fractured Rocks, SKB Technical Report 87-05, 1987

Gelhar L.W., Mantoglou A., Welty C., Rehfeldt K.R. A review of field scale physical solute transport processes in saturated and unsaturated media, EPRI EA-419OS, Aug 1985

Gentier S. Morphlologie et comportement hydromécanique d'une fracture naturelle dans un granite sous contrainte normale. Etude expérimentale et théoretique, Thèse de Doctorat à l'Université d'Orléans, Mar. 1986

Gilling D., Jeffries N.L., Lineham T.R. An experimental study of solute transport in mudstones, Harwell report AERE R12809, 1987

Jefferies N.L. Long term solute diffusion in a granite block immersed in sea water, CEC, Nuclear science and technology report EUR 11627, 1988

KBS-3, 1983, Final storage of spent nuclear fuel, Report by Swedish Nuclear Fuel Supply Co, SKBF, Stockholm, Sweden, May, 1983

Lallemand-Barres A., Peaudecerf P. Recherche des relations entre la valeur de la dispersivité macroscopique d'un milieu aquifère, ses autres caractéristiques et les conditions de mesure, Bull. BRGM (2) III, 4, 277, 1978

Landström O., Klockars C-E., Holmberg K-E., Westerberg S. In situ experiments on nuclide migration in fractured crystalline rocks, KBS TR 110, 1978

Lever D.A., Bradbury M.H., Hemingway S.J. The effect of dead end porosity on rock matrix diffusion, J. Hydrology **80**, p 45-76, 1985

Long J.C.S., Endo H.K., Karasaki K., Pyrak L., MacLean P., Witherspoon P.A. Hydrological Behavior of Fracture Networks. Hydrogeology of Rocks of Low Permeability, IAH Conference Jan 7-12, 1985, Tucson Arizona. Volume XVII, p 44-468, 1985

Long J.C.S., Billaux D.M. From field data to fracture network modelling: An example incorporating spatial structure, Water Resources Research **23,** p 1201-1216, 1987

Maloszewski P., Zuber A. On the theory of tracer experiments in fissured rock with a porous matrix, J. Hydrol. **79**, p 333-358, 1985

Moreno L., Neretnieks I., Klockars C-E. Evaluation of some tracer tests in the granitic rock at Finnsjön, KBS TR 83-38, 1983

Moreno L., Neretnieks I., Eriksen T. Analysis of some laboratory tracer runs in natural fissures, Water Resources Res. **21**, p 951-958, 1985

Moreno L., Neretnieks I. Channeling and its potential consequences for radionuclides transport, presented at MRS Symposium at Boston, Nov 30 - Dec 3, Proceedings, p 169-178, 1987

Moreno L., Tsang Y.W., Tsang C.F., Neretnieks I. Flow and solute transport in a single fracture. A two-dimensional statistical model, Nuclear Fuel Safety Project, Technical report TR 88-03, Stockholm, 1987

Moreno L., Tsang Y.W., Tsang C.F., Hale F.V., Neretnieks I. Flow and tracer transport in a single fracture. A stochastic model and its relation to some field observations, Water Resources Research, **24**, p 2033-3048, 1988

Moreno L., Neretnieks I. Channeling in fracture zones and its potential impact on the transport of radionuclides, Symposium on scientific basis for nuclear waste management. Berlin Oct 10-13, proceedings in print, 1988

Moreno L., Neretnieks I., Landström O. An evaluation of some tracer tests performed at Studsvik, KBS TR 89-09, 1989

NAGRA Project Gewähr. Endlager Für Hochaktive Abfälle: Das System der Sicherheitsbarriären, Nagra, Baden, Switzerland, Jan 1985

Neretnieks I. Diffusion in the Rock Matrix: An Important Factor in Radionuclide Retardation? J. Geophys. Res. **85**, p 4379-4397, 1980

Neretnieks I. Age dating of groundwater in fissured rock. Influence of water in micropores, Water Resources Res. **17**, p 421, 1981

Neretnieks I. A note on fracture flow mechanisms in the ground, Water Resources Res. **19**, p. 364-370, 1983

Neretnieks I. Transport in Fractured Rocks. Paper at IAH 17th congress, Tucson Arizona, Jan. 1985, Memoires vol XVII, part 2, Proceedings, p 301-318, 1985

Neretnieks I. Channeling in crystalline rocks. Its possible impact on transport of radionuclides from a repository, Colloque international Impact de la physico-chimie sur l'étude, la conception et l'optimisation des procédes en milieu poreux naturel, Nancy, 10-12 Juin 1987a

Neretnieks I. Channeling effects in flow and transport in fractured rocks - Some recent observations and models, Paper presented at GEOVAL symposium, Stockholm, Proceedings, p 315-335, 1987b

Neretnieks I. The Swedish repository for low and intermediate level reactor waste-SFR. Radioactivity release and transport calculations, Symposium on scientific basis for nuclear waste management, Berlin Oct 10-13, Proceedings, p 537-544, 1988

Neretnieks I., Eriksen T., Tähtinen P. "Tracer movement in a single fissure in granitic rock: Some experimental results and their interpretation," Water Resources Res. **18**, p 849, 1982

Neretnieks I., Rasmuson A. An approach to modelling radionuclide migration in a medium with strongly varying velocity and block sizes along the flow path, Water Resources Res. **20**, p 1823-1836, 1984

Neretnieks I., Abelin H., Birgersson L. Some recent observations of channeling in fractured rocks. Its potential impact on radionuclide migration, In DOE/AECL conference Sept 15-17, 1987, San Francisco, Proceedings p 387-410, 1987

Novakowski K.S., Flavelle P.A., Raven K.G., Cooper E.L. Determination of groundwater flow pathways in fractured plutonic rock using a radioactive tracer, Intern J. Appl. Radiat. Isot., **36**, p 399-404, 1985a

Novakowski K.S., Evans G.V., Lever D.A. Raven K.G. A field example of measuring hydrodynamic dispersion in a single fracture, Water Resources Research **21**, p 1165-1174, 1985b

Pocos de Caldas project: Progress report March through May 1987, SKB, Sweden, 1987

Rasmuson A., Analysis of Hydrodynamic Dispersion in Discrete Fracture Networks Using the Method of Moments, Water Resources Res. **21**, p 1677-1683, 1985

Rasmuson A., Neretnieks I. Exact solution of a model for diffusion in particles and longitudinal dispersion in packed beds, AIChE J. **26**, p 686, 1980

Rasmuson A., Neretnieks I. Surface migration in sorption processes, SKBF/KBS Technical Report 83-37, March 1983

Rasmuson A., Neretnieks I. Radionuclide transport in fast channels in crystalline rock, Water Resources Res. **22**, p 1247-1256, 1986a

Rasmuson A., Neretnieks I. Radionuclide migration in strongly fissured zones - The sensitivity to some assumptions and parameters, Water Resources Research **22**, p 559-569, 1986b

Raven K.G., Novakowski K.S., Lapcevic P.A. Interpretation of field tracer tests of a single fracture using a transient solute storage model, Water Resources Research, **24**, p 2019-2032, 1986

Robinson P.C., Connectivity, flow and and transport in network models of fractured media, Ph. D. Thesis, St. Catherine's College, Oxford University, Ref TP 1072, May 1984

Robinson P.C. Flow Modelling in Three Dimensional Fracture networks, Report AERE R 11965 UK Atomic Energy Authority Harwell Theoretical Physics Division, May 1986

Skagius K. Diffusion of dissolved species in the matrix of some Swedish crystalline rocks, Ph.D. Thesis, Dept. Chemical Engineering, Royal Institute of Technology, May 1986

Skagius K., Svedberg G., Neretnieks I. A study of strontium and cesium sorption on granite, Nuclear technology **59**, p 302-313, 1982

Skagius K., Neretnieks I. Porosities of and diffusivities in crystalline rock and fissure coating materials, Scientific basis for nuclear waste management VII, Boston, Nov. 1983, Elsevier, p 835, 1984

Skagius K., Neretnieks I. Porosities and diffusivities of some nonsorbing species in crystalline rocks, Water Resources Res. **22**, p 389, 1986a

Skagius K., Neretnieks. I. Diffusivity measurements and electrical resistivity measurements in rock samples under mechanical stress, Water Resources Research **22**, p 570, 1986b

Skagius K., Neretnieks I. Measurements of cesium and strontium diffusion in biotite gneiss, Water Resources Research **24**, p 75-84, 1988

Smith L., Schwartz F., Mase C. Applications of stochastic methods for the simulation of solute transport in discrete and continuum models of fractured rock systems, Proceedings of Conference on Geostatistical, Sensitivity and Uncertainty Methods for Ground-Water Flow and Radionuclide Transport Modelling, San Francisco, California, September 15-17, p 425-440, 1987

Tsang Y.W., Tsang C.F. Channel model of flow through fractured media, Water Resources Res. **23**, p 467-479, 1987

Tsang Y.W., Tsang C.F., Neretnieks I., Moreno L. Flow and tracer transport in fractured media - A variable aperture channel model and its properties, Water Resources Research **24**, p 2049-2060, 1988

Webster D.S., Proctor J.F., Marine I. W. Two well tracer tests in fractured crystalline rock, U.S. Geol. Surv. Water Supply paper 1544-I1, 1970

Witherspoon P.A., Wang J.S.K., Iwai K., Gale J.E. Validity of cubic law for fluid flow in a deformable rock fracture, Water Resources Res. **16**, p 1016-1024, 1980

WP-Cave: reference to a report under preparation.

KBS - technical reports can be obtained from: INIS CLEARING HOUSE, International Atomic Energy Agency, P.O. Box 100, A-1400 VIENNA, Austria.

10 NOTATION

a	Specific surface	m^2/m^3 water
C	Concentration	mol/m^3
C_p	Concentration in pores	mol/m^3
D_a	Apparent diffusion coefficient	m^2/s
D_e	Effective diffusion coefficient in matrix	m^2/s
D_p	Pore diffusion coefficient	m^2/s
D_L	Dispersion coefficient	m^2/s
D_s	Surface diffusion coefficient	m^2/s
D_w	Diffusion coefficient in water	m^2/s
F_f	Formation factor	-
K	Volumetric sorption coefficient	m^3/m^3
K_a	Surface sorption coefficient	m^3/m^2
K_d	Mass sorption coefficient	kg/m^3
K_p	Hydraulic conductivity	m/s
N	Flowrate of dissolved species	mol/s
Pe	Peclet number	-
R_d	Retardation factor	-
t	Time	s
t_w	Water residence time	s
u_f	Water velocity	m/s
W	Width of channel	m
x	Distance into matrix	m
z	Distance in flow direction	m

α	Rock capacity factor	-
δ_D	Constrictivity	-
δ	Fracture aperture	m
ε	Porosity	-
ε_p	Porosity of matrix	-
ε_t	Total porosity	-
$\overline{\eta}$	Penetration thickness	m
ρ_p	Density of rock	kg/m^3
τ	Tortuosity	-

List of SKB reports

Annual Reports

1977-78
TR 121
KBS Technical Reports 1 – 120
Summaries
Stockholm, May 1979

1979
TR 79-28
The KBS Annual Report 1979
KBS Technical Reports 79-01 – 79-27
Summaries
Stockholm, March 1980

1980
TR 80-26
The KBS Annual Report 1980
KBS Technical Reports 80-01 – 80-25
Summaries
Stockholm, March 1981

1981
TR 81-17
The KBS Annual Report 1981
KBS Technical Reports 81-01 – 81-16
Summaries
Stockholm, April 1982

1982
TR 82-28
The KBS Annual Report 1982
KBS Technical Reports 82-01 – 82-27
Summaries
Stockholm, July 1983

1983
TR 83-77
The KBS Annual Report 1983
KBS Technical Reports 83-01 – 83-76
Summaries
Stockholm, June 1984

1984
TR 85-01
Annual Research and Development Report 1984
Including Summaries of Technical Reports Issued during 1984. (Technical Reports 84-01 – 84-19)
Stockholm, June 1985

1985
TR 85-20
Annual Research and Development Report 1985
Including Summaries of Technical Reports Issued during 1985. (Technical Reports 85-01 – 85-19)
Stockholm, May 1986

1986
TR 86-31
SKB Annual Report 1986
Including Summaries of Technical Reports Issued during 1986
Stockholm, May 1987

1987
TR 87-33
SKB Annual Report 1987
Including Summaries of Technical Reports Issued during 1987
Stockholm, May 1988

1988
TR 88-32
SKB Annual Report 1988
Including Summaries of Technical Reports Issued during 1988
Stockholm, May 1989

1989
TR 89-40
SKB Annual Report 1989
Including Summaries of Technical Reports Issued during 1989
Stockholm, May 1990

Technical Reports

List of SKB Technical Reports 1990

TR 90-01
FARF31 –
A far field radionuclide migration code for use with the PROPER package
Sven Norman[1], Nils Kjellbert[2]
[1]Starprog AB
[2]SKB AB
January 1990

TR 90-02
Source terms, isolation and radiological consequences of carbon-14 waste in the Swedish SFR repository
Rolf Hesböl, Ignasi Puigdomenech, Sverker Evans
Studsvik Nuclear
January 1990

TR 90-03
Uncertainties in repository performance from spatial variability of hydraulic conductivities –
Statistical estimation and stochastic simulation using PROPER
Lars Lovius[1], Sven Norman[1], Nils Kjellbert[2]
[1]Starprog AB
[2]SKB AB
February 1990

TR 90-04
Examination of the surface deposit on an irradiated PWR fuel specimen subjected to corrosion in deionized water
R. S. Forsyth, U-B. Eklund, O. Mattsson, D. Schrire
Studsvik Nuclear
March 1990

TR 90-05
Potential effects of bacteria on radionuclide transport from a Swedish high level nuclear waste repository
Karsten Pedersen
University of Gothenburg, Department of General and Marine Microbiology, Gothenburg
January 1990

TR 90-06
Transport of actinides and Tc through a bentonite backfill containing small quantities of iron, copper or minerals in inert atmosphere
Yngve Albinsson, Birgit Sätmark,
Ingemar Engkvist, W. Johansson
Department of Nuclear Chemistry,
Chalmers University of Technology, Gothenburg
April 1990

TR 90-07
Examination of reaction products on the surface of UO_2 fuel exposed to reactor coolant water during power operation
R. S. Forsyth, T. J. Jonsson, O. Mattsson
Studsvik Nuclear
March 1990

TR 90-08
Radiolytically induced oxidative dissolution of spent nuclear fuel
Lars Werme[1], Patrik Sellin[1], Roy Forsyth[2]
[1]Swedish Nuclear Fuel and waste Management Co (SKB)
[2]Studsvik Nuclear
May 1990

TR 90-09
Individual radiation doses from unit releases of long lived radionuclides
Ulla Bergström, Sture Nordlinder
Studsvik Nuclear
April 1990

TR 90-10
Outline of regional geology, mineralogy and geochemistry, Poços de Caldas, Minas Gerais, Brazil
H. D. Schorscher[1], M. E. Shea[2]
[1]University of Sao Paulo
[2]Battelle, Chicago
December 1990

TR 90-11
Mineralogy, petrology and geochemistry of the Poços de Caldas analogue study sites, Minas Gerais, Brazil
I: Osamu Utsumi uranium mine
N. Waber[1], H. D. Schorscher[2], A. B. MacKenzie[3], T. Peters[1]
[1]University of Bern
[2]University of Sao Paulo
[3]Scottish Universities Research & Reactor Centre (SURRC), Glasgow
December 1990

TR 90-12
Mineralogy, petrology and geochemistry of the Poços de Caldas analogue study sites, Minas Gerais, Brazil
II: Morro do Ferro
N. Waber
University of Bern
December 1990

TR 90-13
Isotopic geochemical characterisation of selected nepheline syenites and phonolites from the Poços de Caldas alkaline complex, Minas Gerais, Brazil
M. E. Shea
Battelle, Chicago
December 1990

TR 90-14
Geomorphological and hydrogeological features of the Poços de Caldas caldera, and the Osamu Utsumi mine and Morro do Ferro analogue study sites, Brazil
D. C. Holmes[1], A. E. Pitty[2], R. Noy[1]
[1]British Geological Survey, Keyworth
[2]INTERRA/ECL, Leicestershire, UK
December 1990

TR 90-15
Chemical and isotopic composition of groundwaters and their seasonal variability at the Osamu Utsumi and Morro do Ferro analogue study sites, Poços de Caldas, Brazil
D. K. Nordstrom[1], J. A. T. Smellie[2], M. Wolf[3]
[1]US Geological Survey, Menlo Park
[2]Conterra AB, Uppsala
[3]Gesellschaft für Strahlen- und Umweltforschung (GSF), Munich
December 1990

TR 90-16

Natural radionuclide and stable element studies of rock samples from the Osamu Utsumi mine and Morro do Ferro analogue study sites, Poços de Caldas, Brazil

A. B. MacKenzie[1], P. Linsalata[2], N. Miekeley[3], J. K. Osmond[4], D. B. Curtis[5]
[1]Scottish Universities Research & Reactor Centre (SURRC), Glasgow
[2]New York Medical Centre
[3]Catholic University of Rio de Janeiro (PUC)
[4]Florida State University
[5]Los Alamos National Laboratory
December 1990

TR 90-17

Natural series nuclide and rare earth element geochemistry of waters from the Osamu Utsumi mine and Morro do Ferro analogue study sites, Poços de Caldas, Brazil

N. Miekeley[1], O. Coutinho de Jesus[1], C-L Porto da Silveira[1], P. Linsalata[2], J. N. Andrews[3], J. K. Osmond[4]
[1]Catholic University of Rio de Janeiro (PUC)
[2]New York Medical Centre
[3]University of Bath
[4]Florida State University
December 1990

TR 90-18

Chemical and physical characterisation of suspended particles and colloids in waters from the Osamu Utsumi mine and Morro do Ferro analogue study sites, Poços de Caldas, Brazil

N. Miekeley[1], O. Coutinho de Jesus[1], C-L Porto da Silveira[1], C. Degueldre[2]
[1]Catholic University of Rio de Janeiro (PUC)
[2]PSI, Villingen, Switzerland
December 1990

TR 90-19

Microbiological analysis at the Osamu Utsumi mine and Morro do Ferro analogue study sites, Poços de Caldas, Brazil

J. West[1], A. Vialta[2], I. G. McKinley[3]
[1]British Geological Survey, Keyworth
[2]Uranio do Brasil, Poços de Caldas
[3]NAGRA, Baden, Switzerland
December 1990

TR 90-20

Testing of geochemical models in the Poços de Caldas analogue study

J. Bruno[1], J. E. Cross[2], J. Eikenberg[3], I. G. McKinley[4], D. Read[5], A. Sandino[1], P. Sellin[6]
[1]Royal Institute of Technology (KTH), Stockholm
[2]AERE, Harwell, UK
[3]PSI, Villingen, Switzerland
[4]NAGRA, Baden, Switzerland
[5]Atkins, ES, Epsom, UK
[6]Swedish Nuclear and Waste Management Co (SKB), Stockholm
December 1990

TR 90-21

Testing models of redox front migration and geochemistry at the Osamu Utsumi mine and Morro do Ferro analogue sites, Poços de Caldas, Brazil

J. Cross[1], A. Haworth[1], P. C. Lichtner[2], A. B. MacKenzi[3], L. Moreno[4], I. Neretnieks[4], D. K. Nordstrom[5], D. Read[6], L. Romero[4], S. M. Sharland[1], C. J. Tweed[1]
[1]AERE, Harwell, UK
[2]University of Bern
[3]Scottish Universities Research & Reactor Centre (SURRC), Glasgow
[4]Royal Institute of Technology (KTH), Stockholm
[5]US Geological Survey, Menlo Park
[6]Atkins ES, Epsom, UK
December 1990

TR 90-22

Near-field high temperature transport: Evidence from the genesis of the Osamu Utsumi uranium mine analogue site, Poços de Caldas, Brazil

L. M. Cathles[1], M. E. Shea[2]
[1]University of Cornell, New York
[2]Battelle, Chicago
December 1990

TR 90-23

Geochemical modelling of water-rock interactions at the Osamu Utsumi mine and Morro do Ferro analogue sites, Poços de Caldas, Brazil

D. K. Nordstrom[1], I. Puigdomenech[2], R. H. McNutt[3]
[1]US Geological Survey, Menlo Park
[2]Studsvik Nuclear, Sweden
[3]McMaster University, Ontario, Canada
December 1990

TR 90-24
The Poços de Caldas Project: Summary and implications for radioactive waste management
N. A. Chapman[1], I. G. McKinley[2], M. E. Shea[3], J. A. T. Smellie[4]
[1]INTERRA/ECL, Leicestershire, UK
[2]NAGRA, Baden, Switzerland
[3]Battelle, Chicago
[4]Conterra AB, Uppsala

TR 90-25
Kinetics of UO_2(s) dissolution reducing conditions: numerical modelling
I. Puigdomenech[1], I. Casas[2], J. Bruno[3]
[1]Studsvik AB, Nyköping, Sweden
[2]Department of Chemical Engineering, E.T.S.E.I.B. (U.P.C.), Barcelona, Spain
[3]Department of Inorganic Chemistry, The Royal Institute of Technology, Stockholm, Sweden
May 1990

TR 90-26
The effect from the number of cells, pH and lanthanide concentration on the sorption of promethium on gramnegative bacterium (Shewanella Putrefaciens)
Karsten Pedersen[1], Yngve Albinsson[2]
[1]University of Göteborg, Department of General and Marine Microbiology, Gothenburg, Sweden
[2]Chalmers University of Technology, Department of Nuclear Chemistry, Gothenburg, Sweden
June 1990

TR 90-27
Isolation and characterization of humics from natural waters
B. Allard[1], I. Arsenie[1], H. Borén[1], J. Ephraim[1], G. Gårdhammar[2], C. Pettersson[1]
[1]Department of Water and Environmental Studies, Linköping University, Linköping, Sweden
[2]Department of Chemistry, Linköping University, Linköping, Sweden
May 1990

TR 90-28
Complex forming properties of natural organic acids. Part 2. Complexes with iron and calcium
James H. Ephraim[1], Andrew S. Mathuthu[2], Jacob A. Marinsky[3]
[1]Department of Water in Environment and Society, Linköping University, Linköping, Sweden
[2]Chemistry department, University of Zimbabwe, Harare, Zimbabwe
[3]Chemistry Department, State University of New York at Buffalo, Buffalo, NY, USA
July 1990

TR 90-29
Characterization of humic substances from deep groundwaters in granitic bedrock in Sweden
C. Pettersson, J. Ephraim, B. Allard, H. Borén
Department of Water and Environmental Studies, Linköping University, Linköping, Sweden
June 1990

TR 90-30
The earthquakes of the Baltic shield
Ragnar Slunga
Swedish National Defence Research Institute
June 1990

TR 90-31
Near-field performance of the advanced cold process canister
Lars Werme
Swedish Nuclear Fuel and Waste Management Co (SKB)
September 1990

TR 90-32
Radioclide transport paths in the nearfield – a KBS-3 concept study
Roland Pusch
Clay Technology AB and Lund University of Technology
July 1990

TR 90-33
PLAN 90
Costs for management of the radioactive waste from nuclear power production
Swedish Nuclear Fuel and Waste Management Co (SKB)
June 1990

TR 90-34
GEOTAB: User's guide – Version 1.8.2
Ergodata
October 1990

TR 90-35
Dose conversion factors for major nuclides within high level waste
Ulla Bergström, Sture Nordlinder
Studsvik Nuclear
November 1990

TR 90-36

Sensitivity analysis of groundwater flow
Licentiate thesis

Yung-Bing Bao
Royal Institute of Technology, Department of Land and Water Resources, Stockholm, Sweden
December 1990

TR 30-37

The influence of fracture mineral/ groundwater interaction on the mobility of U, Th, REE and other trace elements

Ove Landström[1], Eva-Lena Tullborg[2]
[1]Studsvik AB, Nyköping
[2]SGAB, Gothenburg
December 1990